

Doctoral Thesis

博士論文

Estimation of Global Irrigation Water Demand by Integrating  
Long-term Remote Sensing Dataset

(長期的リモート・センシングデータセット統合を利用したグローバルな灌漑水需  
要予測に関する研究)

Anjar Dimara Sakti

アンジャール ディマラ サクティ

A dissertation submitted to the University of Tokyo in partial fulfilment of the requirements  
for the degree of Doctor of Philosophy

*Academic Supervisor*

Professor Wataru Takeuchi

*Examination Committee*

Professor Sawahiko Shimada

Project Professor Akiyuki Kawasaki

Associate Professor Oki Kazuo

Associate Professor Yoshihide Sekimoto

Department of Civil Engineering

Graduate School of Engineering

The University of Tokyo

Tokyo, Japan

December, 2018

# Estimation of Global Irrigation Water Demand by Integrating Long-term Remote Sensing Dataset

(長期的リモート・センシングデータセット統合を利用したグローバルな灌漑水需要予測に関する研究)

## Abstract

Compared with another sector, irrigation pointed as the highest water demand, with 70 % of global fresh water consumption is dominated for irrigation purpose. This sector also counted as the biggest contributor to global water loss problem, where 44% water in irrigation sector wasted. Irrigation Water Demand (IWD) defines as the amount of water needed for the crop to achieve optimal growth. As basis data information of water use in agriculture sector, improving the estimation of global water demand in agriculture sector can improve the irrigation water efficiency estimation, which is an important factor to achieve SDGs targets, especially goal no. 2: to double food production, goal no.6: to give drinking water access for the rapidly growing population and goal no.12: to achieve the sustainable management and efficient use of natural resources. Five main parameters to calculate IWD are Potential evapotranspiration (PET), precipitation, cropping intensity (CI), crop calendar - sowing date and cropping pattern. Monitoring accurately the long-term dynamic of global cropping intensity crop calendar, and rice non-rice cropping pattern is important to support global food security especially to estimate accurately water demand in agriculture sector. In this study our objective is to estimate long-term IWD from 2001 to 2015 at a spatial resolution of 1 km in the global scale. To achieve the main goal, we divide the main goal into three specific goals. The first goal is to harmonize and integrate cropland classes of current global land cover (GLC) datasets into cropland agreement level product. Second, to estimate long-term global cropping intensity, sowing month and dominant cropping pattern of rice and non-rice by integrating MODIS NDVI (optic) and AMSR LSWC (microwave). The last goal is to produce global Irrigation water demand (IWD) and its change by combining remote sensing of climate and dynamic crop coefficient with CROPWAT empirical model.

For developing long-term global Irrigation water demand, first, we estimate cropping intensity, sowing month, and dominant cropping pattern based on combination MODIS and AMSR-E/2. We investigate time series of satellite-sensed normalized difference vegetation index (NDVI)

from 16-Day MODIS (MOD13A2) composite from 2001 to 2015 and divide these 15 years archived data into three group of year (2001-2005, 2006-2010, 2011-2015). For estimating specific rice paddy cropping pattern and flooding session as well, we used Land Surface Water Coverage (LSWC) from daily AMSR-E/2 in three group of year (2003 – 2005, 2008 – 2010, and 2013 – 2015). Second, we develop Crop Coefficient (KC) by combining Cropland Agreement level, MODIS Cropping intensity, MODIS-AMSR Sowing month and MODIS-AMSR Cropping Dominant products. The final analysis is applying Doll and Siebert approach by multiplying MODIS potential evapotranspiration product (MOD16A2) with the developed KC. We include GSMaP precipitation, IIASA crop fraction, FAO-GMIA irrigated and HYDE rice paddy fraction to produce final product of long-term global IWD.

The results of cropland agreement level (CAL) analysis proposed four agreement levels, and the correlation factor obtained from the CAL product and IIASA crop fraction comparison had successfully estimated the percentage of cropland area from four agreement levels. The cropland estimate results from the CAL analysis were observed along with FAO data statistics and showed the highest accuracy, with a 0.70 and 0.71 regression value for 2005 and 2010 respectively. The presented MODIS-AMSR sowing month and cropping pattern products, to our knowledge are the first satellite-based products which derived from integration of vegetation and water index phenology from optic and microwave satellite sensor, that can analyze dynamic change of crop activities as one of essential input for estimating irrigation water demand. The advantages of the MODIS-AMSR sowing month product are capable to detect short period crop cultivation, distinguish rice and non-rice crop type and analyze trend of sowing month change from 15 years' data monitoring.

The final result of global irrigation water demand (IWD) products are the first satellite-based products that can analyze 15 years' dynamic change of water demand in cropland area. The total water use by irrigated and rainfed are 6,137 km<sup>3</sup>/ year in 2001-2005, 5,834 km<sup>3</sup>/ year in 2006-2010, and 7,491 km<sup>3</sup>/ year in 2006-2010. This calculation derived from three water use estimation categories: 1) total blue water (irrigation) used by irrigated crop, 2) total green water (precipitation) used by irrigated crop and 3). Green water used by rainfed crops. The long-term global IWD products are projected to simulate global surface water cycle in agriculture area in more realistic way by considering climate and crop activities which derived from actual, consistent and latest remote sensing datasets. This high resolution IWD product will support to achieve SDGs target in regional and country level analysis.

# Contents

|  |    |
|--|----|
| Contents .....   | iv |
| Chapter 1. INTRODUCTION.....   | 7  |
| 1.1 Background.....  | 7  |
| 1.1.1. Global Burden in Food Security .....  | 7  |
| 1.1.2. Dynamic Change of Crop Activity .....   | 9  |
| 1.1.3. Important for Monitoring Water Use in Agriculture Sector for Support SDGs.....                                  | 10 |
| 1.1.4. Rice Paddy mapping for increasing accuracy for Water Use estimation .....                                       | 14 |
| 1.2 Statement of the problem.....  | 18 |
| 1.3 Objective of the study.....  | 19 |
| 1.4 Originality of study.....  | 20 |
| Chapter 2 REVIEW LITERATURE.....   | 21 |
| 2.1 Global Land Cover Datasets .....   | 21 |
| 2.2 Irrigation Water Demand.....   | 21 |
| Chapter 3 DEVELOPMENT OF GLOBAL CROPLAND AGREEMENT LEVEL.....  | 24 |
| 3.1 Background.....  | 24 |
| 3.2 Material.....  | 25 |
| 3.2.1 Global Land Cover (GLC) datasets.....  | 25 |
| 3.3 Methods .....  | 27 |
| 3.3.1 Pixel Comparison Using CRISPS Approach .....   | 27 |
| 3.3.2 Re-projection.....   | 27 |
| 3.3.3 Rescaling Analysis.....  | 28 |
| 3.3.4 Legend Harmonization.....  | 29 |
| 3.4 Result and Discussion.....   | 30 |
| 3.4.1 Thematic Similarity.....   | 30 |
| 3.4.2 Cropland Level Agreement (CAL) Analysis .....  | 32 |
| 3.4.3 Correlation Factor between CAL and Existing IIASA Cropland Fraction .....  | 35 |
| 3.4.4 Comparison of Cropland Area Estimates from the CAL with the FAO Data.....  | 37 |
| 3.4.5 Cropland Agreement Level (CAL) Change Analysis .....   | 40 |
| 3.5 Conclusion .....   | 41 |
| Chapter 4. DEVELOPMENT OF CROP CALENDAR, INTENSITY AND CROPPING<br>PATTERN BY INTEGRATING MODIS AND AMSR DATASETS..... | 42 |
| 4.1 Background.....  | 42 |
| 4.2 Material.....  | 43 |
| 4.2.1 Global MODIS NDVI Datasets .....   | 43 |
| 4.2.2 Global AMSR-E/2 LSWC Datasets Analysis of Endmember Dataset .....  | 43 |

|   |  |     |
|---|--|-----|
| 4.2.3   | Dataset Additional Datasets .....  | 45  |
| 4.3   | Methods .....  | 47  |
| 4.3.1   | Peak and Lowest Month of MODIS NDVI Extraction .....                                   | 47  |
| 4.3.2   | Peak Month of AMSR-E/2 LSWC Extraction .....   | 50  |
| 4.3.3   | Sowing Month Estimation .....  | 51  |
| 4.3.4   | Dominant Cropping Pattern of Rice and Non-Rice Paddy .....                             | 53  |
| 4.4   | Result and Discussion .....  | 53  |
| 4.4.1   | Long-term MODIS Cropping Intensity Product .....                                       | 53  |
| 4.4.2   | Cropping Intensity Change 2001-2015 .....  | 55  |
| 4.4.3   | Long-term MODIS-AMSR Sowing Month Product .....  | 58  |
| 4.4.4   | MODIS-AMSR Sowing Month Change 2001-2015 .....   | 60  |
| 4.4.5   | Rice and Non-Rice Dominant Cropping Pattern .....                                      | 62  |
| 4.5   | Comparative Analysis .....   | 68  |
| 4.5.1   | Comparison of the MODIS Cropping Intensity and SACRA product .....                     | 68  |
| 4.5.2   | Comparison of Cropping Intensity Change with HYDE V.3.2 Annual Irrigated Rainfed ..... | 79  |
| 4.5.3   | Comparison of the MODIS-AMSR Product with other Sowing Month Products .....            | 80  |
| 4.6   | Conclusion .....   | 87  |
| Chapter 5. DEVELOPMENT OF CROP COEFICIENT USING CROPWAT EMPIRICAL MODEL ..... |  | 88  |
| 5.1   | Background .....   | 88  |
| 5.2   | Material .....   | 89  |
| 5.3   | Methods .....  | 89  |
| 5.3.1   | CROPWAT Empirical Model .....  | 89  |
| 5.4   | Result and Discussion .....  | 90  |
| 5.4.1   | CROPWAT Crop Coefficient Product .....   | 90  |
| 5.4.2   | Monthly Gridded Crop Coefficient Product .....   | 93  |
| 5.5   | Conclusion .....   | 95  |
| Chapter 6. DEVELOPMENT IRRIGATION WATER DEMAND .....                          |  | 96  |
| 6.1   | Background .....   | 96  |
| 6.2   | Material .....   | 96  |
| 6.3   | Methods .....  | 98  |
| 6.3.1   | Crop Water Balance Approach .....  | 98  |
| 6.4   | Result and Discussion .....  | 100 |
| 6.4.1   | Effective Precipitation Product .....  | 100 |
| 6.4.2   | Long-term Crop Water Demand .....  | 101 |
| 6.4.3   | Irrigation Water Demand .....  | 105 |
| 6.5   | Conclusion .....   | 119 |

|   |     |
|---|-----|
| Chapter 7. CONCLUTIONS AND RECOMMENDATIONS..... | 121 |
| 7.1 Conclusions.....                            | 121 |
| 7.2 Recommendations.....                        | 122 |
| 7.3 Future Works .....                          | 122 |
| <b>ACKNOWLEDGMENT</b> .....                     | 123 |
| <b>BIBLIOGRAPHY</b> .....                       | 123 |

# Chapter 1 INTRODUCTION

## 1.1 Background

### 1.1.1. Global Burden in Food Security

The year 2015 was the United Nations Millennium Development Goals (UN-MDGs) evaluation of achievement, where one of the important target issues was to eradicate hunger that faced by around 800 million people. As a result, the share of undernourished had decreased significantly in the last 15 years, especially in the developing countries (figure 1-1). Undernourishment means that a person is not able to acquire enough food to meet the daily minimum dietary energy requirements, over a period of one year. FAO defines hunger as being synonymous with chronic undernourishment [FAO, 2015].

Stability in economic growth which has been supported by the massive development of irrigation infrastructure becoming one of the important factors that cause an escalation in agricultural extensification and intensification. This condition made a great contribution in increasing the global food production that leads to the decrease in hunger problem [See et al., 2015; Ramankutty et al., 2008].

However, in some region such as in Southern Asia, Oceania, the Caribbean, Southern and Eastern Africa, the decrease was slow [FAO, 2015]. The reasons behind this slow progress are the escalation of food demand due to a rapidly growing population that exceeds the rate of food production. With growth value of more than four times during the 20<sup>th</sup> century, the global population have been exceeding from 1.6 billion in 1900 to 7.4 billion in 2015 and are expected to reach 8.5 billion of people in 2030 according to FAO report [2007]. Consequently, the food production has to increase by 60 percent to feed an additional 1 billion people by 2030 [Doxsey-Whitfield et al., 2015; Davis et al., 2015]. This condition is getting worse by the unpredictable climate change impacts such as drought, flood, tropical storms and extreme weather changes [Ramankutty et al., 2018; Heino et al., 2018].

From eighteen countries were still facing high and very high hunger level based on FAO report (i.e: 1. Afghanistan, 2. Central African Republic, 3. Chad, 4. Congo, 5. Ethiopia, 6. Haiti 7. Liberia, 8. Madagascar, 9. Malawi, 10. Mozambique, 11. Namibia, 12. North Korea, 13. Rwanda, 14. Tajikistan, 15. Uganda, 16. Yemen, 17. Zambia, and 18. Zimbabwe), where 15 countries are located in Africa regional (Figure 1-2).

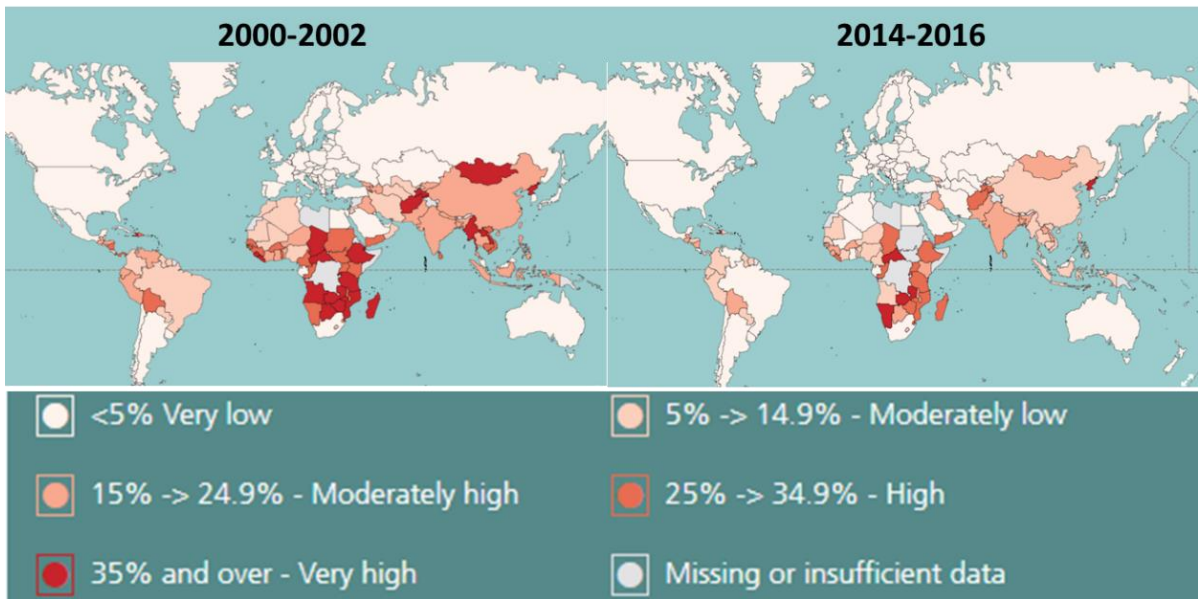


Figure 1-1. MDGs report on hunger and undernourished [Image Source: FAO., 2016]

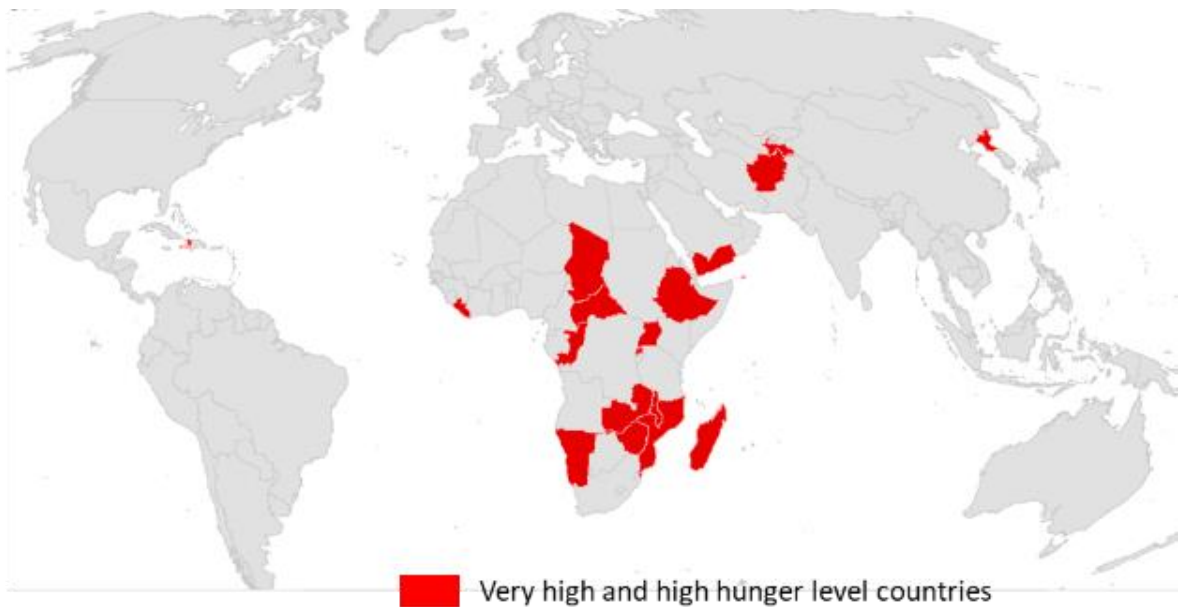


Figure 1-2. Distribution of 18 countries target that is still facing very high and high hunger levels [Data Source: FAO., 2016]

Increasing crop production in Africa is needed to meet future food demand. Africa population is projected to reach 1,634 million by 2030 (+ 500 million) [NEPAC, 2003]. Undernourished population increases by 35 million over the last 20 years. Crops represent 89%

of the diet in Sub-Sahara Africa (SSA). Human food commodity to increase by 15% in the next 40 years. Crop production growth in SAA is mainly due to the extension of cultivated area and cropping intensities while crop yield improvement is low. With this condition showed optimizing groundwater irrigation can play a significant role in increasing food production in Africa, although the development of area equipped for irrigation is slow (+ 6.2 million hectare over 45 years) [Villholth, 2013].

### 1.1.2. Dynamic Change of Crop Activity

The trend of widespread abandonment agricultural land and shrinking cropland area due to urbanization, makes extensification strategy become not preferred to mitigate the unavoidable increase of agricultural production [D'amour et al., 2016; Wue et al., 2018]. Where a limitation of the suitable land area and high environmental cost become major reasons for this extend agriculture land difficulty in the current situation. With the climate change pressure, global cropland area is facing the uncertainty not only in the number of crop intensity but also shifting for planting date. Since some crop influenced by weather and climate condition, which impress the farmer to changing the timing of sowing. This farmer decision making is an effort for adaptation strategies [Tubiello et al., 2000] (figure 1-3).



Figure 1-3. Dynamics of Rice Intensification System in Nepal  
(Source; Rajendra Uprety -Wageningen University)

As the response of this condition, several countries tried to intensify land-use on already cultivated lands, since it provides promising opportunity to boost global crop production more effectively instead expand agricultural land [Rufin, 2018]. However, this strategy facing high risk, since high crop water demand will follow high cropping intensity and estimated produce more GHG emissions which will be centered in specific area.

### 1.1.3. Important for Monitoring Water Use in Agriculture Sector for Support SDGs

Compared with another sector, irrigation pointed as the highest water demand, with 70% of global water consumption is for Irrigation purpose [UNEP, 2000; Oki et al, 2006] (Figure1-4) (Figure1-5). This sector also counted as the biggest contributor to global water loss problem, where 44% water in irrigation sector wasted [FAO, 2012], mainly caused by three dominant factors that are extreme evaporation, infrastructure problem, and low water management [Vanham et al., 2018] (Figure1-6).

As next generation of global pledge -development, Sustainable Development Goals (SDGs) are targeting not only to achieve zero hunger in 2030 but also to ensure sustainable food production systems [FAO, 2016]. Learn how to deal with tradeoffs between global food security and water demand are needed, to boosting food production in more sustainable approaches to achieve the goal.

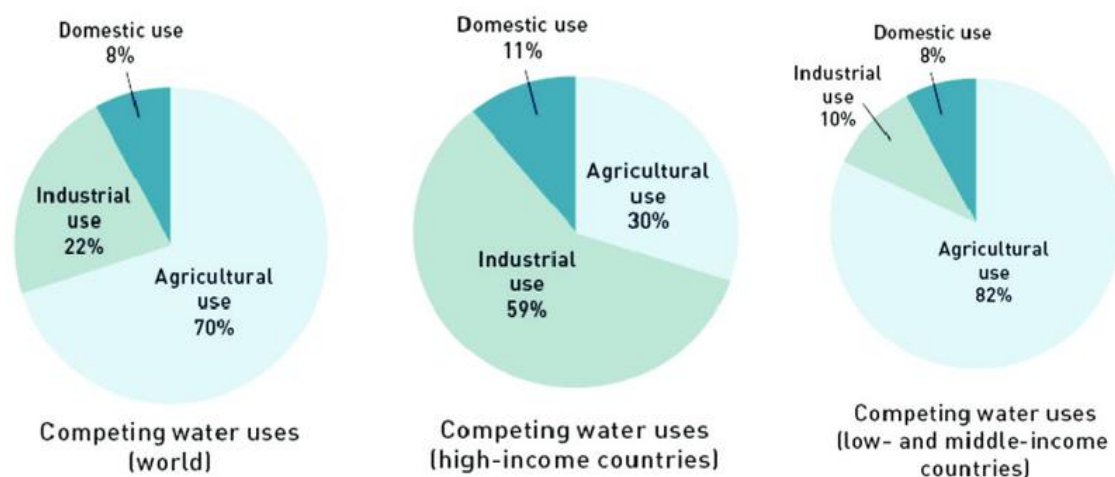


Figure1-4. Percent distribution of water use among domestic use, industrial use, and agricultural use in the world, in high-income countries and in low- and middle-income countries. (source; [World Water Development report, 2005])

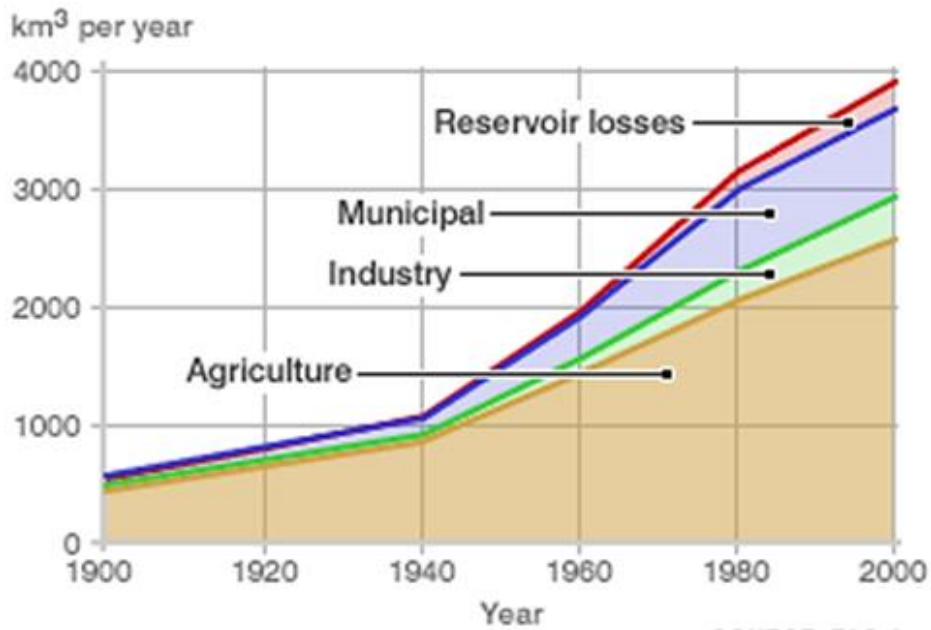


Figure 1-5. Estimated annual world water use (source; FAO Aqua stat 2010)

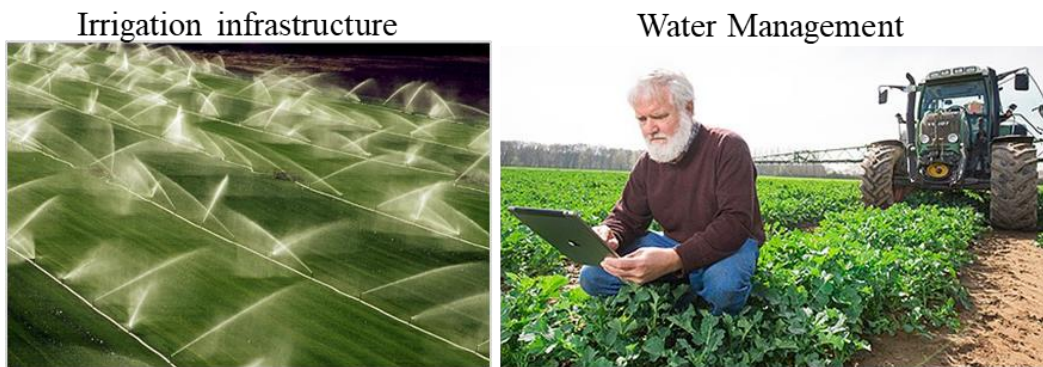


Figure 1-6. Irrigation infrastructure and water management issues on water loss problem

Irrigation water demand (IWD) means the amount of water that must be applied to the crop to achieve optimal growth [Doell, 2002; Rockstrom, 2006]. Increasing accuracy of IWD product can contribute to improve the analysis of several issues. There are include; A. To reduce water demand in irrigation [FAO, 2012; Nelson, 2015; Davis et al., 2017], B. To Improve Hydraulic Cycle Estimation [Oki and Kanae, 2006; Dalin et al., 2012; Wada, 2016; Biigs, 2015], C. To find new water Source for Irrigation [Altchenko et al., 2015], D. To improve crop emission estimation [Han et al., 2016; Carlson et al., 2016], E. Climate Change – Impact and Projection [Heino et al., 2018; Mehran et al., 2017] (figure 1-7).

Improving water irrigation efficiency can possible to reduce water loss problem by Improvement in irrigation infrastructure in intensively cultivated area. Such Improvement for

water management strategies such as agricultural drainage water (ADW) also has great near-term potential to reduce the GHG emissions intensity of global agriculture, without compromise with reduction in food production [Russ, 2016]. This contribution, can be one of the important factors to achieve SDGs targets, especially Goal no. 2: to double food production, Goal no.6: to give drinking water access for the rapidly growing population and Goal no.12: to achieve the sustainable management and efficient use of natural resources. This efficiency reflects to volume of water evapotranspired by the crop as a ratio of the water volume diverted from reservoirs/ground water. Water use efficiency has improved during the 22-y period (globally averaged VWC of all five crops has decreased and yields have increased) [Dalin et al., 2011].

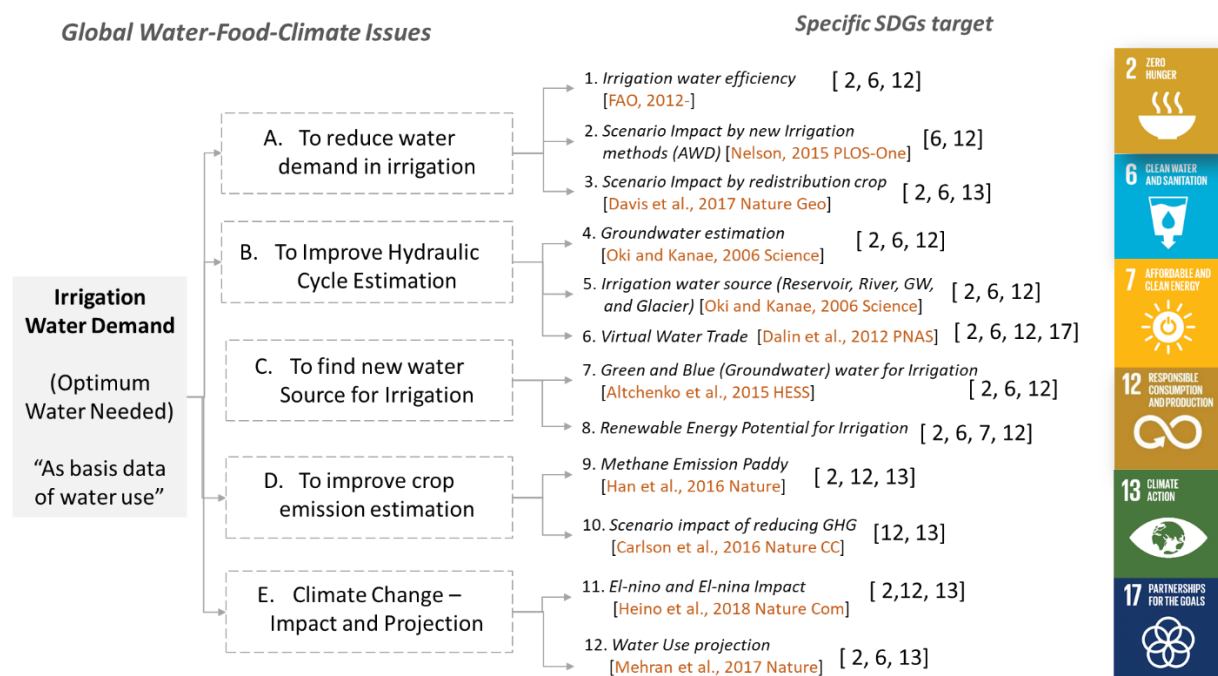


Figure 1-7. Contributions of Irrigation Water Demand estimation in SDGs in target number 2, 6, 7, 12, 13 and 17

One of contribution of IWD is for finding a new source of water especially ground water recharge [Altchenko, 2015]. Since extreme hunger occurs predominantly in remote areas with minimum irrigation infrastructure, groundwater becomes an alternative source of water for irrigation development. Groundwater can play a significant role to help both extensification and intensification since there is large groundwater potential storage [Margat et al., 2013]. To date, however, a complex array of factors has impeded its widespread introduction.

Development of areas equipped with groundwater irrigation is relatively low and unevenly distributed in a relatively small share of cultivated land, with only limited space available for abstraction [Foster and Perry, 2010]. Presently, groundwater covers around 2,106-ha area in Africa, equivalent to 1% of the developed land [Siebert et al., 2013]. In Asia, it covers about 38,106 ha or 14% of cultivated land [Siebert et al., 2013]. Groundwater has been most intensively developed in South Asia and North America - where it provides all irrigation water for about 57% and 54% respectively [Doll and Fiedler., 2008].

Groundwater recharge is one of the groundwater types that can provide an essential buffer to climate variability. The groundwater recharge is defined as the amount of water that infiltrates from precipitation through the unsaturated zone of the water table and reaches the aquifer. Groundwater recharge is estimated to provide 43% of all water used for irrigation. It is relatively affordable, safe and reliable, compared with non-renewable (fossil) groundwater [Altchenko, 2015].

Irrigation water demand also important input for emission estimation especially in rice paddy area [Han et al., 2016]. The food system, including crop production, is responsible for up to 1/3 of total anthropogenic GHG emissions. This emission is come from: 1. CH<sub>4</sub> emissions from paddy (flooded) rice cultivation, 2. CO<sub>2</sub>, N<sub>2</sub>O and CH<sub>4</sub> flux from agricultural peatland draining, 3. Direct and indirect N<sub>2</sub>O emissions from synthetic N fertilizer and manure application [Carlson et al., 2016]. International agreements now focus on reducing emissions from such agricultural extensification and intensification up to 2% per year [UNFCCC, 2015]. In 2010, agricultural production emissions were greater than land change emissions. GHG reduction strategies targeted to crop management practices are essential to address agriculture's contribution to climate change. (Improving yields on existing croplands supports future food demand).

Another contribution of Irrigation water demand estimation is to calculate Virtual Water Trade. It is defined as volume of water that an exporting nation consumes to produce the commodities that it trades abroad [Hanasaki et al., 2010]. Food trade may help save water by exchanges of virtual water. This activity can solve inequalities in global water use. The virtual water trade not only generates water savings for importing countries but also represents water “losses” for the exporting countries. [Chapagain et al. 2006]. Temporal analysis of the global VWT network would allow for an assessment of key impacts of policy, economic, and biophysical factors. Dalin et al, [2011] found that international food trade is leading to global water savings (from a relatively more efficient country (with lower VWC) to a relatively less efficient country) Represented 18% of the global VWT volume in 1986 and 42% in 2007.

#### 1.1.4. Rice Paddy mapping for increasing accuracy for Water Use estimation

Rice is one of the most consumed grains in the world and produced more than 114 countries, that is why it become an important factor in view of food security [USDA, 2015]. Long year rice field distribution monitoring in global scale will become an important method in order to evaluate the accomplishment of SDGs in decreasing hunger and also to assess the impact of environmental changing especially for water use monitoring in agriculture sector [Xiao et al., 2005; Mosleh et al., 2015].

Rice is very important crop with specific planting characteristic and has highest water demand. Based on CROPWAT crop coefficient [FAO, 2009] shows rice has higher crop coefficient compare with non-rice crop type. Where compare with non-rice of major crops, rice consumed the greatest water especially blue water. Hence, understanding rice paddy phenology to separate rice and non-rice crop type can improve the accuracy of sowing month estimation and irrigation water demand as well. The result of analysis that conducted from this method can be used to construct a strategy for achieving Sustainable Development Goals (SDGs) target in food security 15 years later.



Figure 1-8. Understanding rice paddy phenology can improve the accuracy of Irrigation Water Demand.

#### 1.1.5. Source of Global Crop Water Demand: Blue and Green Water

Monitoring Croplands have resulted in changes in land use and cover through land clearing, deriving redistribution of evapotranspiration and increasing it in many irrigated areas with associated impacts on microclimate and regional climate impacts [Gordon et al., 2008].

Continued increase in demand for water and recent water shortages have intensified the need for better utilization of our water resources; its has also forced us to think more innovatively about different components of water available in the hydrological cycle [Sevenije, 2004; Jewit et al., 2006]. The source of water for irrigation can be classified into two groups: the green and blue water resorces.

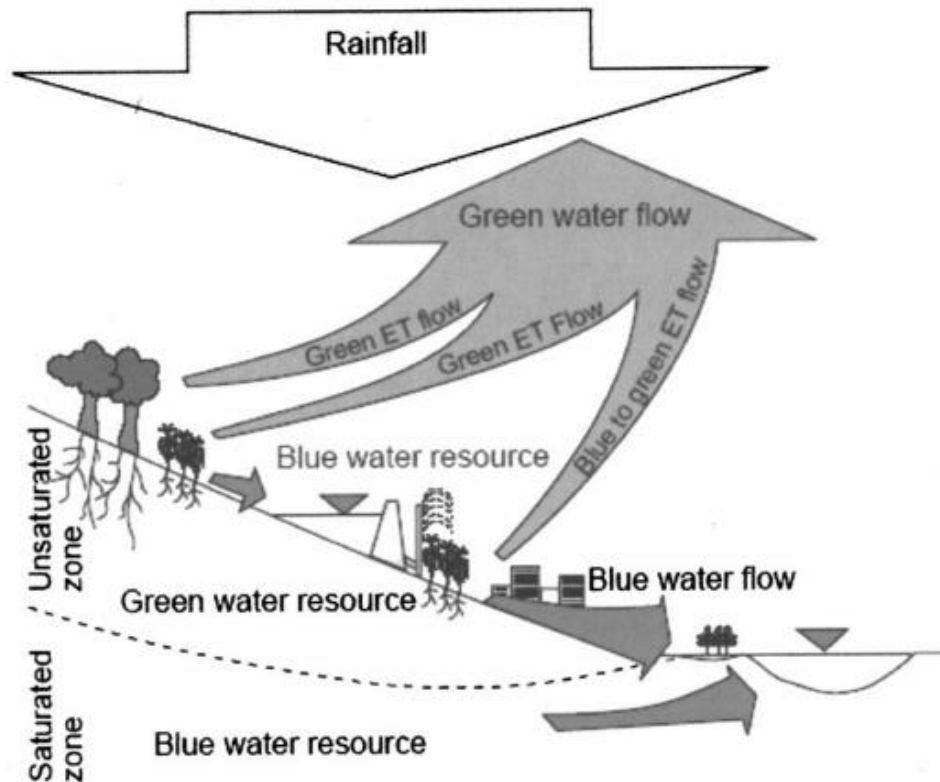


Figure 1-9. Conceptualization of a widened green-blue approach to water-resource planning and management. (Source: [Falkenmark and Rockstrom, 2006])

**Green water resources:** Precipitation as undifferentiated freshwater resource, is partitioned in a Green-water resource as moisture in the unsaturated zone [Falkenmark and Rockstrom, 2006]. In other word, Green water (productive green water) can describe as water that located in the soil moisture that transpires through crops and vegetation since this water is available for crop productivity and vegetation [Foster and Perry, 2009]. This water is in the unsaturated zone and readily available for consumptive use by crops.

Green water is typically associated with crop production under rainfed conditions and constitutes bulk of the water used by croplands. Siebert and Döll [2009] used an “Effective Precipitation ( $P_{eff}$ )” to compute green water use of crops, where effective rainfall refers to that portion of rainfall that can effectively be used by plants, that generate flows, as green-water

flow from terrestrial biomass producing systems in cropland area. In other words, Effective Precipitation is the fraction of the total precipitation as rainfall and snowmelt that is available to the crop and does not run off. Without detailed site-specific information, Effective Precipitation is very difficult to determine. Siebert and Döll [2002] use a simple approximation of Effective Precipitation which developed by U.S. Department of Agriculture Soil Conservation Method Smith [1992].

**Blue water resources:** Water in lakes, reservoirs, rivers, ice caps, and ground-water (saturated zone) are called “blue water”. Blue water is typically associated with crop production under irrigated conditions. Blue-water flow in rivers, through wetlands, and through base flow from groundwater [Falkenmark and Rockstrom, 2006] (figure 1-9).

The distinction between blue and white water has many implications for water management for food security. For instance, the lesser the blue water used for producing food the greater will be the water productivity and water use efficiency; however, the implications for the environment may not always be straightforward. The blue and green water metaphor has enhanced policy discussion regarding water scarcity and food security. In green water as most sustainable water resources, strategies that improve green water management offer potential to enhance food production even in places with serious water scarcity issues [Rockstrom et al., 2009].

However, in Blue water resources has the level of sustainability which derived from each type of blue water (figure 1-10). The one of blue water resource that had become global issues is groundwater. Groundwater is water source for irrigation without any conjunctive use and is usable, accessible, and locally available. This condition would overestimate groundwater use in several areas. There are some areas are the ones that had confirmed by Postel et al. [1999] where there has been excessive use of groundwater in areas such as the high plain aquifer in the US, Punjab in PAKISTAN-INDIA, and North China plain in China.

Excessive use of groundwater can disrupt the sustainability of the water balance in soils. World Resource Institute [2015] estimate that 54% of Indian territory faces high and extremely high water stress followed by decreasing groundwater levels. The use of glaciers to irrigate agriculture fields such as in the Punjab region of Pakistan [Piracha and Majeed, 2011] can also be one of the regional issues in the South Asia region, and if the use is inappropriate, that can lead to regional disasters in the region.

### Water Demand of Cropland originates from:

- Effective Precipitation (Green Water)
- Irrigation (Blue Water)
  - River
  - Reservoir
  - Lake/Wetland
  - Aqueduct
  - Aquifer
  - Glacier

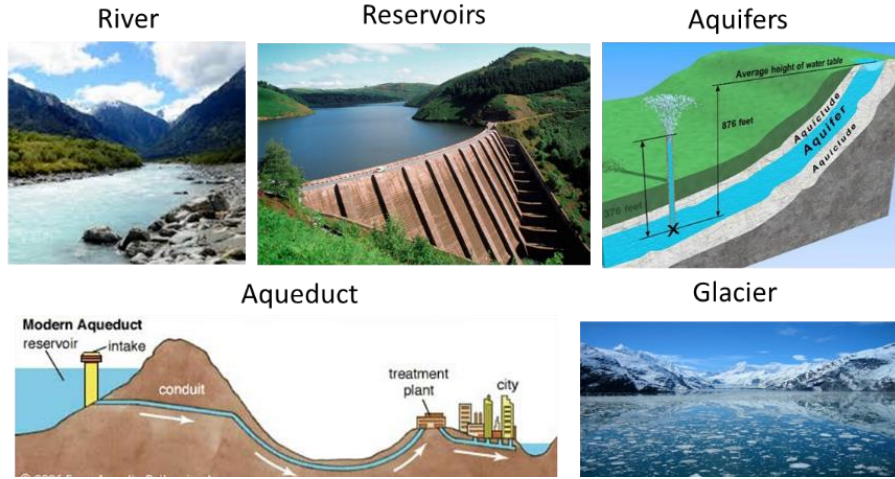
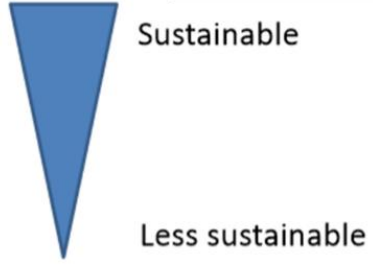


Figure 1-10. Source of Global Cropland Water Demand: Blue and Green.  
 (Source: [Falkenmark and Rockstrom, 2004])

## 1.2 Statement of the problem

Based on current issues, the year of MDGs period (2001-2015) is the year that has significant reduction in hunger because of the increase of food production. However, a distinct effect of climate change that leads to the decrease in food production also happened in this period. Crop activity that resembles the food productivity was facing a dynamic change during this MDGs period. Understanding the cause of dynamic change in cropping activity in the MDGs period become important as it will give the lesson to the future food security.

Based on the above explanation, there are four big problems that elaborated in this study. The four big problems are:

1. The high discrepancy between global land cover (GLC) product in cropland class. Moreover, there is no previous GLC dataset comparison that considered data collection time and used similar two-year term GLC datasets (year 2005 and 2010).
2. There are no such datasets that describe the distribution of rice paddy globally in the last fifteen years. Moreover, there is limited information in cropping pattern change phenomena of rice paddy, especially in multi-cropping intensity area.
3. There is no information regarding cropping calendar and cropping intensity that can explain the phenomena of cropping intensity change and sowing month change in the last fifteen years
4. There is no available product of irrigation water demand estimation that uses high resolution, consistent, and latest data input.

### 1.3 Objective of the study

In this study our objective is to estimate long-term IWD from 2001 to 2015 at a spatial resolution of 1 km in the global scale. Figure 1-11 show overall study. To achieve the main goal, we divide the main goal into four specific goals:

1. To integrate the combined cropland classes from current GLC datasets to produce a 1 km cropland agreement level (CAL) analysis through two main processes of dataset harmonization and pixel comparison.
2. To develop dominant cropping pattern (CP) of rice and non-rice by combination of MODIS NDVI (optic) and AMSR LSWC (microwave).
3. To develop long-term sowing month from 2001 to 2015 at a spatial resolution of 1 km in the global scale.
4. To develop crop coefficient based on the integration of cropland agreement level, cropping intensity, sowing month and cropping pattern with CROPWAT empirical model.
5. To Produce 1 km high resolution of 15-year global Irrigation water demand by integrating various remote sensing datasets.

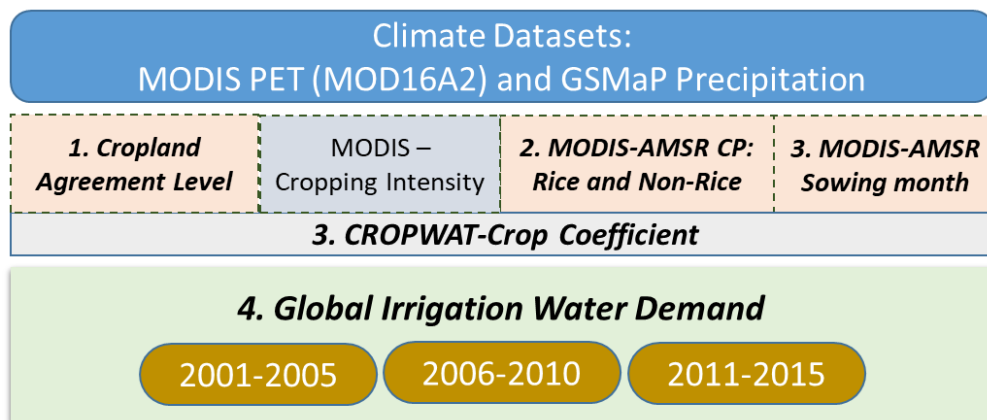


Figure 1-11. Overall studies of four objective for developing global irrigation water demand based on long-term remote sensing data integration

## 1.4 Originality of study

- The presented cropland agreement level (CAL) analysis, to our knowledge is the first study to compare the four current versions of GLC datasets (ESA CCI-LC, GlobCover, GLCMNO and MODIS LC) that were focused on worldwide cropland classes while taking into consideration data collection time.
- The presented MODIS-AMSR sowing month and dominant cropping pattern of rice and non-rice, to our knowledge are the first satellite-based products which derived from integration of vegetation and water index phenology that can analyze dynamic change of global sowing month and cropping pattern in multi cropping intensity area.
- The presented 1 km global irrigation water demand product are the first satellite-based products which derived from climate and crop remote sensing datasets that can analyze 15 years' dynamic change of water demand in agriculture sector, which developed by integrating consistent and latest remote sensing data input.

Figure 1-12 shows the summarize of detail flowchart for three original products in this study. 1. Cropland agreement level development, 2. Sowing month and cropping pattern development and 3. Irrigation water demand development.

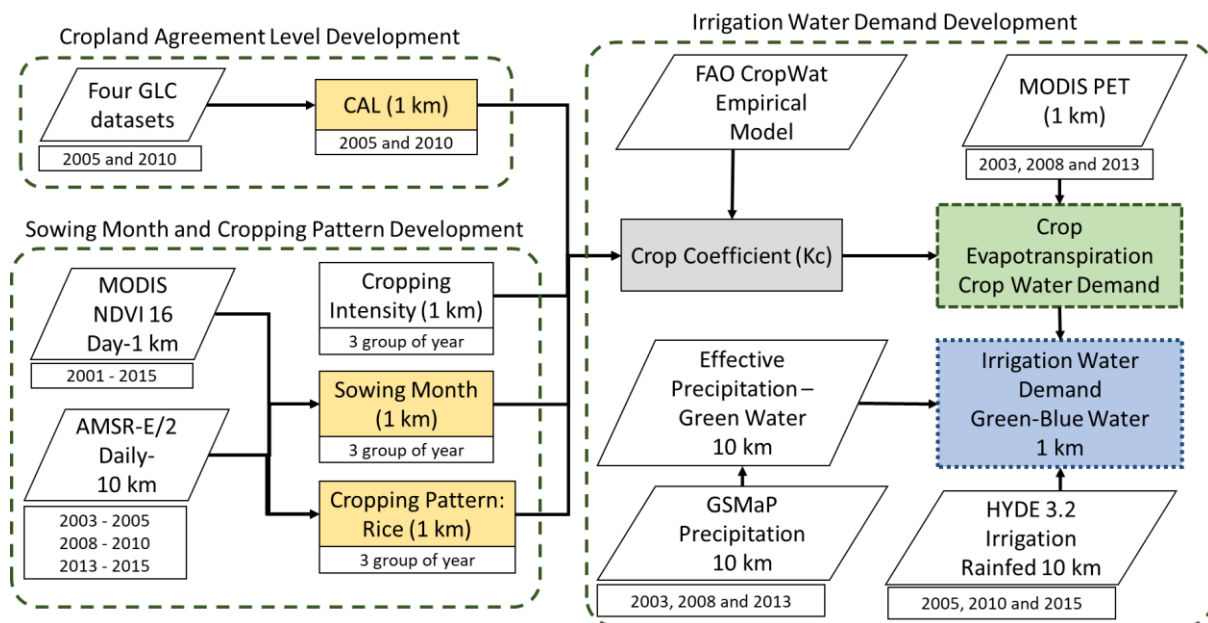


Figure 1-12. Shows overall flowchart from three original products in this study.

## Chapter 2 REVIEW LITERATURE

### 2.1 Global Land Cover Datasets

Over the last two decades, many institutions have published different global land cover (GLC) datasets that provide cropland class information. Since the first one released in 1993, the trend in the improvement of the production of GLC datasets has been in an increase of spatial resolution and accuracy [Grekousis, et al., 2015]. However, each GLC dataset has a different production year, data input method, classification technique, class definition and accuracy distribution value [Fritz et al.,2008; Ran et al., 2010]. These datasets are released as independent datasets, which make them incomparable, especially for a multitemporal analysis [Bai et al., 2004].

To evaluate the differences between each GLC dataset, researchers have tried to analyze land cover class agreement using a relative pixel comparison approach. The results of this kind of analysis produce a spatial agreement analysis that is effective for determining regions with levels of high confidence as a reference [Giri et al., 2005; Trsendbazar et al., 2015]. Previous pixel comparison analyses were carried out by comparing GLC datasets, which does not take into consideration when the data was collected. This condition makes the differences that result from a comparison analysis ambiguous as the differences may be a result of real physical changes to the cropland area during that period of time (not because of the different characteristics or classification system of the dataset). Therefore, the method for selecting GLC datasets for a comparison analysis must be reliable and consider time.

### 2.2 Irrigation Water Demand

Irrigation water demand (IWD) defined as the amount of water that must be applied to the crop to achieve the optimal growth [Doell and Siebert, 2002]. To estimate the IWD, previous studies are dominantly using global hydrological model. This model is using two main input, climate and crop coefficient. For the climate input, there are two data category which are evapotranspiration and precipitation. For the crop coefficient, there are three data category which are crop intensity (CI), crop calendar (CC), and crop type.

Previous studies are using this kind of model. However, different study using different

source of datasets for the input. This condition gives different result of estimation that cause discrepancy. Besides, the data input also using the old datasets. Hence, those studies produce low resolution products of 50 km. The low resolution product leads to the difficulties in country level analysis. Figure 2-2 summarize the input data used in previous studies.

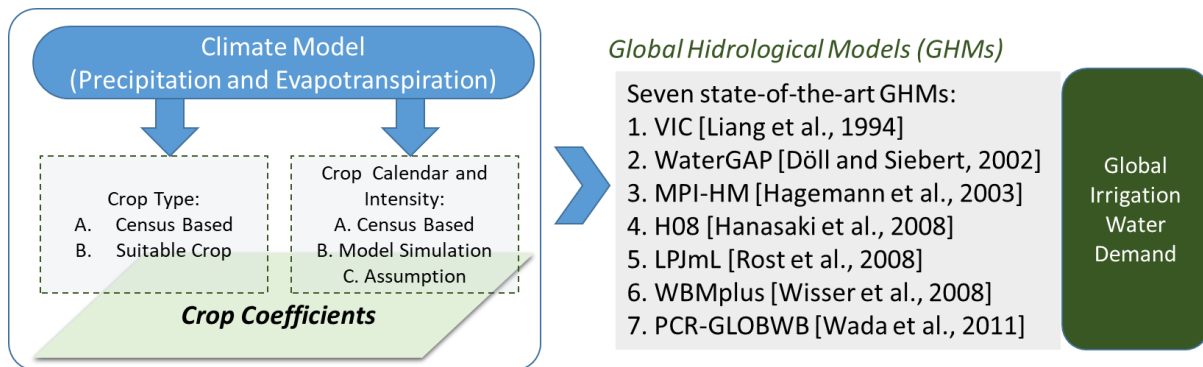


Figure 2-2. General concept of previous Irrigation water demand estimation

Table 2-1. Previous studies of irrigation water demand products

| Reference               | Year baseline  | Blue Water use by Irrigated Crop<br>km <sup>3</sup> /yr | Green water use by Irrigated crop<br>km <sup>3</sup> /yr | Green water use by rainfed crops<br>km <sup>3</sup> /yr | Total water use by Irrigated-rainfed crop<br>km <sup>3</sup> /yr | Spatial resolution |
|-------------------------|----------------|---|--|---|--|--------------------|
| Postel [1998]           | 1995           |   |  |   | 7,500  |                    |
| Doll and Siebert [2002] | Avg. 1961–1990 | 2,452   |  |   |  | 0.5°               |
| Hanasaki et al. [2006]  | Avg. 1987–1988 | 2,254   |  |   |  | 0.5°               |
| Falkenmark [2006]       | 1950-2000      | 1,800   |  | 5,000   | 6,800  | 0.5°               |
| Rost et al. (2008)      | Avg. 1971–2000 | 2,555   |  |   |  | 0.5°               |
| Siebert and Doll [2009] | Avg. 1998–2002 | 1,180   | 919  | 4,586   | 6,685  | 0.0083°            |
| Hanasaki et al. [2010]  | Avg. 1985–1999 | 1,530   |  |   |  | 0.5°               |
| Sulser et al. [2010]    | 2000           | 3,128   |  |   |  |                    |
|                         | 2025           | 4,060   |  |   |  |                    |
|                         | 2050           | 4,396   |  |   |  |                    |
| Wada et al. [2011]      | Avg. 1958–2001 | 2,057   |  |   |  | 0.5°               |
| Pokhrel et al. [2012]   | 1983–2007      | 2,158   |  |   |  | 0.5°               |
|                         | 2000           | 2,462   |  |   |  | 1°                 |

There are various approaches used to estimate and stimulate the global CC and CI. MIRCA2000 [Portmann et al., 2010] collected the census-based information of global CC using in 2000-year baseline. Other CC product, WAHA12 [Waha et al., 2012], simulated the growing period of dominant crop using H08 model simulation. SACRA product [Kotsuki et al., 2015] estimated weeks of crop sowing and harvesting by combining satellite drive SPOT NDVI product and census based datasets. The problems that were faced in all previous studies are only represent one-year data product, produced in coarse pixel resolution and high discrepancy among CC data products. CC product derived from simulation model by Zabel et al. [2014], can analyze its changes in 100 years' long-term, otherwise the product was based on crop suitability model and not based on real ground condition.

Table 2-2. Previous input data products which used for global irrigation water demand estimation

| Variable input        | Existing input data products  |
|-----------------------|---|
| 1. Evapotranspiration | 1. SLSCP [Meeson et al., 1995], 2. CRU TS 1.0 [New et al., 2000], 3. CRU TS 2.1 [Mitchel, 2005], 4. JRA-25 [Kim et al., 2009] , 5. MIROC-ESM-CHEM [Weedon et al., 2011]   |
| 2. Precipitation      |   |
| 3. Crop Type          | 1. Rice and non-Rice FAO [Döll and Siebert, 2002], 2. 18 crops [Leff et al., 2004], 3. 20 crops [You et al., 2006], 4. Multiple crop type [Monfreda et al., 2008] , 5. MIRCA 26 crops [Portmann et al. 2010].   |
| 4. Crop Intensity     | 1. Optimal growth, 2. FAO stat Regional level [FAO,1995], 3. SWIM model [Krysanova et al.,1998], 4. Assumption: Temperature and Precipitation [Doell Siebert, 2002], 5. Simulate a cropping calendar by H08 [Hanasaki et al.,2008], 6. MIRCA [Portmann et al. 2010], 7. |
| 5. Crop calendar      | Zabel Crop Suitability [Zabel et al., 2014], 8. SACRA product [Kotsuki et al., 2015]  |

## Chapter 3

### DEVELOPMENT OF GLOBAL CROPLAND AGREEMENT LEVEL

#### 3.1 Background

Global trends of the last 25 years show that for the developing world as a whole, the share of undernourished people among the total population has decreased significantly. Some important factors that have affected this reduction have been stability in economic growth and the massive development of irrigation systems, which have caused an escalation in agricultural productivity [FAO, 2015]. Sustainable development goals (SDGs), as part of the development of a global pledge, are targeting to eradicate hunger by 2030 and ensure sustainable food production systems [FAO, 2016]. To achieve this target, the availability of accurate information about global and regional cropland distribution that can be monitored periodically is becoming important for the construction of strategies for achieving food sustainability targets [See et al., 2015]. Satellite-derived cropland dataset can be one alternative source of information since it directly correlates with food resource distribution [Leff et al., 2004] and water requirements [Doll and Siebert, 2002].

The goal of this research was to integrate the combined cropland classes from current GLC datasets to produce a 1 km cropland agreement level (CAL) analysis and its changes (year 2005 and 2010) through two main processes of dataset harmonization and pixel comparison. This study also focused on analyzing the potential use of a cropland agreement level for cropland area estimate and cropland change phenomena.

The presented model of cropland agreement was, to our knowledge, the first study to compare the four current versions of GLC datasets (GlobCover, MODIS LC, GLCNMO and ESA CCI LC) that were focused on worldwide cropland classes while taking into consideration data collection time. There was no previous GLC dataset comparison [McCallum et al., 2006] [Nakaegawa, 2011] that considered data collection time and used similar two-year term GLC datasets. It was the first study to estimate total cropland area on a national level by converting the levels of agreement into percentage values using a correlation model between the CAL analysis and an IIASA cropland fraction map.

## 3.2 Material

### 3.2.1 Global Land Cover (GLC) datasets

During this study, we explored all existing GLC datasets in the low spatial resolution category (300–1,000 m) and distributed those GLC datasets according to data collection time. After distributing the GLC datasets on a timeline, we grouped the data based on the proximity of data collection time and got five groups of GLC datasets. Figure 3-1 shows the five groups of data in the timeline of GLC datasets. This grouping strategy made those datasets more comparable for pixel comparison and integration analysis. Within each group, the maximum difference in data collection time was two years. The reason for setting two years as the maximum time difference was to minimize any extreme changes that could occur in cropland fields over long periods.

To create this CAL analysis, the GLC datasets were put through two processes, which were a harmonization and pixel comparison. In the harmonization process, we standardized the analysis depth for all GLC datasets within five groups. Those five groups consisted of 14 GLC datasets from the seven GLC dataset versions listed below:

- (1) IGBP GLCC v 2.0 (1993 dataset) using the International Geosphere-Biosphere Programme (IGBP) classification system produced by the United States Geological Survey (USGS) [Loveland et al., 2000];
- (2) UMD (1993 dataset) using the simplified IGBP classification system developed by the University of Maryland [Hansen et al, 2000];
- (3) GLC2000 (2000 dataset) using the Land Cover Classification System (LCCS) of Food and Agricultural Organizations (FAO) generated by the European Commission's Joint Research Center (EC-JRC) [Bartholomé et al., 2005];
- (4) GlobCover V 2.2 and V 2.3 (2005 and 2009 datasets) using the FAO LCCS created by the European Space Agency (ESA) [Bontemps et al., 2009];
- (5) MODIS LC MCD12Q1 collection 5.1 (2001, 2005, 2010 and 2013 datasets) using the IGBP classification system produced by Boston University [Friedl et al., 2010];
- (6) GLCMNO V.1 and V.2 (2003 and 2008 datasets) using the FAO LCCS created by Chiba University [Tateishi et al., 2011; Tateishi et al., 2014];
- (7) ESA CCI-LC v 2.5 (2000, 2005 and 2010 datasets) using the FAO LCCS generated by the ESA [ESA, 2014], in 2017 ESA CCI have published maps from 1993 -2015 that can be

useful for long year monitoring of land cover change.

For the pixel comparison process, we used datasets from the 2005 and 2010 groups from the same GLC dataset versions. These GLC datasets were the ESA CCI LC, GlobCover, MODIS LC and GLCMNO datasets. The same GLC datasets from each group were paired to produce two CAL analyses for further analysis of cropland change. Table 3-1 shows the characteristics of each of the GLC datasets in the 2005 and 2010 groups that were used in the pixel comparison process.

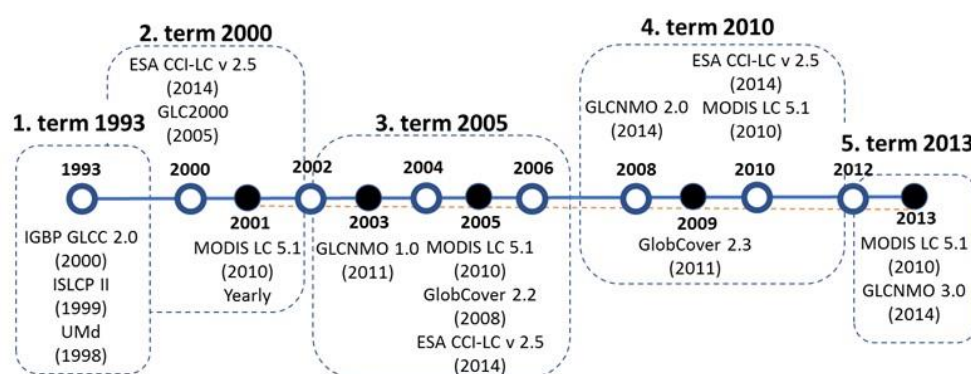


Figure 3-1. Timeline of the GLC datasets in five groups of data

Table 3-1. Characteristics of the four GLC datasets used in the pixel comparison analysis.

| Dataset name            | Data provider                    | Satellite sensor     | Spatial resolution | Time of data collection  | Projection/ Datum            | Input data  | Classification technique                                       | Classification scheme | Data for Validation                     |
|-------------------------|----------------------------------|----------------------|--------------------|--------------------------|------------------------------|---|--|-----------------------|---|
| <b>GLOBCOVER</b>        |                                  |                      |                    |                          |                              |   |  |                       |   |
| GlobCover 2005 v 2.2    | ESA, MEDIAS-France               | Envisat (MERIS)      | 300 m (1/360)      | December 2004- June 2006 | Plate-Carrée                 | MERIS L1B data                                    | Unsupervised classification                                    | FAO LCCS / 22 Classes | SPOT-VEG NDVI, and Google Earth         |
| GlobCover 2009 v 2.3    | ESA, Univ. Catholique de Louvain |                      |                    | January-December 2009    |                              | MERIS FR mosaics (13 Spectral bands)              | Classification using local/regional expertise                  |                       |   |
| <b>MODIS LC MCD12Q1</b> |                                  |                      |                    |                          |                              |   |  |                       |   |
| MODIS LC (v.5.1)        | Boston University, NASA          | Terra Aqua (MODIS)   | 500 m (1/240)      | Yearly since 2001-2013   | MODIS sinusoidal WGS1984     | MODIS L2 L3, MODIS 16day EVI, MODIS 8day LST, DEM | Supervised classification using decision tree, neural networks | IGBP / 17 Classes     | High resolution land cover information  |
| <b>GLCNMO</b>           |                                  |                      |                    |                          |                              |   |  |                       |   |
| GLCNMO 2003(v.1)        | GSI Japan, Univ. Chiba, ISCGM    | Terra Aqua (MODIS)   | 1000 m (1/120)     | January-December 2003    | Geographic (lat-lon) WGS1984 | 500-m MODIS 16-day, Landsat ETM+, DMSO-OLS        | Supervised classification                                      | FAO LCCS / 20 Classes | Google Earth and regional existing maps |
| GLCNMO 2008 (v.2)       |                                  |                      | 500 m (1/240)      | January-December 2008    |                              |   |  |                       |   |
| <b>ESA CCI-LC v 2.5</b> |                                  |                      |                    |                          |                              |   |  |                       |   |
| CCI-LC 2005             | ESA                              | MERIS Full, SPOT VGT | 300 m (1/360)      | 2003-2007 epoch          | Geographic (Lat-lon) WGS1984 | MERIS 10-year LC map as baseline SPOT-VGT         | Unsupervised classification                                    | FAO LCCS/ 22 classes  | 2600 Primary Sampling Units             |
| CCI-LC 2010             |                                  |                      |                    | 2008-2012 epoch          |                              |   |  |                       |   |

This study used a relative accuracy assessment, which was the use as a reference of another dataset that was considered to use accurate datasets. We explored the reference data in order to convert agreement levels into percentage values. As reference data, a 1 km global IIASA-IFPRI cropland percentage map with a 2005 baseline year [Fritz et al., 2015] was developed by integrating a number of individual global and regional cropland maps. This IIASA-IFPRI cropland percentage map was validated by high-resolution satellite imagery via Geo-Wiki (<http://www.geo-wiki.org>) [Fritz et al., 2009] with an overall accuracy result of 82.4%. The reason for choosing the IIASA data was because this dataset was a recent one that gave a highly accurate overview of cropland area distribution in percentage values.

### **3.3 Methods**

#### **3.3.1 Pixel Comparison Using CRISPS Approach**

To achieve the study's first goal, there were two main methods for producing the CAL analysis, which were the harmonization and pixel comparison processes. The different characteristics and classification systems for each dataset made these two processes important for getting reliable CAL analysis results. During the harmonization process, we standardized all GLC datasets to produce comparable cropland classes for the pixel comparison process. The result of the cropland harmonization process was evaluated by comparing the result to each group. A balanced distribution verified that the data was standardized and comparable. Finally, datasets within the same group were overlaid using the CRISPS approach for a pixel comparison processes to produce the CAL analysis. As the fourteen GLC datasets from each group had different mapping standards, we applied the following cross-walking methods to get comparable products:

#### **3.3.2 Re-projection**

To facilitate different projections, these data sets were co-registered and re-projected to a geographic (latitude-longitude) image with map datum WGS 84, which is a pseudocylindrical equal-area map projection [See et al., 2015]. This projection has been used in many GLC datasets. ESA CCI-LC, GlobCover and GLCNMO are GLCs that have used this projection. Its

use was also supported by the use of this projection system in similar studies of GLC datasets comparisons [Jung et al, 2006].

### 3.3.3 Rescaling Analysis

The resampling process had an important role in standardizing the different pixel resolutions of the GLC datasets because during the comparison process the GLC datasets needed to have the same pixel size. Different rescaling processes were a special concern in this study as a mistake in the resampling process could have caused changes in the class area. When considering the goals of this study, which was to resample all GLC datasets to a 1 km resample target, this study attempted to adopt and combine some important parts of the resampling process from another study with an aim of minimizing errors from the resampling process.

For the cropland rescaling process, we used two resampling processes, which were the nearest neighbor and maximum area methods. We used these two techniques because both would not change the value of cells. For datasets that have coarser resolutions, direct resampling using the nearest neighbor method might have caused a non-ignorable disagreement between the original and the rescaled dataset [Bai et al., 2014]. This is based on the fact that the footprint of the sensor is not at the same location during each revisit [Tchuenté, 2011]. The maximum area method, however, has been proven a more powerful approach for aggregating discrete land cover data [ Zhang et al., 2013]. Furthermore, it also tends to give a smoother result than the nearest neighbor method because the new value resulting from this approach is obtained based on the most common values around the pixel. The GLC datasets that already have a 1 km resolution did not need a rescaling process, which minimized the changes from resampling the results data [Tchuenté, 2011].

Taking into consideration the facts from this previous explanation, the steps that were taken in the rescalling process during this study were as follows: (i) Global land cover datasets that have a large resolution, such as the GlobCover and ESA CC-LC (300 m), MODIS LC (500 m), and GLMNO 2008 V.2 (500 m) datasets, were resampled on a grid with a 250 m resolution using the nearest neighbor method. (ii) After that, the entire GLC 250 m grid was aggregated using a majority area method to 1 km for all datasets. (iii) For GLMNO 2003 v1 since they were already in a 1 km spatial resolution, the datasets were kept in their original resolution without a rescaling process.

### 3.3.4 Legend Harmonization

For this study, legend harmonization played a crucial role because the focus of this study was on analyzing cropland classes among several GLC datasets. Differences in the definitions and characteristics of each class correlating with the cropland in each individual GLC would produce ambiguities among the comparisons of the GLC datasets. To overcome this problem, we evaluated all the classes used by the different GLC datasets and then analyzed those classes to determine how they correlated with a standardized cropland classification system, which was the Land Cover Classification System (LCCS). The rationale for choosing LCCS rather than IGBP was: (i) LCCS was developed after an analysis of existing relevant FAO nomenclature documents [26] that can explain some categories of cropland classes in detail. (ii) MODIS LC v 6, one of the GLC products that use IGBP, would soon change to LCCS with their next dataset [Friedl et al., 2010].

One step in the legend harmonization process was to convert the original class numbers to LCCS-labels. Table 3-2 shows the conversion results for some of the original class numbers to cropland LCCS-labels. The class definition followed the LCCS hierarchy based on the dichotomous phase and the modular-hierarchical phase [Di Gregorio, 2016]. As in Table 3-2, the cropland class of the MODIS LC, LCCS-label is “A11-A3”. A11 is the dichotomous phase of “Cultivated and Managed Land” and A3 is the modular-hierarchical phase of “Herbaceous Crop”. The fact that the original class descriptions from the GLC datasets had a great impact on choosing the type of dichotomous phase and modular-hierarchical phase, we adopted the descriptions of the original classes from the GLC datasets from a previous study [Herold et al., 2006; Pflugmacher et al., 2011]. For this conversion, we grouped all classes that correlate with cropland into a new cropland class, including mosaic vegetation cropland that had a smaller cropland percentage when compared to vegetation. Since all the GLC datasets in the five year groups would be harmonized for comparison proposes, Table 3-2 shows information about the type of class that was categorized as “cropland” based on the LCCS-label conversion status of seven GLC datasets.

Table 3-2. The conversion results for the original cropland classes converted to LCCS-labels for all GLC

| Global Land Cover Datasets                              | LCC Level    | LCC Label   |
|---|--------------|---|
| <b>A. MODIS LC (IGBP)</b>                               |              |   |
| Croplands (12)  | A11-A3       | Herbaceous Crop(s)  |
| Cropland/ Natural Vegetation Mosaic (14)                | A11-A3       | Herbaceous Crop(s)  |
|   | A12          | Natural and Semi-natural Primarily Terrestrial Vegetation |
| <b>B. GLCNMO (LCCS)</b>                                 |              |   |
| Cropland (11)   | A11-A3       | Herbaceous Crop(s)  |
| Paddy field (12)  | A11-A4.A5    | Graminoid Crops //Non-Graminoid Crops                     |
| Cropland /Other Vegetation Mosaic (13)                  | A11          | Cultivated and Managed Terrestrial Area(s)                |
|   | A12          | Natural And Semi-Natural Primarily Terrestrial Vegetation |
|   | A23          | Cultivated Aquatic or Regularly Flooded Area(s)           |
| <b>C. GlobCover (LCCS)</b>                              |              |   |
| Post-flooding or irrigated croplands (11)               | A11-A1XXXXD3 | Irrigated Tree Crop                                       |
|   | A11-A2XXXXD3 | Irrigated Shrub Crop                                      |
|   | A11-A3XXXXD3 | Irrigated Herbaceous Crop                                 |
|   | A11-A3XXXXD2 | Post Flooding Herbaceous Crop                             |
| Rainfed croplands (14)                                  | A11-A2XXXXD1 | Rainfed Shrub Crop  |
|   | A11-A1XXXXD1 | Rainfed Tree Crop   |
|   | A11-A3XXXXD1 | Rainfed Herbaceous Crop                                   |
| Mosaic cropland/vegetation (20)                         | A11          | Cultivated and Managed Terrestrial Area(s)                |
|   | A12          | Natural and Semi-natural Primarily Terrestrial Vegetation |
| Mosaic vegetation/ cropland (30 )                       | A12          | Natural and Semi-natural Primarily Terrestrial Vegetation |
|   | A11          | Cultivated and Managed Terrestrial Area(s)                |
| <b>D. ESA CCI-LC (LCCS)</b>                             |              |   |
| Cropland, rainfed (10)                                  | A11-A2XXXXD1 | Rainfed Shrub Crop  |
|   | A11-A1XXXXD1 | Rainfed Tree Crop   |
|   | A11-A3XXXXD1 | Rainfed Herbaceous Crop                                   |
| Cropland, irrigated or post-flooding (20)               | A11-A1XXXXD3 | Irrigated Tree Crop                                       |
|   | A11-A2XXXXD3 | Irrigated Shrub Crop                                      |
|   | A11-A3XXXXD3 | Irrigated Herbaceous Crop                                 |
|   | A11-A3XXXXD2 | Post Flooding Herbaceous Crop                             |
| Mosaic cropland (>50%) / natural vegetation (<50%) (30) | A11          | Cultivated and Managed Terrestrial Area(s)                |
|   | A12          | Natural and Semi-natural Primarily Terrestrial Vegetation |
| Mosaic natural vegetation (>50%) / cropland (<50%) (40) | A12          | Natural and Semi-natural Primarily Terrestrial Vegetation |
|   | A11          | Cultivated and Managed Terrestrial Area(s)                |

### 3.4 Result and Discussion

#### 3.4.1 Thematic Similarity

Following the M. C. Hansen and B. Reed [Hansen et al, 2000] strategy, we evaluated the harmonization results for the cropland classes by analyzing cropland pixel similarity in each dataset group. A successful result in the harmonization process would produce a balanced

proportion among the GLC datasets in the same groups of GLC data. Figure 3-2 shows the proportion of the cropland classes from the harmonization results and figure 3-3 shows the spatial distribution of harmonized cropland area.

In general, four out of five groups showed a balanced proportion of cropland classes. The subtraction value of the highest from the lowest percentage in each group were 7 %, 6 %, 6%, 8 %, 8 % for 2000, 2005, 2010 and 2013 group respectively. However, in the 1992 group, there was a large difference in cropland classes between UMd and GLCC of 38 %. The absence of mosaic agricultural classes in the UMd datasets was the cause of this difference [Hansen et al., 2000]. This shows that the differences in the goals and focus of an analysis caused conspicuous differences between cropland and vegetation by classifying more area as a vegetation class. This explanation shows that the harmonization result was acceptable especially for the 2005 and 2010 groups. So, both were eligible to be analyzed in the next step.

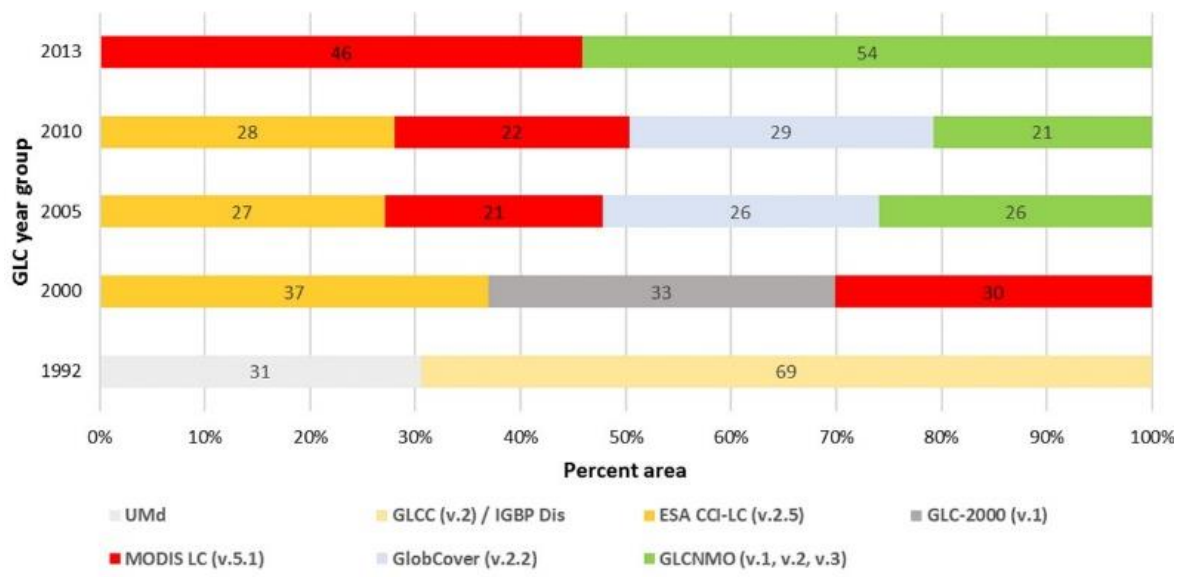


Figure 3-2 Proportion value of cropland analyses as the result of the harmonization of the five groups.

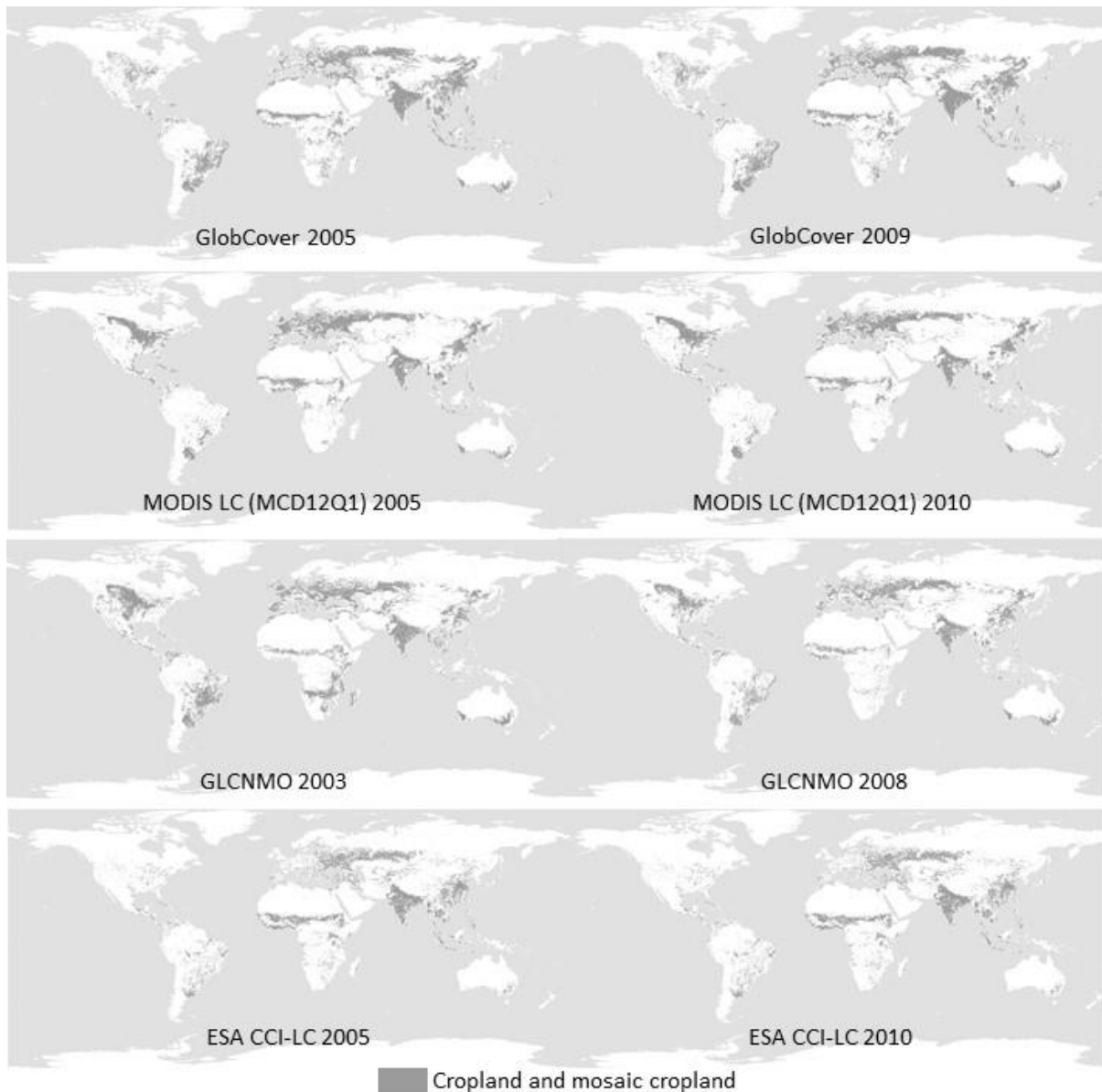


Figure 3-3. Spatial distribution of harmonized cropland area from four selected GLC datasets in the two year-groups of 2005 and 2010. Only groups of GLC datasets that are located within these two year-groups are used for the cropland class comparison process.

### 3.4.2 Cropland Level Agreement (CAL) Analysis

After assigning the harmonized dataset target and proving the balance proportion value, we compared and observed for pixel similarity within the four GLC datasets in the two year-groups by overlaying the datasets using the CRISPS approach, which is based upon cross-walking between classes [Bai et al., 2014]. Since we only focused on one cropland class (not analyzing multiple classes), utilizing a CRISPS approach that matches using one-to-one

mapping was sufficient [McCallum et al.,2006; See, et al.,2006]. Another technique is the Fuzzy approach, which can allow an overlap between legend definitions to be taken into consideration. It requires expert knowledge to quantify uncertainty in the classification and transition zones of boundaries [See, et al.,2006; Fritz, et al.,2005]. In the previous study explained by McCallum et.al [2006], the result of this pixel comparison technique could indicate an agreement level among these datasets.

The comparison result of these cropland classes produced four agreement levels, which in this study were also referred to as the Cropland Agreement Level (CAL) analysis. The four levels that were obtained from the CAL analysis in this study were as follows (Figure 3-4):

- Level 1; No agreement for pixels with a unique aggregated class in each data set
- Level 2; Low agreement for pixels where only two of the four data sets were in agreement
- Level 3; Medium agreement for pixels where three of the four data sets were in agreement.
- Level 4; Full agreement for pixels where all the five data sets within a pixel were in agreement.

Since we focused on analyzing cropland class similarity within four GLC datasets in two groups of data from 2005 and 2010, we produced two CAL analyses from those years.

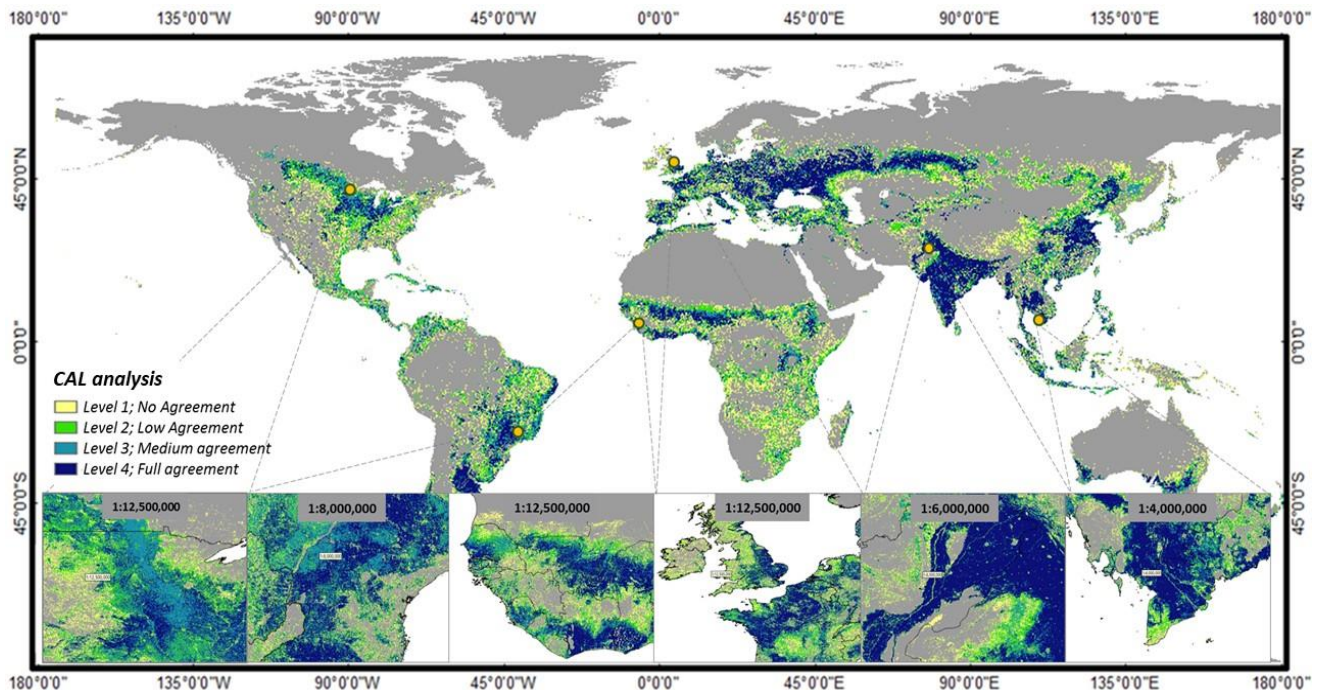


**Figure 3-4.** Cropland Agreement Level (CAL) analysis from 2005, based on pixel comparison analysis between four selected recent GLC datasets.

To study this CAL analysis more deeply, we divided the study area into seven test sites according to size. Those study areas were South America, North America, Europe, Africa, Australia, Russia and Asia. Table 3-3 shows the percentage calculation result for four CAL analysis levels for seven test sites. Four GLC datasets were used and the underlined value shows the highest percentage value whereas the bolded value shows the lowest percentage for the site area.

Comparison results for the seven sites in the two years of analysis showed that Europe was indicated as the area with highest full agreement level whereas Australia, Russia and Africa had the three highest no agreement level areas. A short time period for cultivation and a small cropland area combined with a large area of vegetation were the causes of a mix in cropland classes (Figure 3-5). This triggered different classification results in each GLC dataset. Besides this, there were also random changes in levels two and three of the 2005 and 2010 CAL analyses.

**Figure 3-5.** Comparison two different CAL model in 2005 and 2010 term, in Africa and Asia Continental.

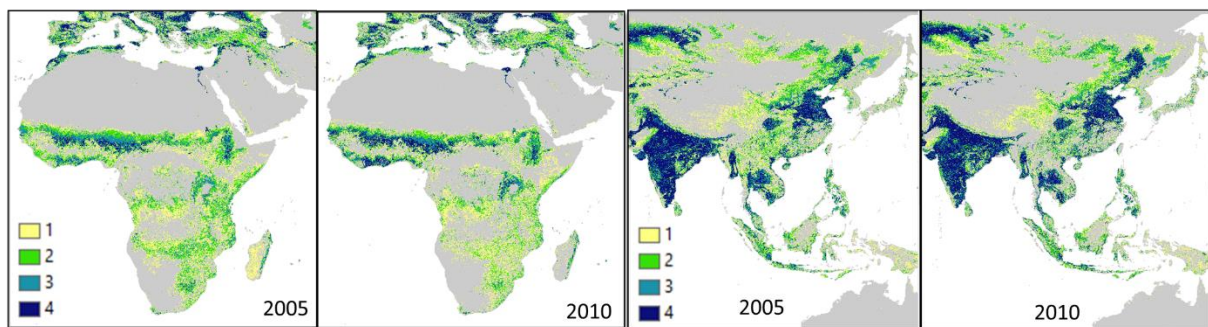


**Table 3-3.** Agreement percentage of the CAL analysis across the seven test sites in 2005 and 2010

| Test Sites    | No Agreement |             | 2 of 4 Agree |             | 3 of 4 Agree |             | Full Agreement |             |
|---------------|--------------|-------------|--------------|-------------|--------------|-------------|----------------|-------------|
|               | 2005         | 2010        | 2005         | 2010        | 2005         | 2010        | 2005           | 2010        |
| South America | 0.32         | 0.27        | 0.24         | 0.23        | <u>0.25</u>  | <u>0.24</u> | 0.19           | 0.26        |
| Nort America  | 0.44         | 0.32        | <u>0.26</u>  | <u>0.28</u> | 0.2          | 0.26        | 0.1            | 0.15        |
| Europe        | <b>0.21</b>  | <b>0.18</b> | 0.19         | <b>0.16</b> | 0.24         | 0.19        | <u>0.36</u>    | <u>0.47</u> |
| Africa        | 0.4          | 0.39        | 0.29         | 0.26        | 0.22         | 0.19        | 0.08           | 0.16        |
| Australia     | <u>0.6</u>   | <u>0.49</u> | <b>0.17</b>  | 0.21        | <b>0.17</b>  | 0.21        | <b>0.06</b>    | <b>0.09</b> |
| Russia        | 0.32         | 0.26        | 0.2          | 0.19        | 0.22         | <b>0.17</b> | 0.27           | 0.38        |
| Asia          | 0.33         | 0.27        | 0.21         | 0.2         | 0.19         | 0.19        | 0.27           | 0.34        |

### 3.4.3 Correlation Factor between CAL and Existing IIASA Cropland Fraction

To obtain a correlation model between the CAL analysis and cropland percentage, first we analyze the trend correlation between the CAL analysis with the original cropland classes from the four selected GLC datasets (Table 3-4). The dominant distribution of “cropland” classes (class numbers 10 and 20 for ESA CCI-LC, numbers 11 and 14 for GlobCover, numbers 11 and 12 for GLCNMO and number 12 for MODIS LC) is in level 4, compared with the “mosaic cropland” that is dominant in level 1 and level 2, indicating that the four levels in the CAL analysis correlate with the amount of actual cropland area in one pixel.

**Table 3-4.** The conversion results for the original cropland classes converted to LCCS-label for all GLC datasets

| GLC Cropland Classes (class number)                     | Cropland agreement level |         |         |         |
|---|--------------------------|---------|---------|---------|
|   | Level 1                  | Level 2 | Level 3 | Level 4 |
| <b>A. MODIS LC</b>                                      |                          |         |         |         |
| Croplands (12)  | 2.1                      | 7.4     | 18.3    | 34.3    |
| Cropland/ natural vegetation mosaic (14)                | 6.5                      | 10.6    | 11.7    | 9.0     |
| <b>B. GLCNMO</b>  |                          |         |         |         |
| Cropland (11)   | 12.5                     | 13.9    | 19.2    | 28.6    |
| Paddy field (12)  | 0.3                      | 0.3     | 0.7     | 2.2     |
| Cropland /other vegetation mosaic (13)                  | 6.4                      | 5.2     | 4.8     | 5.8     |
| <b>C. GlobCover</b>                                     |                          |         |         |         |
| Post-flooding or irrigated croplands (or aquatic) (11)  | 0.2                      | 0.5     | 1.4     | 5.7     |
| Rainfed cropland (14)                                   | 2.5                      | 4.3     | 8.4     | 14.8    |
| Mosaic cropland/vegetation (20)                         | 3.0                      | 4.9     | 7.8     | 10.9    |
| Mosaic vegetation/ cropland (30)                        | 6.5                      | 10.2    | 11.1    | 7.7     |
| <b>D. ESA CCI-LC</b>                                    |                          |         |         |         |
| Cropland, rainfed (10)                                  | 3.7                      | 11.4    | 22.3    | 27.3    |
| Cropland, irrigated or post-flooding (20)               | 0.4                      | 0.9     | 1.9     | 5.5     |
| Mosaic cropland (>50%) / natural vegetation (<50%) (30) | 1.9                      | 4.0     | 4.6     | 3.6     |
| Mosaic natural vegetation (>50%) / cropland (<50%) (40) | 3.1                      | 4.6     | 3.2     | 1.5     |

To investigate the meaning of each CAL analysis level in percentage values, we analyze the pixel correlation between the CAL analysis and the IIASA-IFPRI cropland percentage map by using a 2D Scatter Plot (Figure 3-5). Results show that level 4 of the CAL analysis mainly corresponds with 80% of cropland fraction and with the same approach, the following correlations were also obtained: level 3 with 40%, level 2 with 20% and level 1 with 10% (Table 3-6). Figure 3-6 shows a comparison between the CAL model and IIASA-IFPRI map using a 2D Scatter Plot. To estimate cropland area from the CAL analysis, the pixel area from each agreement level is multiplied by the correlation percentage.

**Table 3-5.** Correlation factor (percent) between CAL analysis and IIASA cropland fraction.

| CAL product | IIASA cropland fraction |      |      |      |      |      |      |      |      |      |
|-------------|-------------------------|------|------|------|------|------|------|------|------|------|
|             | 10%                     | 20%  | 30%  | 40%  | 50%  | 60%  | 70%  | 80%  | 90%  | 100% |
| Level 1     | 41.1                    | 25.5 | 16.4 | 11.1 | 7.9  | 4.7  | 2.5  | 2.3  | 4.9  | 16.4 |
| Level 2     | 34.4                    | 35.1 | 29.1 | 24   | 18.6 | 12.8 | 7.5  | 5.8  | 9.2  | 36.6 |
| Level 3     | 19.6                    | 28.1 | 34.6 | 37   | 35.1 | 31.6 | 25.6 | 19   | 21.7 | 27.5 |
| Level 4     | 5.0                     | 11.3 | 19.8 | 27.9 | 38.3 | 50.9 | 64.4 | 72.9 | 64.2 | 19.5 |
| Total       | 100                     | 100  | 100  | 100  | 100  | 100  | 100  | 100  | 100  | 100  |

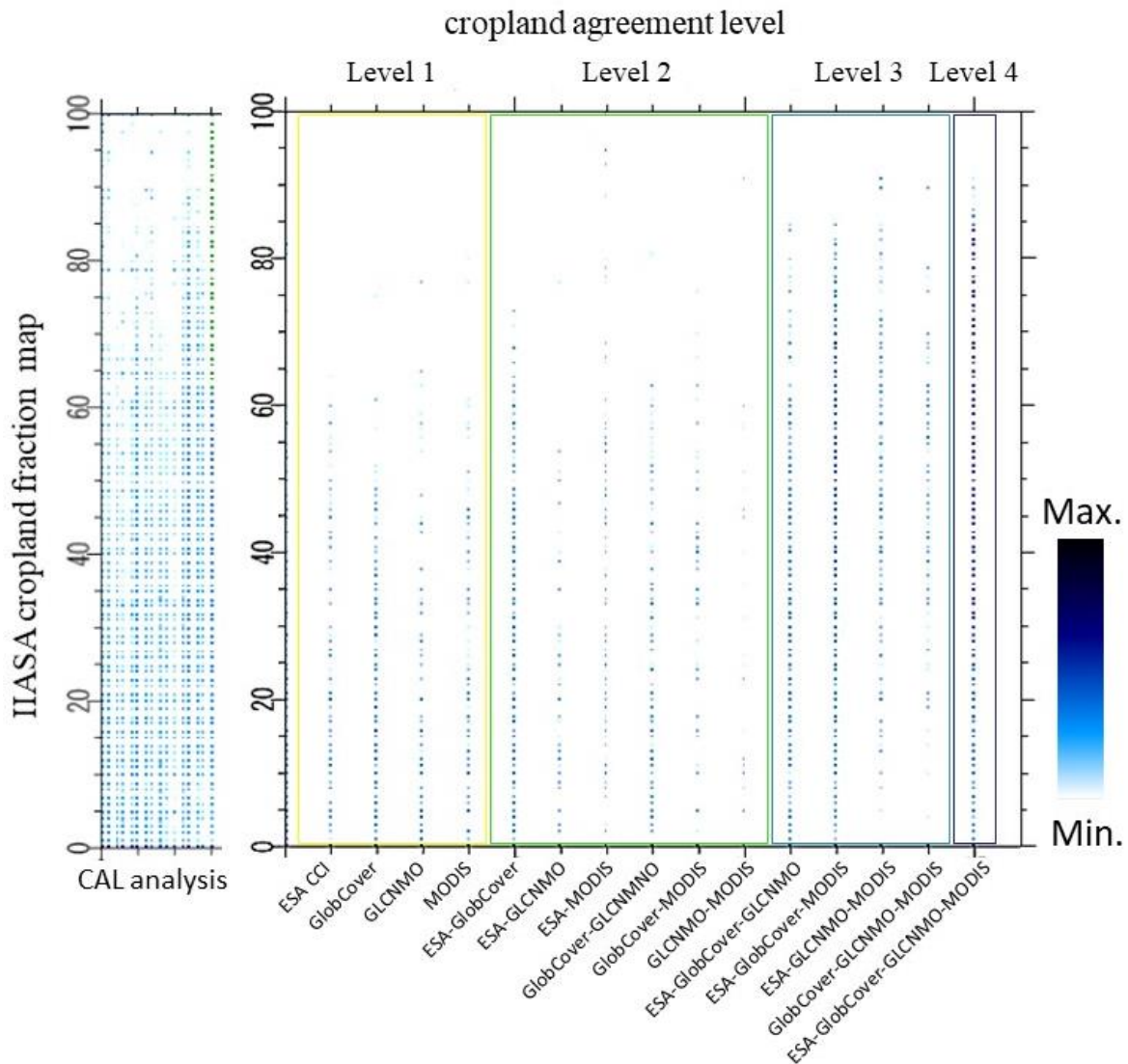


**Figure 3-6.** Comparison between the CAL analysis and IIASA cropland fraction using scatter plot

#### 3.4.4 Comparison of Cropland Area Estimates from the CAL with the FAO Data

To evaluate cropland estimation results on the national level, cropland areas derived from the CAL analysis are compared to the cropland area estimates from FAO-stat 2005 as a statistical data reference. Based on the definition from FAO statistics, cropland is defined as “arable land and permanent crops” [Vancutsem et al., 2013]. Overall correlation also is observed for 2005 and 2010 respectively and shows some proximity between the CAL analysis and the FAO with a 0.70 and 0.71 regression value (Figure 3-7).

We also analyze the accuracy of the four selected GLC datasets to FAO statistics. We divide countries into two groups based on the subtraction value of the cropland area. The groups are (i) small, which have a cropland area from 5,000 to 140,000 km<sup>2</sup>, and (ii) medium to large, which have cropland area from 180,000 to 1,700,000 km<sup>2</sup> (Figure 3-8). In this framework, the regression value and relative error to the FAO (%) have been observed as 0.574; 42.2 for small cropland area countries and 0.858; 29.8 for medium to large cropland area countries between FAO-stat and the CAL analysis (Table 3-6). Those values promote the CAL analysis as the most accurate dataset compared to FAO-stat within all datasets in estimating cropland area. Good correlation of the results to FAO statistics is still not enough for quality assessment of the product. To provide accurate validation it is worth to compare the product with some more precise country level cropland map which have higher resolution. Globland30 [Chen et al., 2014] and Unified Cropland layer [Waldner et al., 2016] as one of the alternative for the analysis in next study.

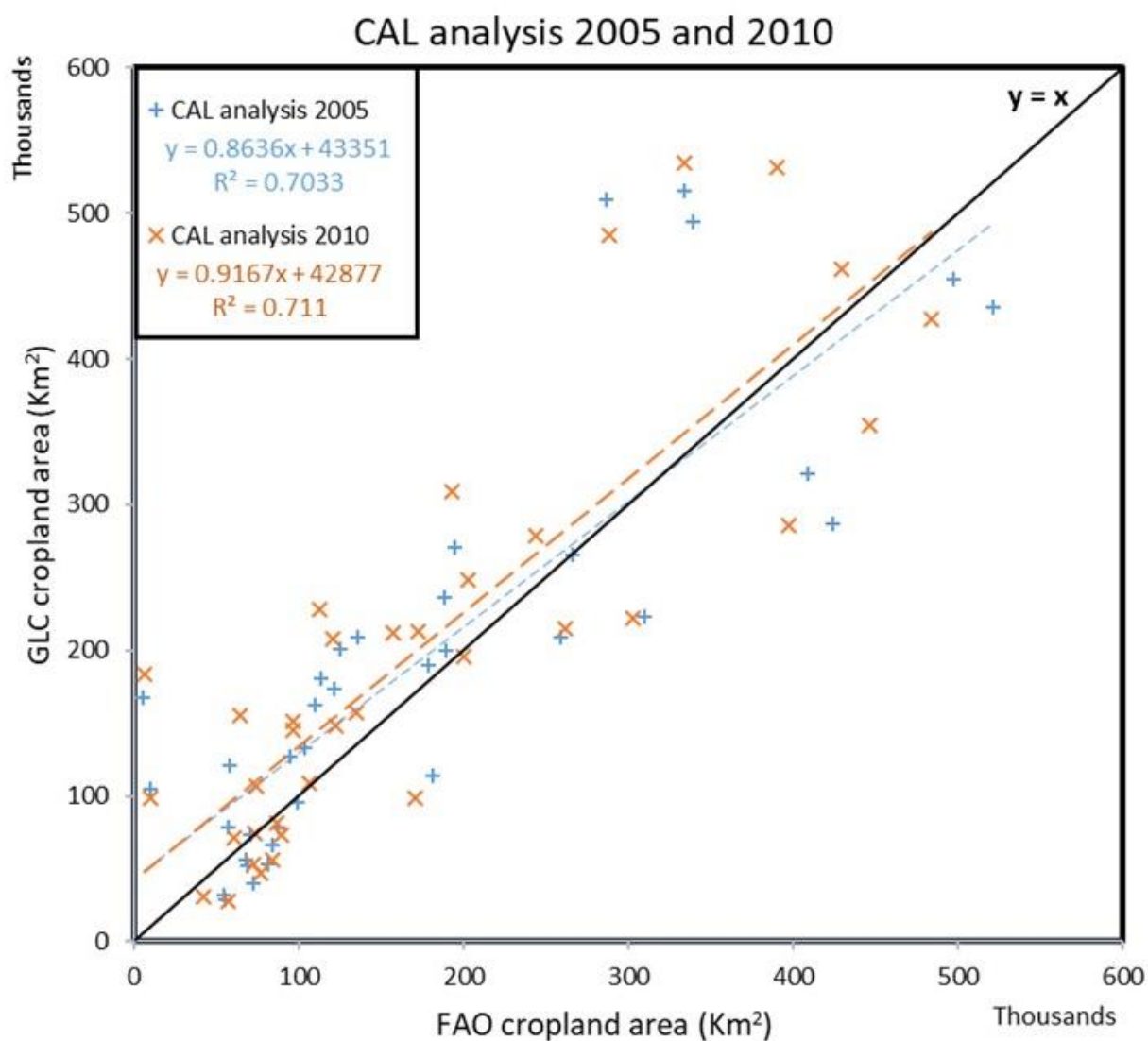


**Figure 3-7.** Regression of cropland area estimates derived from two years of the CAL analysis with FAO cropland area statistics

**Table 3-6.** Regression value and relative error of the CAL analysis and the four GLC datasets to FAO-stat data

| GLC datasets       | Small cropland area countries |                           | Medium to large cropland area countries |                           |
|--------------------|-------------------------------|---------------------------|---|---------------------------|
|                    | R2                            | Relative error to FAO (%) | R2                                      | Relative error to FAO (%) |
| CAL Product        | 0.57                          | 42.2                      | 0.86                                    | 29.8                      |
| GlobCover (v.2.3)  | 0.34                          | 85.6                      | 0.65                                    | 79.3                      |
| MODIS LC (v.5.1)   | 0.37                          | 104.2                     | 0.79                                    | 99.2                      |
| GLCNMO (v.2)       | 0.55                          | 45.1                      | 0.79                                    | 75.2                      |
| ESA CCI-LC (v.2.5) | 0.32                          | 144.5                     | 0.66                                    | 77.6                      |

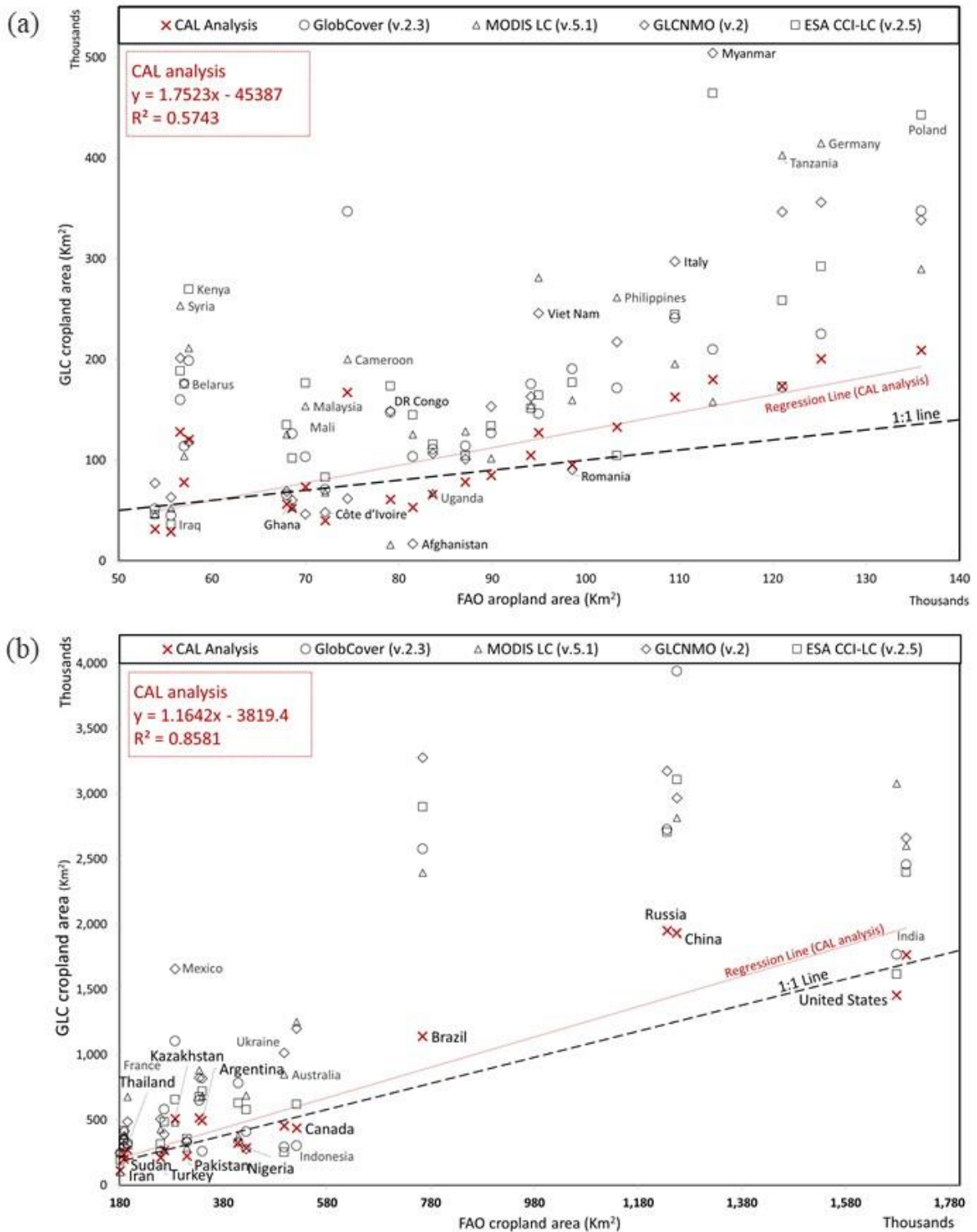


**Figure 3-8.** Comparison on the national level between the CAL analysis and the four original GLC datasets with cropland area estimates from the FAO in (a) small cropland area countries and (b) medium to large cropland area countries.

### 3.4.5 Cropland Agreement Level (CAL) Change Analysis

The CAL analysis is used to study the potentiality of cropland area changes monitored between 2005 and 2010. Figure 3-9 shows global cropland Agreement Level change. Almost all of the CAL analysis and the four GLC datasets are not able to produce similar cropland area change data comparable to the cropland change statistical data from the FAO. However, the CAL analysis has the highest proximity of cropland change compared to the other GLC datasets.

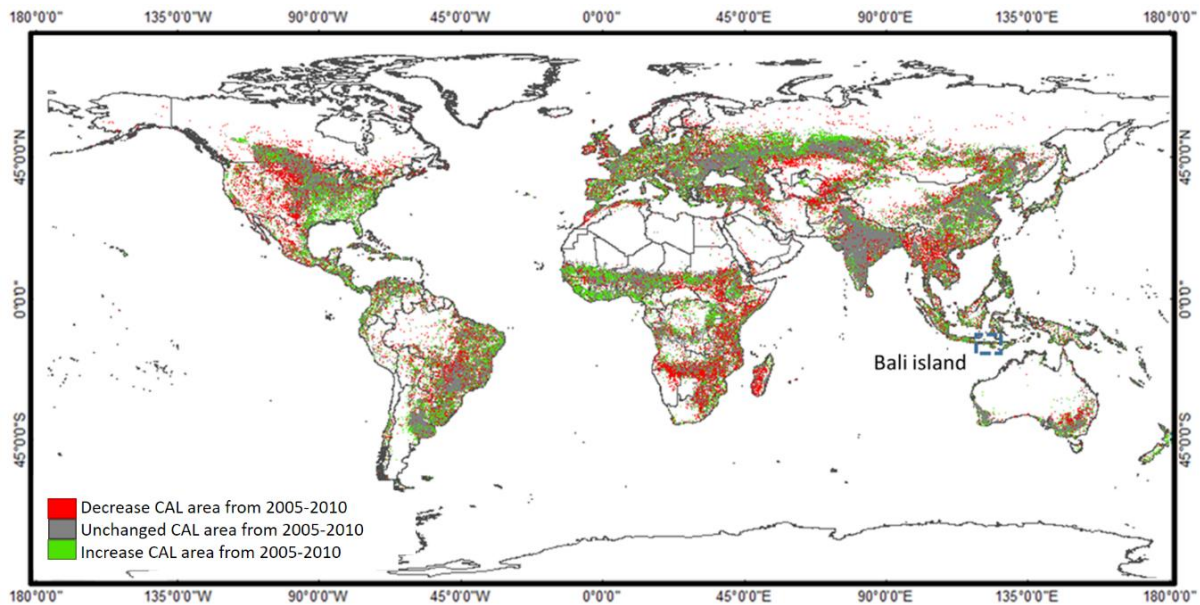


**Figure 3-9.** Global CAL change analysis from 2005 to 2010

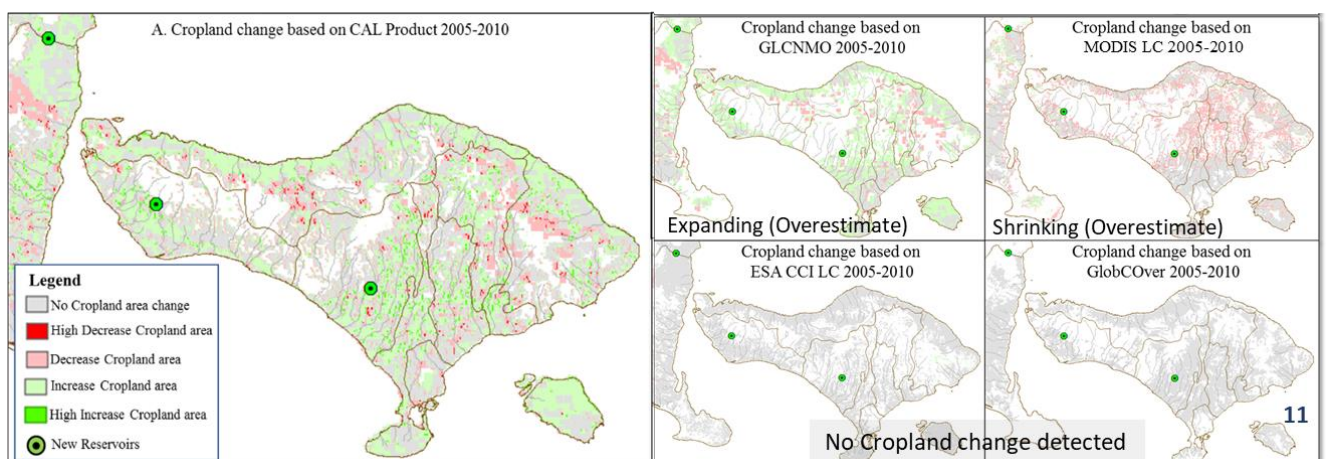


**Figure 3-10.** Cropland agreement level change of Bali Island, Indonesia

Moreover, the development of three new reservoirs in Bali and East Java built within the 2005-2010 time period expanded the cropland area around the reservoirs [Suputra et al., 2012]. Figure 3-10 shows that in ESA CCI LC and GlobCover, almost all of the cropland area in 2005 and 2010 had no change, whereas in the MODIS data, there is a decline in cropland change. In contrast, GLCMNO shows an expansion in cropland area. Cropland change results from the CAL analysis can accommodate the results from the four GLC datasets, and it also accommodates an area with an extreme level of changes.

### **3.5 Conclusion**

This study shows that integrating recent GLC datasets can be considered for estimating cropland area with the highest accuracy among original datasets. The CRISPS approach is also used to analyze per pixel comparisons between cropland map datasets and produce a Crop Agreement Level (CAL) analysis by integrating four GLC datasets in the two year-groups (2005 and 2010). To calculate cropland area from the CAL analysis, an IIASA-IFPRI cropland percentage map is used. The correlation model obtained from the CAL analysis and IIASA comparison successfully estimated the percentage value of four agreement levels. When the correlation between the CAL analysis and cropland percentage is studied, the result shows a good correlation where level 1 correlates with 10%, level 2 with 20%, level 3 with 40% and level 4 with 80% cropland area. The regression value for the CAL analysis is 0.70-0.71, this value was the highest compared to other datasets, which are ESA CCI-LC (0.47-0.49), GlobCover (0.41-0.43), GLCMNO (0.43-0.59) and MODIS LC (0.63-0.65). Cropland area estimates for each country in 2005 and 2010 show that the CAL analysis is more accommodating for cropland change calculation based on FAO cropland change statistical data

## Chapter 4

# DEVELOPMENT OF CROP CALENDAR, INTENSITY AND CROPPING PATTERN BY INTEGRATING MODIS AND AMSR DATASETS

### 4.1 Background

The trend of shrinking cropland area due to urbanization, makes extensification strategy become not preferred to achieve sustainable food production [D'amour et al., 2016; Wu, 2018]. The rising demand of food that is accompanied by GDP growth, increases the agriculture production by improving irrigation infrastructure. Several countries tried to intensify land-use on existing cultivated lands to boost global crop production [Rufin, 2018]. In the other hand, this massive improvement has been facing challenging problem in negative climate change impact such as drought and extreme weather changes [Ramankutty et al., 2018]. With this climate change pressure, global cropland area is facing the uncertainty the number of crop intensity and crop calendar as well especially in the beginning of 21<sup>st</sup> century. [Heino et al., 2018]. Issues like global monitoring of emission and water demand change in cropland are becoming important to understand the present and future challenges in food sustainability trade off [Wua et al., 2018]. Here, the information about the cropping intensity and crop calendar parameters are essential inputs for estimating the food production, water demand and GHG emissions [Takeuchi, 2009; See, 2013]. CC defines as the date or month when farmers are sowing crops whereas CI is the number of cropping cycle per year. Monitoring accurately the long-term dynamic of global Crop intensity and crop calendar is important to support global food security. Rice is very important crop type with specific planting characteristic, with highest water demand and produce methane emission. Understanding rice paddy phenology can improve the accuracy of global crop calendar.

In this study we tried to fill the information gap by estimating the long term Sowing month and cropping pattern of rice and non-rice by using combination MODIS NDVI and AMSR LSWC from 2001 to 2015 at a spatial resolution of 1 km in the global scale. These sowing month and cropping pattern products are the first satellite-based products which derived from water and vegetation index phenology that can analyze 15 years' dynamic change of crop activities for crop security purpose.

## 4.2 Material

### 4.2.1 Global MODIS NDVI Datasets

We investigate time series of global satellite-sensed normalized difference vegetation index (NDVI) from 16-Day MODIS (MOD13A2) composite data with 1 km spatial resolution from 2001 to 2015. We divide these 15 years archived data into three group of year (2001-2005, 2006-2010, 2011-2015) to mitigate the effect of cloud contamination.

Cropland Agreement Level (CAL) product [Sakti et al., 2017] used as the cropland base map. This CAL product integrated four global croplands that are GlobCover, MODIS LC, GLCNMO and ESA CCI LC. The aims of this CAL product are to accommodate different global cropland and reduce the less accurate area by eliminating the lowest agreement area among GLC datasets.

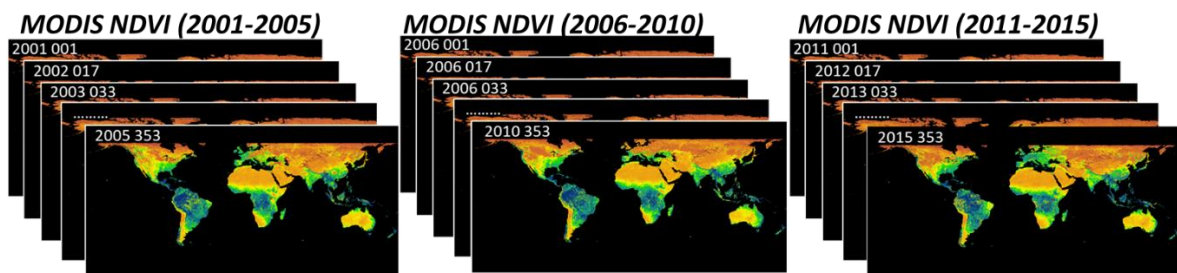


**Figure 4-1.** Global MODIS NDVI (MOD13A2) 1 km 16-Day composite data from 2001 – 2015.

315 global MODIS NDVI dataset in total (600 GB size datasets)

### 4.2.2 Global AMSR-E/2 LSWC Datasets Analysis of Endmember Dataset

For extract water index, we used Advanced Microwave Scanning Radiometer (AMSR)-E/2 LSWC (land surface water coverage). The AMSR instruments are dual-polarized, conical scanning, passive microwave radiometers. Each is placed in a near-polar orbit which allows for up to twice daily sampling of a given Earth location. A key feature of these AMSR instruments is the ability to see through clouds, thereby providing an uninterrupted view of the ocean measurements.

AMSR-E measures geophysical parameters supporting several global change science and monitoring efforts, including precipitation, oceanic water vapor, cloud water, near-surface wind speed, sea surface temperature, soil moisture, snow cover, and sea ice parameters [Xi and Takeuchi, 2016]. AMSR-2 measures weak microwave emission from the surface and the atmosphere of the Earth. From about 700 km above the Earth, AMSR-2 provides highly accurate measurements of the intensity of microwave emission and scattering. This enables AMSR-2 to acquire a set of daytime and nighttime data with more than 99% coverage of the Earth every 2 days [Zabolotskikh et al., 2015; Pang et al., 2018].

We investigate time series of LSWC from daily AMSR-E/2 data with 10 km spatial resolution. We divide these 15 years archived data into three group of year (2003-2005, 2008-2010, 2013-2015). Takeuchi and Gonzalez [2009] found that the algorithm accurately predicted daily LSWC of AMSR-E/2 by blending MODIS NDWI and AMSR-E. AMSR-E Daily Normalized Difference Frequency Index (NDFI) [Takeuchi et al., 2006] was used to map LSWC in 10 km which was effective to agriculture monitoring issues [Jonai and Takeuchi, 2012; Ngoc Van et al., 2012].

$$NDFI = \frac{TB_{18.7V} - TB_{23.8V}}{TB_{18.7V} + TB_{23.8V}}$$

W 1 here  $TB_{18.7V}$  and  $TB_{23.8V}$  are the brightness temperature of vertical (V) polarization at 18.7GHz and 23.8GHz.

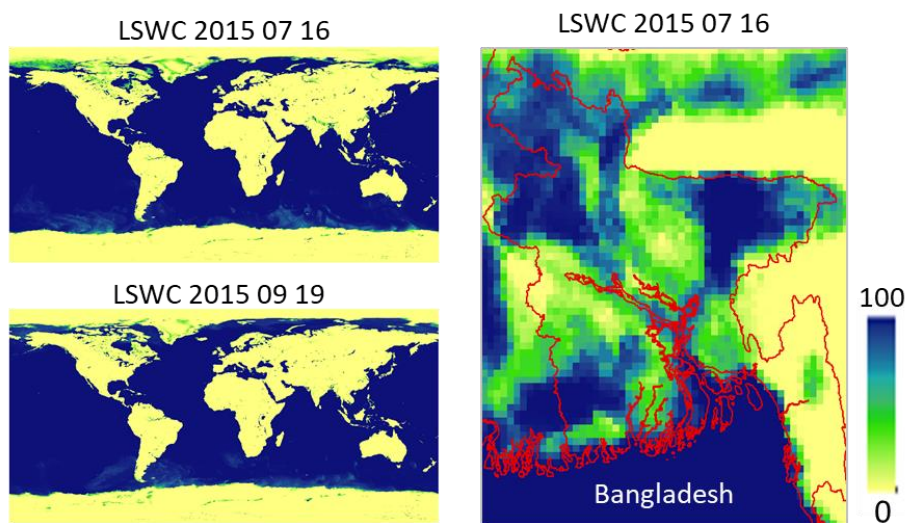


**Figure 4-2.** Daily global AMSR-E/2 LSWC 10 km data (2003 – 2005, 2008 – 2010, and 2013 – 2015).

### 4.2.3 Additional Datasets

#### 4.2.3.1 HYDE V 3.2 Annual Global Irrigated Rainfed of Rice Paddy Data

HYDE presents (gridded) time series of population and land use for the last 12,000 years. Cropland and pasture statistics are combined with satellite information, specific allocation algorithms, and weighting maps of the HYDE rules to create spatially explicit maps, which are fully consistent on a 5 longitude/ latitude grid resolution, and cover the period 10,000 bc to ad 2000. Input data are derived from total rice area statistics per country from FAO, Rice-growing countries from Mitchell [2007], Reference maps for rice from MAP SPAM [You et al., 2014] and Literatures of ratio of physical area to harvested in China, Bangladesh, Vietnam and India.

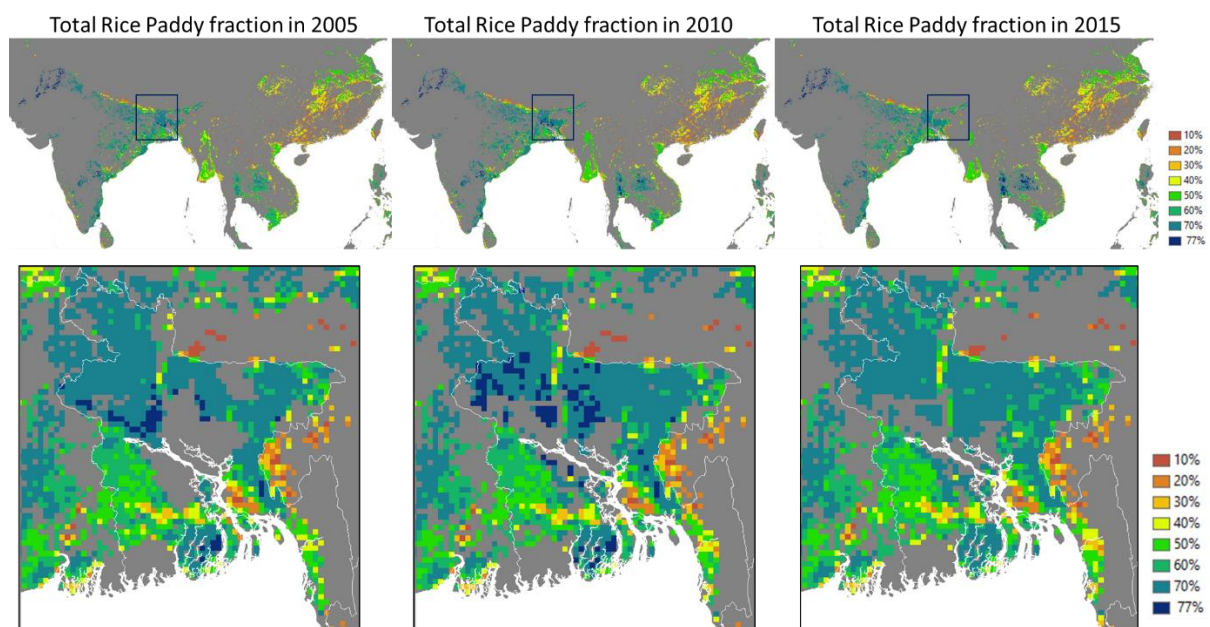


**Figure 4-3.** HYDE V.3.2 of rice paddy fraction for Irrigated and rainfed

#### 4.2.3.2 The GFSAD1KCD Crop Type, Irrigated, and Rainfed Dataset

The GFSAD products at 1 km resolution include the Crop Dominance product and Crop Mask product. First, the Global Crop Extent 1 km Crop Dominance [Thenkabail et al., 2012, Thenkabail et al., 2011, Thenkabail et al., 2009a, 2009b] provides cropland extent, irrigated-rainfed, and crop dominance. The GCE 1 km Crop Dominance provides spatial distribution of the five major global cropland types (wheat, rice, corn, barley and soybeans; which occupy 60% of all global cropland areas) at nominal 1. The map is produced by overlying the five

dominant crops of the world produced by Ramankutty et al. [2008], Monfreda et al. [2008], and Portman et al. [2009] over the remote sensing derived global irrigated and rainfed cropland area map of the International Water Management Institute [IWMI; Thenkabail et al., 2009a, 2009b] Input data used in these various products include remote sensing (e.g., AVHRR, SPOT vegetation, MODIS), crop type distribution, climate, reference and statistics (e.g., country statistics) data were used.

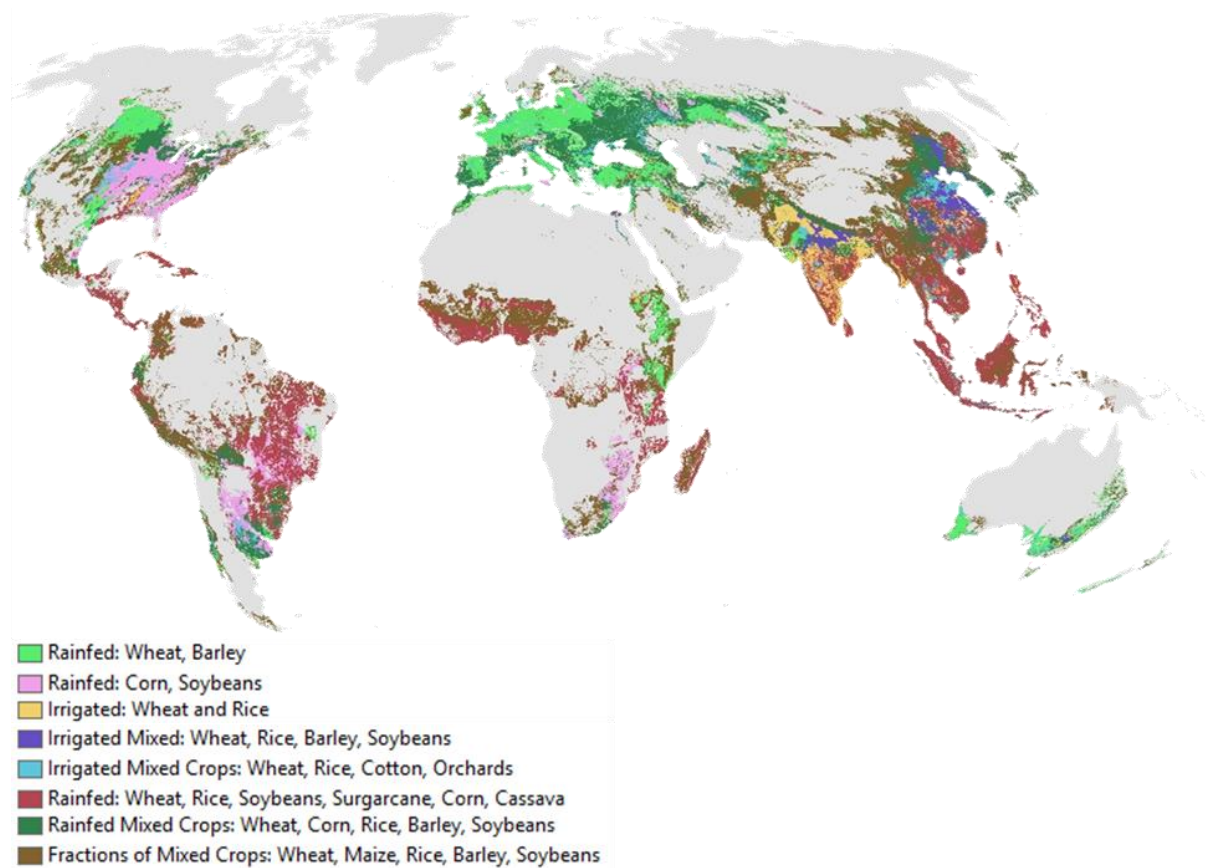


Figure 4-4. The GFSAD1KCD Crop Type Irrigated and Rainfed 1 km dataset [Thenkabail, 2016]

#### 4.2.3.3 The Previous Crop Calendar Products

To verified our cropping intensity and sowing month products, we compare the estimated sowing date within three cropland calendar products. We also compare the product result with other existing census-based (MIRCA 2000) and satellite-based (SACRA) CC products.

Original product of MIRCA2000 is point base, which each point has information about sowing month. This product released in two spatial resolutions that are 30 and 5 arc minute.

Zabel product released in three group year, here we used 1981-2010 product. Zabel product simulate climate model and reflected into 16 crop type dominant where each dominant crop has information of sowing weeks. In this research we calculate distribution of crop based of dominant value to produce dominant crop type and its sowing month in single information data. SACRA product produced by combining NDVI spot 10 days' composite and census based, it released both sowing and harvest in DOY unit with aggregate 10 km pixel resolution. The limitations in previous studies were: (1). Only represented one-year data product, (2) Coarse pixel resolution and (3) High discrepancy among CC data products. Zabel product could tackle those limitations but it uses a simulation model (Figure 4-5).

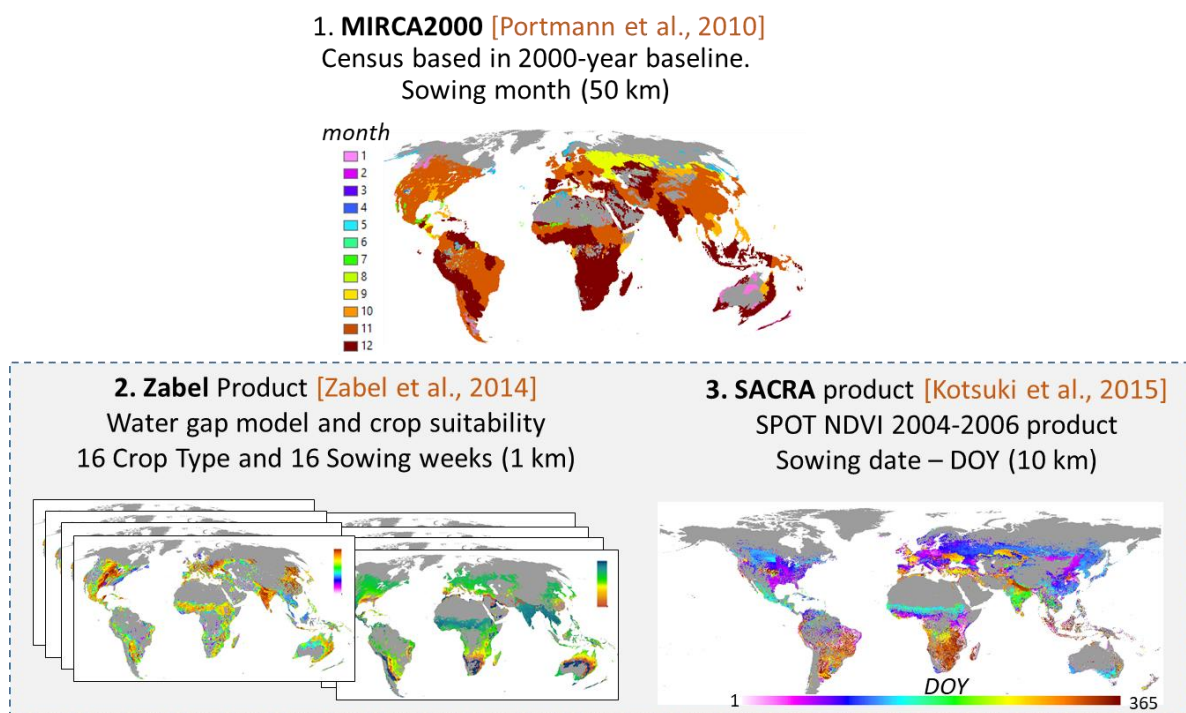


**Figure 4-5.** Previous studies of sowing month products: MIRCA2000, Zabel, and SACRA

## 4.3 Methods

### 4.3.1 Peak and Lowest Month of MODIS NDVI Extraction

Discrete Fourier Transform (DFT) analysis is applied to temporal NDVI dataset to capture the trend of crop phenology. We assume that NDVI time series represent the phenology of one dominant crop in each grid, where the number of NDVI peak counted as intensity [Oyoshi et

al., 2013]. Figure 4-6 shows overall methods to detect peak month and lowest month from MODIS NDVI datasets.

The DFT equation is expressed as:

$$F_n = \sum_{k=0}^{N-1} f_k e^{-j\frac{2\pi}{N}kn}, n = 0,1,2,\dots,N-1 \quad (1)$$

where  $k$  denotes the number of 16-day MODIS NDVI, totally we used 115 samples in each three group year 2001-2005, 2006-2010 and 2011-2015 with total 315 global MODIS NDVI datasets or about 600 GB size of data.

The highest peak ( $t_{pk}$ ) and lowest point ( $t_{low}$ ) calculated by comparing each value within 48 days (3 NDVI data) before and after peak and lowest candidates. The highest and lowest value among those range can be detected as the peak and lowest point. After that we translate the DOY of highest peak and lowest point to unit of month to simplify the final CC product. The equation of peak and lowest estimation are expressed as:

$$\begin{aligned} \text{NDVI}(i) &\leq \text{NDVI}(t_{pk}) \quad (I = t_{pk} - 1, t_{pk} - 2, t_{pk} - 3) \\ \text{NDVI}(i) &\leq \text{NDVI}(t_{pk}) \quad (I = t_{pk} + 1, t_{pk} + 2, t_{pk} + 3) \end{aligned} \quad (2)$$

$$\begin{aligned} \text{NDVI}(i) &\geq \text{NDVI}(t_{low}) \quad (I = t_{low} - 1, t_{low} - 2, t_{low} - 3) \text{ and} \\ \text{NDVI}(i) &\geq \text{NDVI}(t_{low}) \quad (I = t_{low} + 1, t_{low} + 2, t_{low} + 3) \end{aligned} \quad (3)$$

DFT result indicates the highest spectrum at the frequency of one cycle per year. Then, the frequency of the highest spectrum defined as cropping intensity (CI) of the pixel. These process were conducted all over the cropland area defined by CAL product pixel by pixel.

DFT can normalized the unstable NDVI due to cloud contamination. The comparison result before and after converting proses from peak and lowest DOY to month showed in figure 4-7. Here, the result show by converting DOY to month, can simplify for detecting stable average

sowing month. After we find month of peak and lowest we produce peak month and lowest month by applying all flow process from DFT analysis until detecting average peak and lowest month in three group year pixel by pixel.

From the interpretation of peak and valley of DFT NDVI profile phenology (figure 4-7) we can see how in those areas the intensity of cropping frequency seems to be changing from single to triple cropping frequency, in some year are sometime stable, increase and decrease. This phenomenon happens since during 15-year investigation start from 2001 to 2015, development of irrigation infrastructure can increase intensity in some cropland area, and unpredicted failure of harvesting due to disaster may cause reducing intensity in some year. However, there are other reason such as cloud contamination that cannot be investigate in this study.

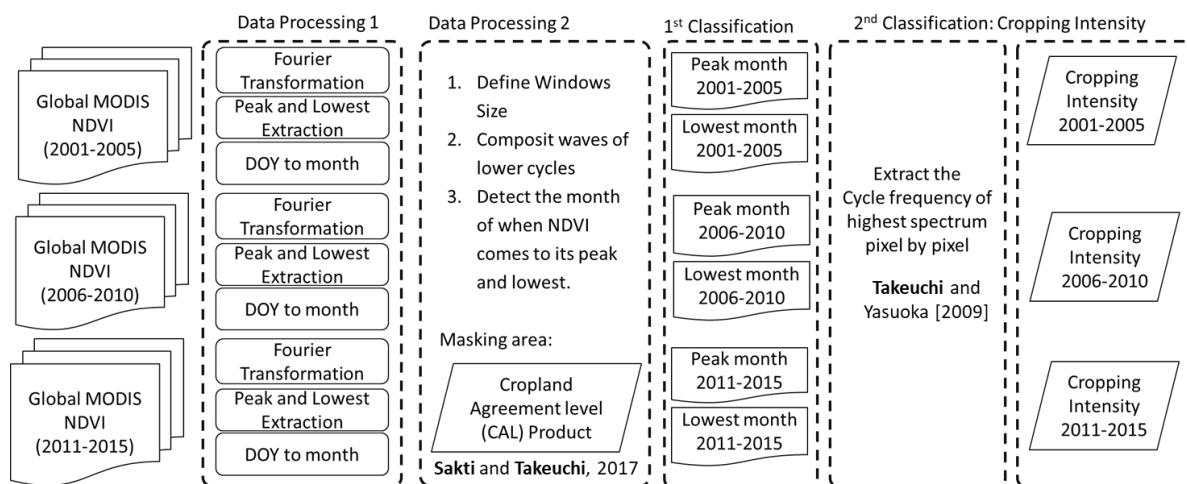


Figure 4-6. Overall MODIS data processing for classified long-term MODIS data into Peak and Lowest month

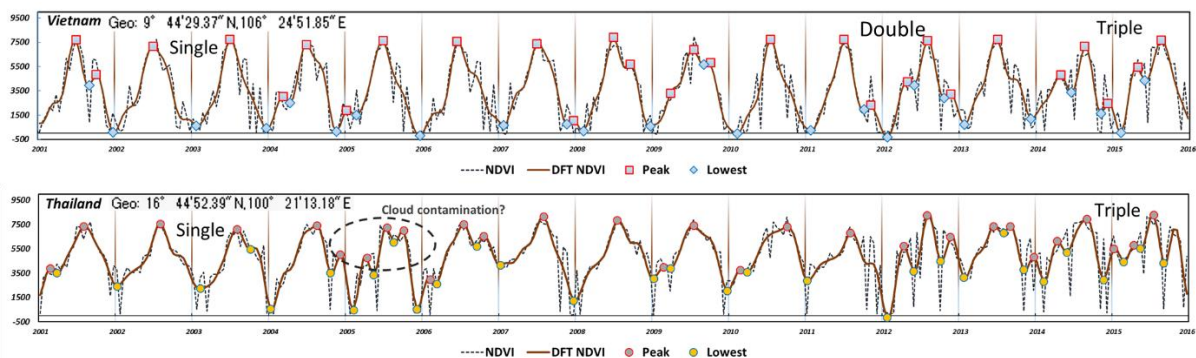
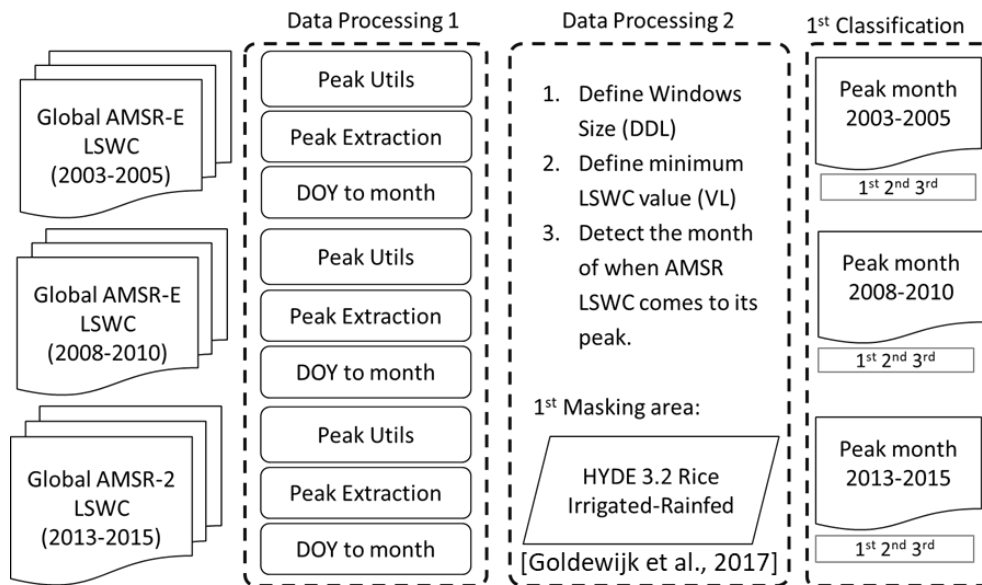


Figure 4-7. analysis of time-series 16 days composite MODIS NDVI and reconstruct DFT NDVI profile during 2001 to 2015 in Vietnam (top) and Thailand (bottom).

### 4.3.2 Peak Month of AMSR-E/2 LSWC Extraction

In AMSR-E/2 data processing we used same approach with MODIS data processing, the different is in AMSR data processing was not using Discrete Fourier Transform (DFT) for detecting peak. We analyses peak average in each group of year using Peak Utils a python library that can be used to detect peak and lowest point in some wavelength time series datasets. For detecting real peak that located in flooding session on rice paddy, we define windows size (DDL) and minimum LSWC value (VL) with 120 days for DDL and 20 for VL (Figure 4-9).



**Figure 4-8.** Overall AMSR-E/2 data processing for classified long-term AMSR-E/2 data into peak month

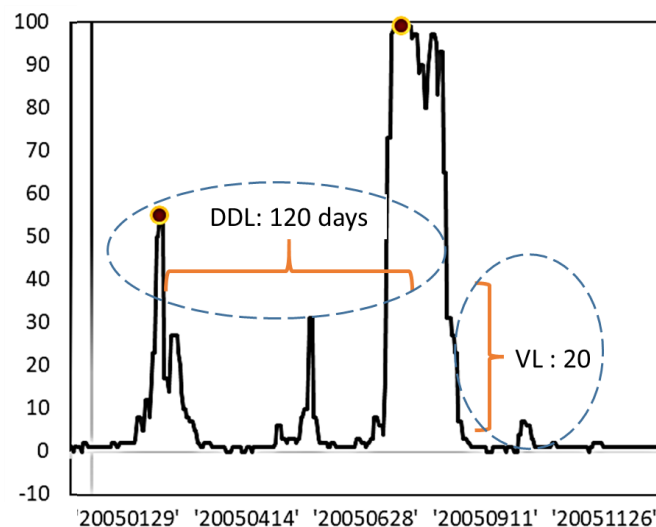


**Figure 4-9.** Analysis of time-series Daily AMSR LSWC

### 4.3.3 Sowing Month Estimation

Crop calendar highly depends on climatic conditions such as rainfall and temperature, because these factors regulate plant growth. Climatic conditions have seasonality and periodicity. Since temporal NDVI profile can indicate seasonal change of crops, spectral analysis of time-series NDVI data has been promising as one of approach to developing crop calendar data product [Sakamoto, 2005].

1). Two month before peak (CROPWAT) [FAO, 2010], 2. Lowest point combine with climate data (SACRA Product) [Kotsuki et al. 2015], 3). Follow 2 : 1 month approach (two month from plantation to peak and one month from peak to harvest [FAO, 2010].

In this study, we propose three approach to estimate global sowing month for both rice and non-rice crop types by integrating MODIS NDVI and AMRS-E/2 LSWC:

#### 4.3.3.1 General crop cultivates length approach

For sowing month estimation, we are follow general crop cultivated length derived from CROPWAT model [FAO, 2009]. In this CROPWAT model, planting date in each cropping cycle is defined to be eight weeks or two months before the peak.

#### 4.3.3.2 Short period crop cultivation

For short crop cultivated period, we identify sowing month as the lowest point before peak, if we find the lowest point occur in two months before peak. Figure 4-10 illustrated the strategy to identify sowing month candidate by combining DFT NDVI phenology and CROPWAT model estimation.

#### 4.3.3.3 Sowing month estimation for rice paddy

Since detecting sowing month using previous approach has limitations where estimating sowing month using both methods such as two months before peak assumption is too simple and using lowest point as reference is too risky since it estimated contain cloud rather than peak. Here, we propose estimation sowing month of rice paddy by using daily AMSR-E/2

LSWC (Microwave) that can be used to identify flooding session in rice paddy. In our data processing we select peak of AMSR LSWC that located around two months before peak of MODIS NDVI. Figure 4-11 shows water and vegetation index pattern in rice paddy phenology.

Figure 4-10 illustrate two approach that used for sowing month estimation in this study.

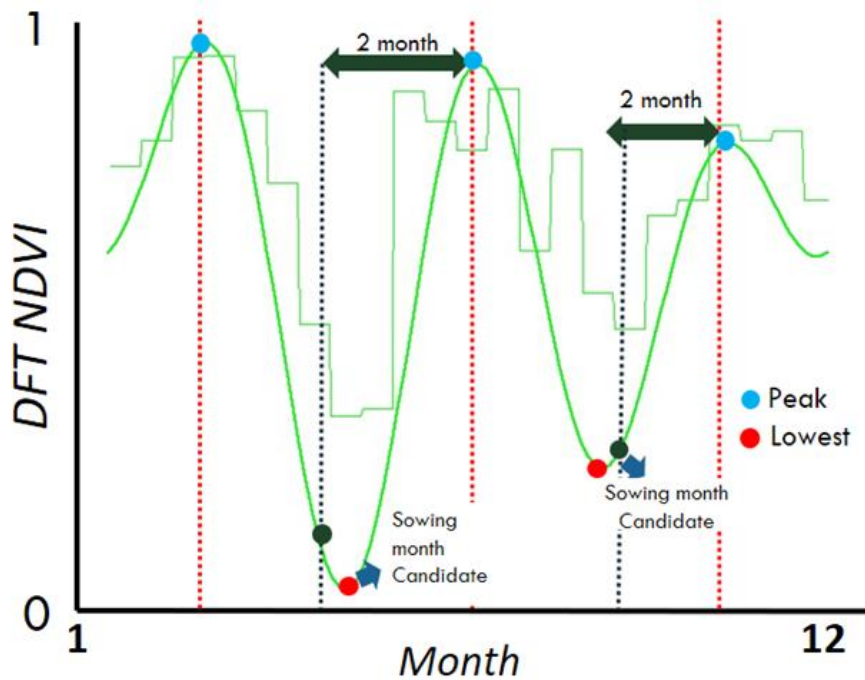


**Figure 4-10.** Two conditions for detecting sowing month candidate, a) two months before the peak and b) a month when lowest occur before peak.

#### 4.3.3.4 Sowing month estimation for rice paddy

Since detecting sowing month using previous approach has limitations where estimating sowing month using both methods such as two months before peak assumption is too simple and using lowest point as reference is too risky since it estimated contain cloud rather than peak. Here, we propose estimation sowing month of rice paddy by using daily AMSR-E/2 LSWC (Microwave) that can be used to identify flooding session in rice paddy. In our data processing we select peak of AMSR LSWC that located around two months before peak of MODIS NDVI. Figure 4-11 shows water and vegetation index pattern in rice paddy phenology.

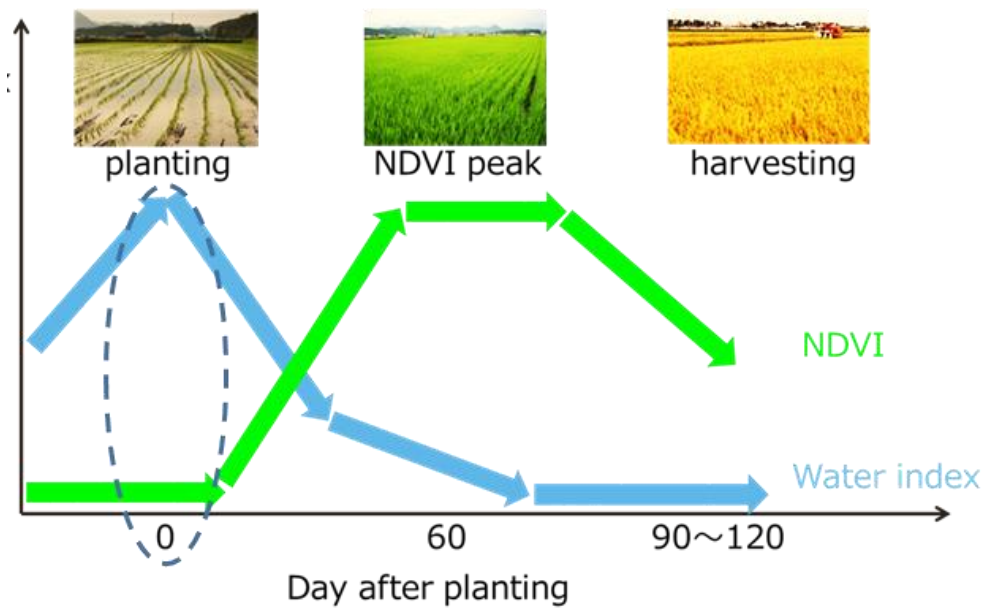


Figure 4-11. Water and vegetation index pattern in rice paddy phenology

#### 4.3.4 Dominant Cropping Pattern of Rice and Non-Rice Paddy

Detecting rice paddy become one important issue in this research, since rice paddy has specific planting characteristic, and has significant water usage compared with other crop type. In multi cropping intensity area, Rice paddy not fully planting in each seasons, farmers are usually change their crop type depet on water source, climate and needs. Detecting rice paddy in multi cropping intensity become important to increase the accuracy of sowing month and water demand estimation. The approach based on integration DFT MODIS NDVI and AMSR LSWC to find suitable condition for detecting flooding session of rice paddy cultivation. We pick up the AMSR LSWC peak month that located in MODIS NDVI peak month. We combine this rice paddy detection with previous research of cropping intensity [Takeuchi and Yasuoka, 2009] for analyzing rice paddy cropping pattern in multi cropping intensity area.

### 4.4 Result and Discussion

#### 4.4.1 Long-term MODIS Cropping Intensity Product

Previous research related to the cropping intensity product can be found in Takeuchi and Yasuoka [2009], Jonai and Takeuchi [2013] and. Based on spectrum analysis, the total of

cropping cycle in 5 years were counted. Then we aligned total cycle to get average cropping per year. Figure 4-12 shows the result of average cropping intensity product in three group of year. The actuary of product methods already described in previous paper [Oyoshi and Takeuchi, 2013].

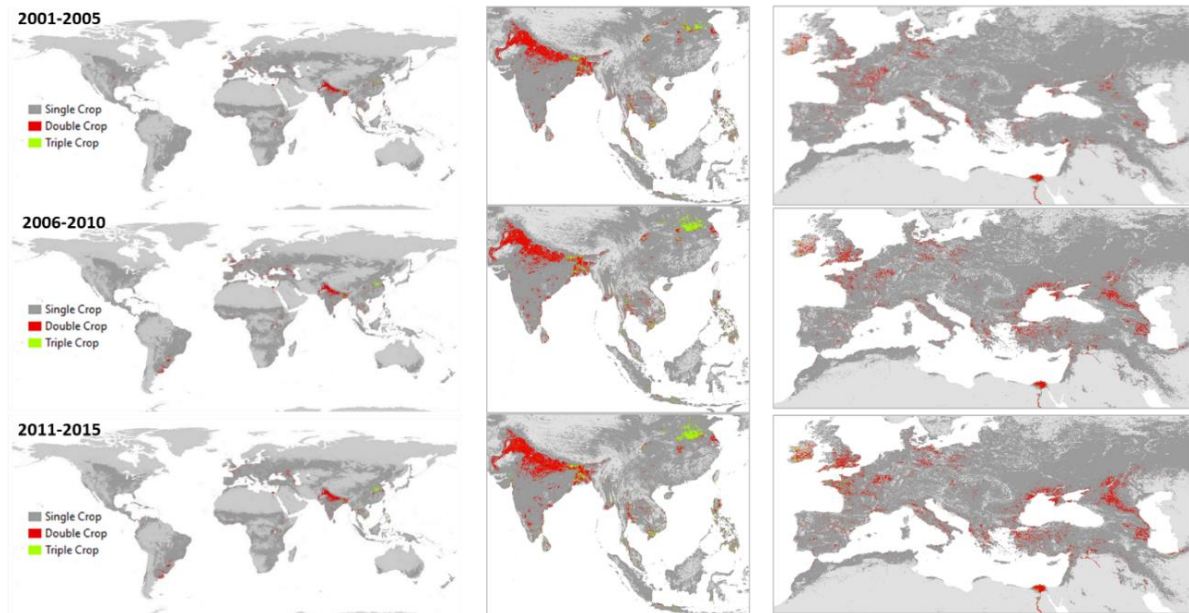


**Figure 4-12.** MODIS Cropping Intensity Product 2001-2015

In order to calculate area of single, double and triple, we used HYDE 3.1 Cropland Fraction data product in 2005, 2006 and 2007 [Goldewijk et al., 2017] for converting single pixel based into fraction based, by using fraction based each pixel can contain percentage of cropland area from 0 to 100 %. The result of cropland area estimation are shown in figure 4-13. Overall we used FAO statistic of cropland area to compare with the product of cropland area in this study derived from combination single, double and triple product. Almost in all regions cropland area derived from cropping intensity product are in underestimation. The reasons of this underestimation because the fraction value which derived from HYDE product is originally compatible with 10 km square pixel resolution, however in this study we used the fraction value for 1 km square product.

The change trend of cropping area in 2005, 2006 and 2007 has similar pattern with cropland area change of FAO-Stat. From comparison of changing single double and triple crop shows that how Africa is only region that increase single cropping area in 15 years. There are some very big gap between Asia and non-asia region regarding growing of double and triple cropping area. Moreover, Asia can increase two time larger of triple cropping area in 15 years, indicated

how Asia region successfully developed irrigation system that can increase number of cultivation period in one year.

For the next analysis we directly try to compare the performance of the MODIS cropping intensity product with other global cropping intensity product derived by remote sensing (SACRA) [Kotsuki et al., 2015] and Model-based climate condition (Zabel) [Zabel et al., 2014] (figure 4-26).

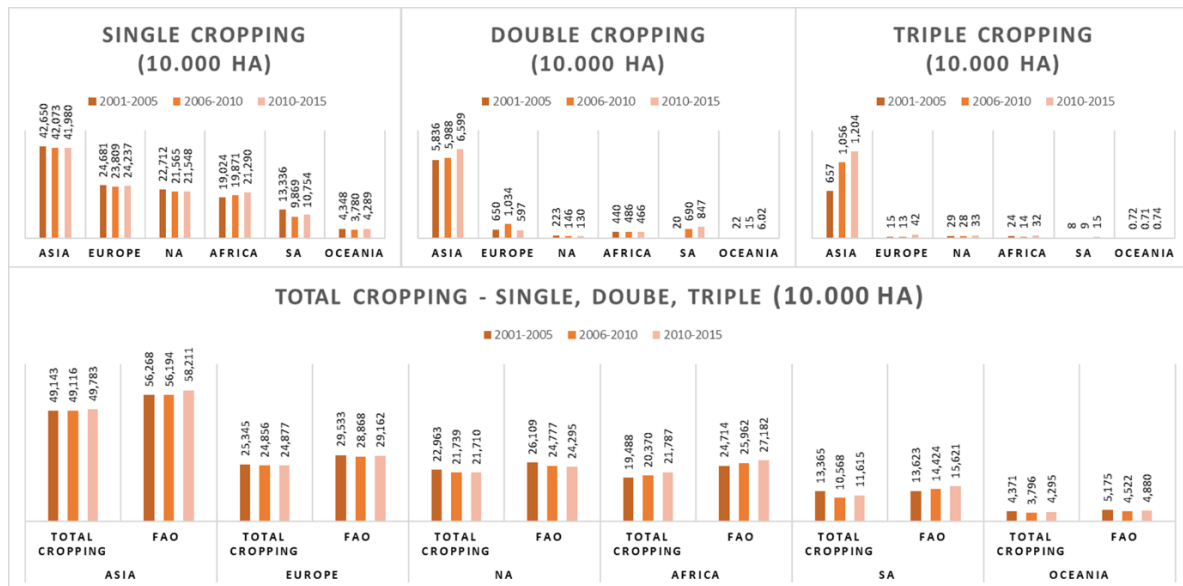


Figure 4-13. Cropping intensity area for single, double and triple in six regional analysis

#### 4.4.2 Cropping Intensity Change 2001-2015

In this study we try to analyze cropping intensity changing in 15 years (Figure 4-14). The product result of this analysis are three level product of increasing intensity and three level product of decreasing intensity. Increasing one level means crop can increase from single to double or double to triple intensity. Two level means from No cultivation to double or single to triple. Three level means from no intensity to triple. This description is same for decreasing level condition (figure 4-14). In figure 4-14. shows the product of cropping intensity change, with the highlight of area A, B, and C that facing high dynamic change of intensity.

For detail information, we calculate area that facing increasing one and two level in all countries. Figure 4-15 Show top 20 countries that facing largest increasing in one and two level cropping intensity. For calculating the area, we used same approach by combined with HYDE Irrigated area. The reason for using Irrigated area is assumption that increasing intensity

phenomena are dominantly contributed by irrigation. Based on the country statistic result, several countries are facing high increase of intensity level in this last 15 years there are India, China, and Argentina (Figure 4-15).

From comparing result of increasing one level and two level, India and china detected have different strategy, since limited area located in China with limited suitable climate condition for cultivation activities, China try to increase two level in existing cultivated land, where 33,324 km<sup>2</sup> cropland area in China had increase two level. Different with India, this country tries to focus to increase one level intensity in large area, where 108,565 km<sup>2</sup> were increased one level compare with only 7,285 km<sup>2</sup> that increase one two level intensity. The different approach between India and China is reflecting their response to the increasing food demand in last 15 years with consider physical condition of arable land in each country.

We investigate in some countries; the high decrease of intensity level is located near urban area. This condition reflect how urban area are facing pressures from urbanisation. Moreover, this decreasing phenomena is worsening by crop failure due to drought and floods.

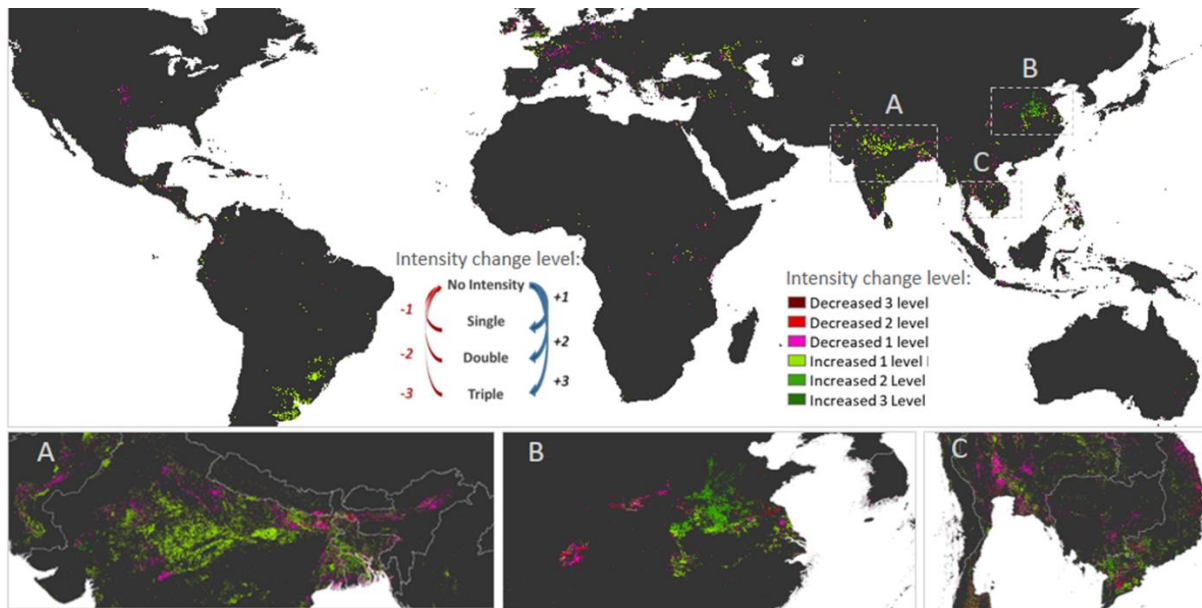


**Figure 4-14.** MODIS Cropping Intensity Change 2001-2015, derived from three group of year cropping intensity (2001-2005, 2005-2010, and 2011-2015).

**Table 4-1.** Top twenty countries with facing rapid increasing of CI, where India China and Brazil are three top countries that can increase the intensity during last 15 year

| Ranking | Increase 1 level |            |                             | Increase 2 Level |            |                             |
|---------|------------------|------------|-----------------------------|------------------|------------|-----------------------------|
|         | Country          | Area (km2) | Irrigated/<br>Rainfed (km2) | Country          | Area (Km2) | Irrigated/<br>Rainfed (Km2) |
| 1       | India            | 108,565    | 73,861<br>11,410            | China            | 33,324     | 35,846<br>4,519             |
| 2       | Argentina        | 42,319     | 6,703<br>126,326            | India            | 7,285      | 5,778<br>174                |
| 3       | Brazil           | 27,871     | 5,084<br>70,138             | Philippines      | 5,231      | 1,865<br>5,804              |
| 4       | China            | 18,337     | 16,232<br>1,866             | Vietnam          | 3,068      | 3,189<br>1,961              |
| 5       | Pakistan         | 17,070     | 12,329<br>3,706             | Bangladesh       | 2,759      | 6,513<br>1,818              |
| 6       | Russia           | 13,565     | 267<br>4,090                | Thailand         | 2,451      | 2,131<br>3,326              |
| 7       | Thailand         | 9,914      | 10,799<br>12,569            | Indonesia        | 2,023      | 2,222<br>2,523              |
| 8       | Uruguay          | 9,511      | 835<br>42,927               | France           | 1,666      | 74<br>22                    |
| 9       | Bangladesh       | 7,510      | 15,836<br>2,673             | Mexico           | 1,337      | 14<br>44                    |
| 10      | France           | 7,131      | 139<br>92                   | Burma            | 1,159      | 561<br>1,154                |
| 11      | Ukraine          | 6,222      | 186<br>2,688                | Malaysia         | 1,068      | 103<br>1,406                |
| 12      | Philippines      | 5,519      | 2,451<br>5,828              | United Kingdom   | 960        | 4<br>1,031                  |
| 13      | United Kingdom   | 4,792      | 21<br>5,724                 | Sri Lanka        | 634        | 227<br>1,175                |
| 14      | Turkey           | 3,551      | 932<br>8                    | Uganda           | 501        | 0<br>911                    |
| 15      | United States    | 3,308      | 863<br>0                    | Argentina        | 485        | 64<br>1,375                 |
| 16      | Burma            | 2,923      | 1,702<br>3,109              | United States    | 423        | 215<br>0                    |
| 17      | Vietnam          | 2,910      | 3,783<br>1,678              | Brazil           | 412        | 158<br>990                  |
| 18      | Uganda           | 2,816      | 8<br>5,087                  | Pakistan         | 386        | 98<br>3                     |
| 19      | Mexico           | 2,432      | 160<br>56                   | Ireland          | 310        | 0<br>1                      |
| 20      | Indonesia        | 2,323      | 1,779<br>3,770              | Cambodia         | 218        | 16<br>311                   |

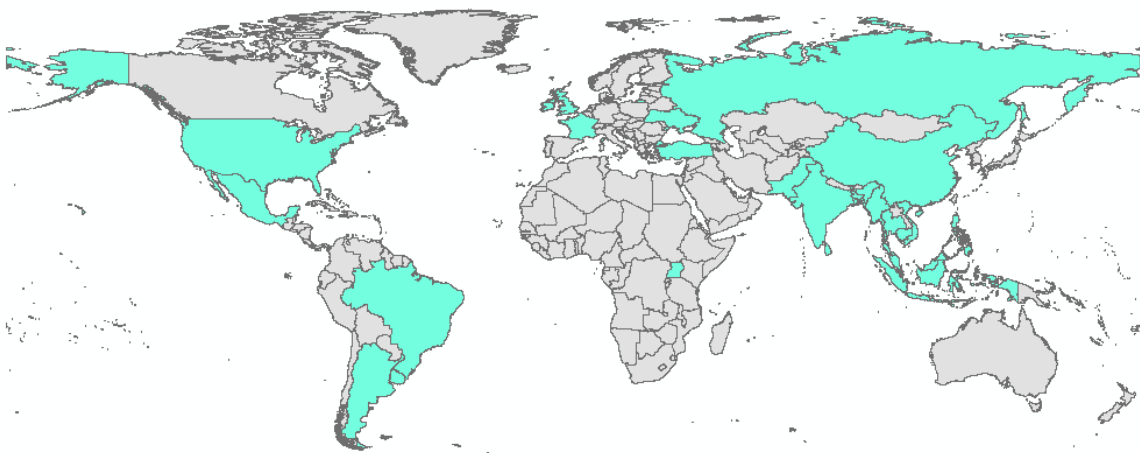


**Figure 4-15.** Distribution of top twenty countries with facing rapid increasing of Cropping Intensity of one and two level during last 15-year

Based on the distribution of top 20 countries with highest increasing of single and double cropping intensity (Figure 4-16), Uganda is the only country from Africa region that facing this increasing cropping intensity. The reasons of this increasing are supply water from precipitation are higher compare with other country in Africa region since the location of Uganda in tropical region. This condition supported with contribution three big lake that located in Uganda which represented function of reservoir to collect water in surface area.

The contribution of irrigated and rainfed change which calculated by integrating Cropping intensity change product with HYDE irrigated and rainfed product data are highlight to understand the water source type contribution behind this increasing phenomena. This water source contribution can be indicator of crop type and also cost for infrastructure development.

In one level increased there are different water source contribution among India, Brazil and Argentina, where pixel with increasing one level in India has dominant contribution from Increasing Irrigated area, however in Brazil and Argentina cases, the pixel of one level increase has detected with increasing rainfed compare with irrigated. This condition is reflected in the crop type that facing increasing intensity. Since Brazil and Argentina are increasing production of Soybean, the increasing water demand are not high compare with India with dominant crop type that facing increase is rice paddy. However, in two level increased of two level, China has balance contribution between Irrigated and rainfed increasing area.

#### 4.4.3 Long-term MODIS-AMSR Sowing Month Product

Three approaches that used in this study (basic approach, first adjustment and second adjustment) are work well to detect sowing month in three group of year. Figure 4-17 shows the estimation result of sowing month based on three approaches. Basic approach is the approach to estimate sowing month by counting two months back from the peak in discrete Fourier transform (DFT) analysis of MODIS NDVI. First adjustment estimates the sowing month by the peak and lowest point information from MODIS NDVI. The target of first adjustment approach is to investigate the area with short cultivation period. From this approach, northern Russia known to have a big area of short cultivated crop. The third approach is second adjustment that use the information of MODIS and AMSR LSWC. This approach can be used to estimate the sowing months of rice paddy area. After we developed the product of sowing month based on three approaches, we combine three approaches product. Figure 4-18 shows

the final product of MODIS-AMSR sowing month by combining the products from three approaches.

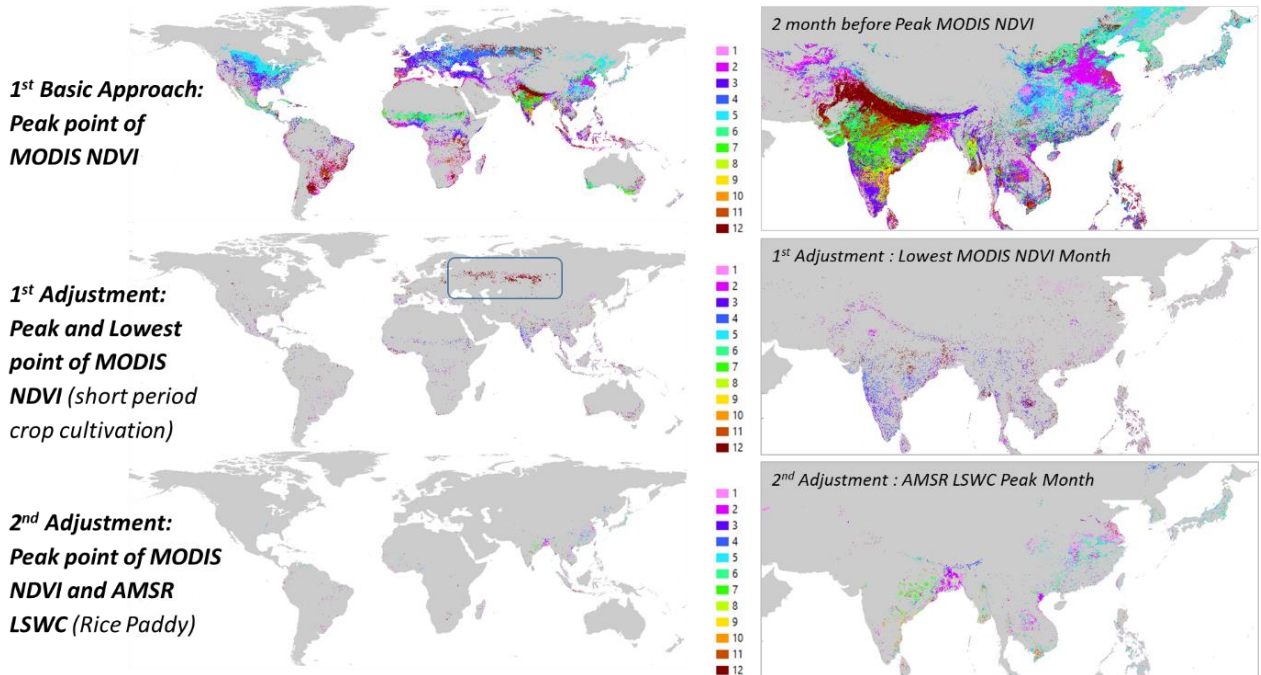


Figure 4-16. Three approaches of sowing month estimation

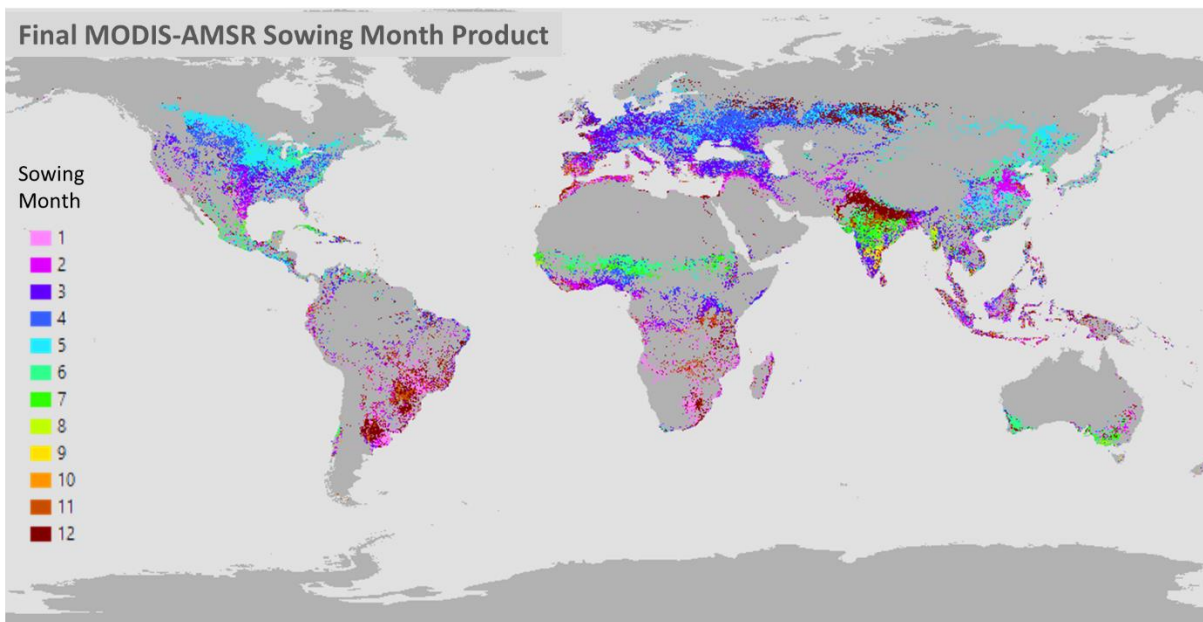


Figure 4-17. The final MODIS-AMSR Sowing month product (2001-2005)

#### 4.4.4 MODIS-AMSR Sowing Month Change 2001-2015

The final product of MODIS AMSR is not only can give an estimation of sowing month in one year, the final products are conduct in long term analysis for fifteen years as shown in figure 4-19. This include first, second and third sowing in each seasons. By 15 years' long-term analysis which represented by sowing month product in three group of year, we can analyze how consistent or how change the sowing month in each pixel in 15 years.

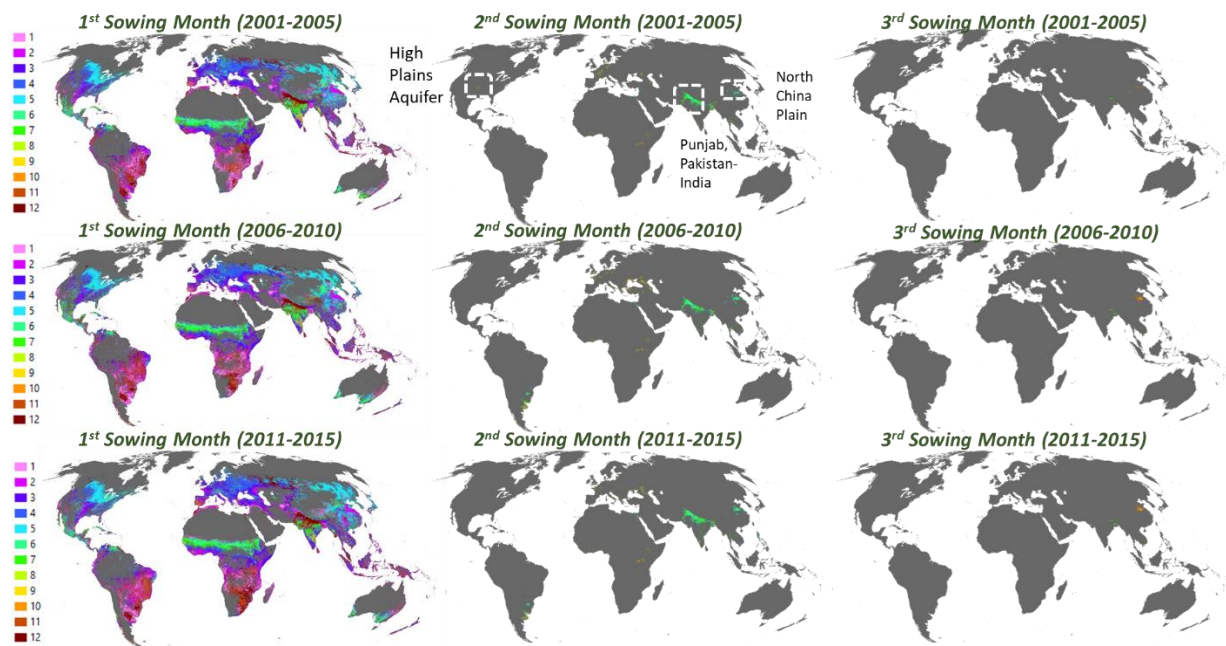


Figure 4-18. Sowing month product in three group of year 2001-2005, 2006-2010 and 2011-2015

In more detail image, we highlight area around boundary of India and Bangladesh that can be seen in Figure 4-20. Form the figure shows how in that area has very high level of intensity that makes analysis of sowing month become more complex. Bangladesh has dominant sowing month in February whereas India has sowing month in March. The different sowing month between two countries are shown in country boundary between two countries. From the result of second and third sowing month period in three group of year, we can interpret how pattern of change in sowing month.

In more detail next analysis will produce agreement product of consistency sowing month product among three group of year. Figure 4-21 shows the sowing month change between 2001-2005 and 2006-2010 also 2006-2010 and 2011-2015. After we analyse the

product two product of sowing month change, we develop final product the agreement level of sowing month consistency from 0 to 12. Value 0 show that in the pixel has very consistent sowing month otherwise value 12 show the most inconsistent sowing month.

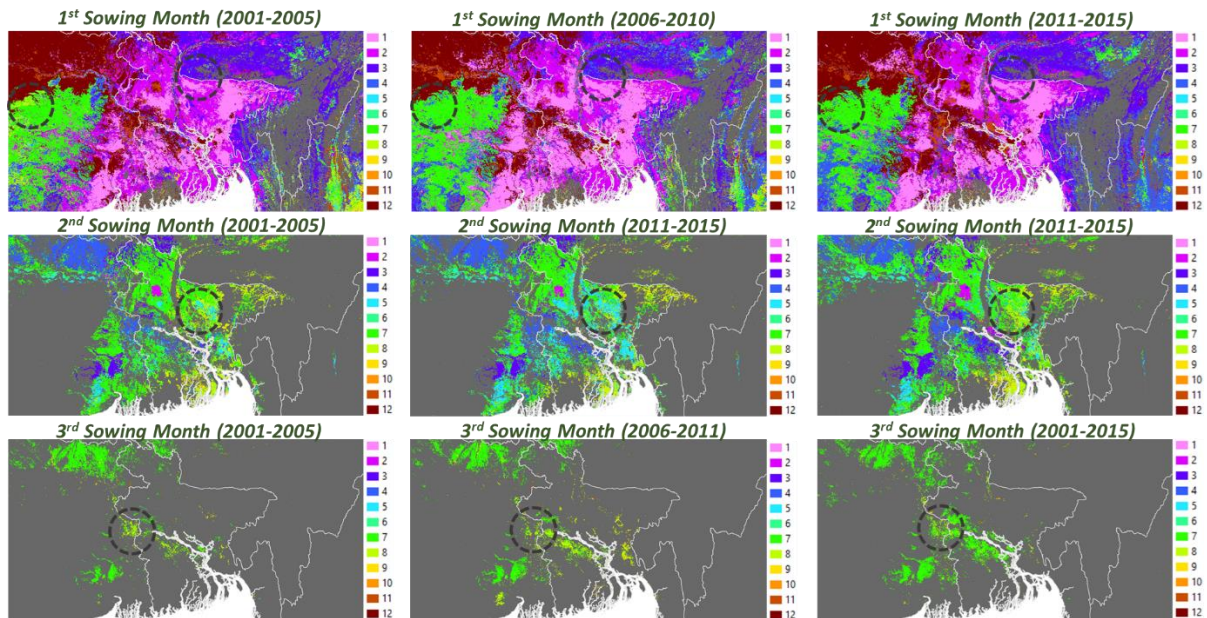


Figure 4-19. Fifteen year sowing month estimation in country boundary of India and Bangladesh

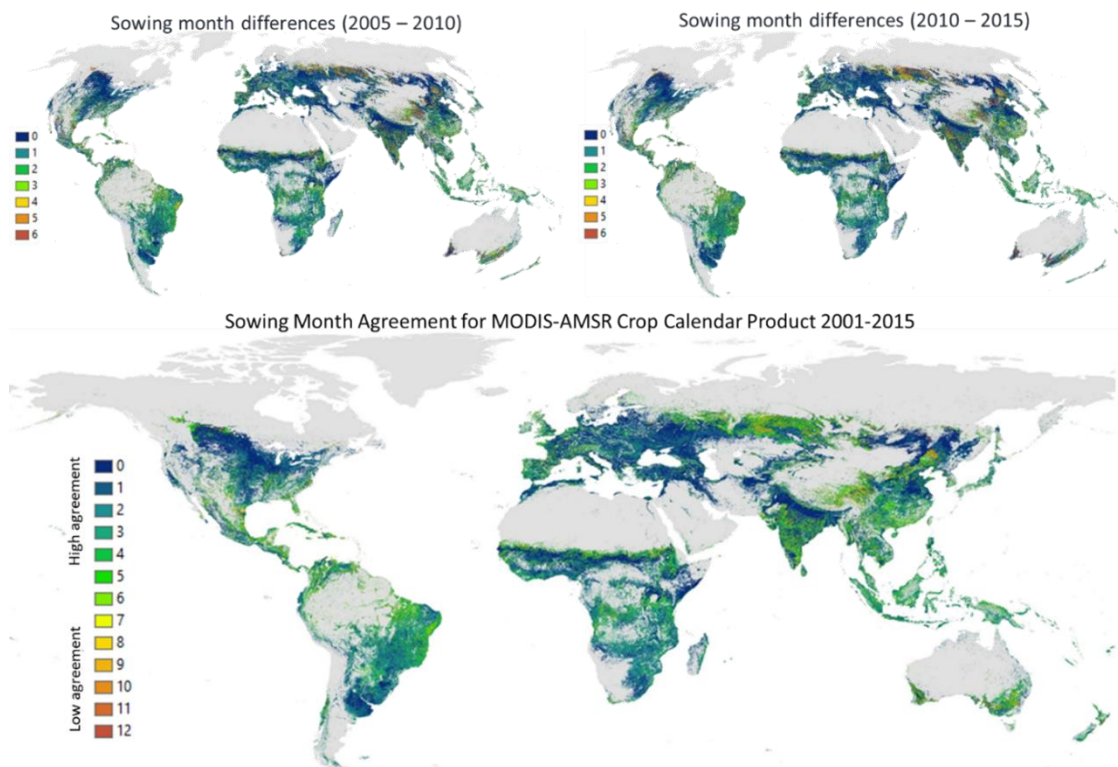


Figure 4-20. Global sowing month difference from 2001 to 2015

The final The sowing month difference among three group of sowing month products was found in dynamic cropping intensity change area such as China, India and Spain. Northern countries like Canada and Russia are also facing different change (figure 4-21). Further investigation needed to describe the reason of this sowing month change and also the impact of this change for food security situation, and projection in future.

#### 4.4.5 Rice and Non-Rice Dominant Cropping Pattern

With the integration of MODIS NDVI and AMSR LSWC products, we were able to classify the cropland types into paddy and non-rice paddy rice crops. By looking at the NDVI and LSWC time series patterns over the average one-year period, the MODIS-AMSR Cropping pattern product can not only distinguish rice paddy and non-paddy in single crop, but also in double and triple crops.

The consequences on double and triple cropping area, cropping pattern of rice and non-rice will produce in multi cropping pattern formation. Double cropping area will have four patterns, i.e. non-rice and non-rice, non-rice-and rice, rice and non-rice, rice and rice, while on triple cropping area there will be eight pattern formations from non-rice, non-rice and non-rice to rice, rice and rice (Triple rice) (Figure 4-22).

Figure 4-22 shows the product of rice non-rice cropping pattern in two contrast regions: Northern part of South Asia and center Africa. In the Northern region of South Asia, rice and non-rice crops in single, double and triple cropping intensities can easily be detected, however in Africa, rice and non-rice crop types are found only in single crop regions. Double crop for non-rice to non-rice is found in small areas in the countries of Ethiopia, Kenya and Uganda. The difficulty to increase crop intensity in Africa region become this region are still facing hunger problem. From eighteen countries were still facing high and very high hunger level based on FAO report (i.e: 1. Afghanistan, 2. Central African Republic, 3. Chad, 4. Congo, 5. Ethiopia, 6. Haiti 7. Liberia, 8. Madagascar, 9. Malawi, 10. Mozambique, 11. Namibia, 12. North Korea, 13. Rwanda, 14. Tajikistan, 15. Uganda, 16. Yemen, 17. Zambia, and 18. Zimbabwe), 15 countries are located in Africa regional.

Increasing crop production in Africa is needed to meet future food demand. Africa population is projected to reach 1,634 million by 2030 (+ 500 million) [NEPAC, 2003]. Undernourished population increases by 35 million over the last 20 years. Crops represent 89% of the diet in Sub-Sahara Africa (SSA). Human food commodity to increase by 15% in the next

40 years. Crop production growth in SAA is mainly due to the extension of cultivated area and cropping intensities while crop yield improvement is low.

To analyze cropping pattern in single, double and triple area, we analyzed the distribution of cropping patterns in several regions. Figure 4-23 shows single crop intensity of rice and non-rice cropping pattern in North America, Europe and South America. Figure 4-24 shows double crop intensity of rice and non-rice cropping pattern in Southeast Asia, China and Europe. Figure 4-25 shows triple crop intensity of rice and non-rice cropping pattern in Bangladesh, Vietnam, China, Thailand and Philippines. The area of double rice is widely found in the northern part of Java province Indonesia and China. For investigations in the triple cropping region we compiled two regions of Bangladesh and the Mekong delta Vietnam which has large area of triple cropping intensity area, the results shows that triple rice only can be widely detected in the Mekong delta Vietnam rather than in Bangladesh (Figure 4-23).

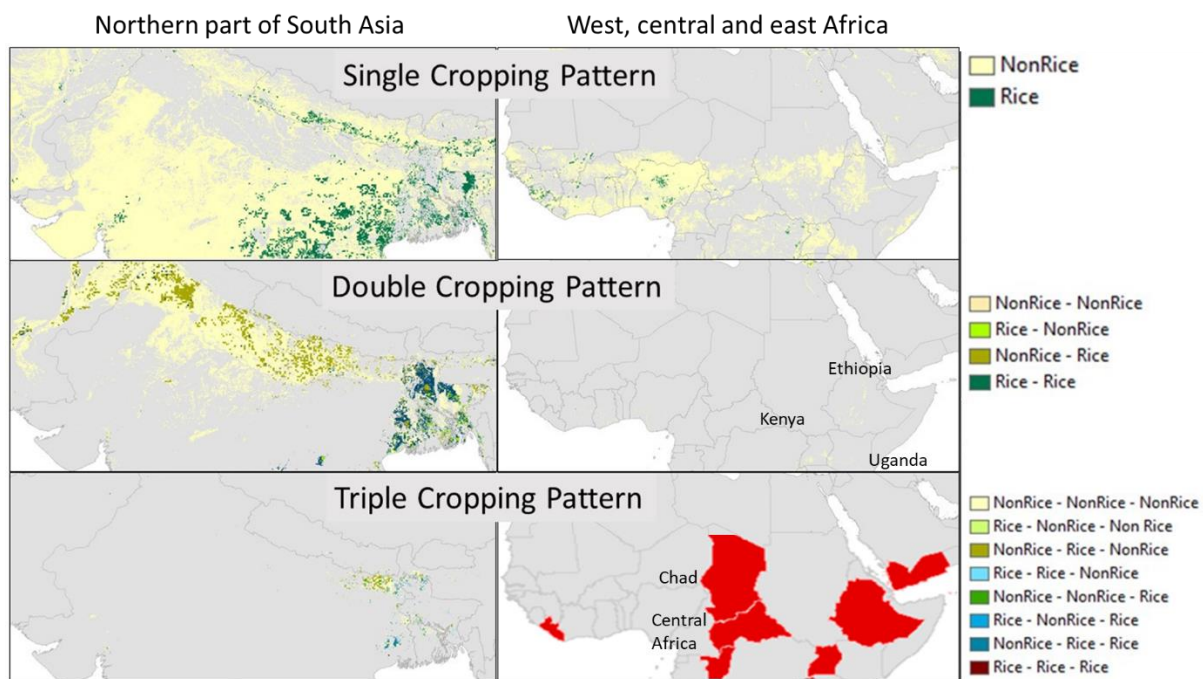


Figure 4-21. Rice and non-rice cropping pattern formation in South Asia and Central Africa for single, double and triple cropping intensity area



**Figure 4-22.** Distribution of 18 countries target that is still facing very high and high hunger levels [Data Source: FAO., 2016]

To investigate how this vegetation and water index of MODIS-AMSR integration are working, we used Bangladesh official data of dominant cropping pattern (figure 4-26). This data derived from ground survey database in 2001 year of data. From the data rice in Bangladesh are categorized into three rice type there are Boro, Ault and Aman. Boro which categorized as the highest quality and highest water demand are mainly planting in first cultivated session.

#### Single Cropping Pattern

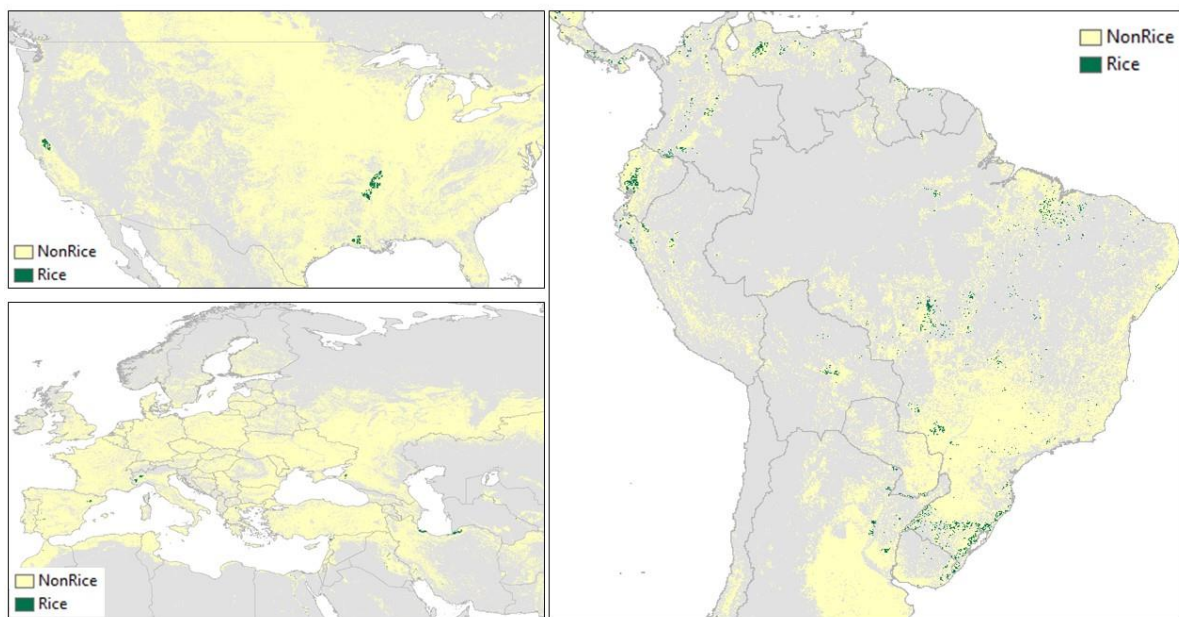


**Figure 4-23.** Single crop intensity of rice and non-rice cropping pattern in North America, Europe and South America

### Double Cropping Pattern

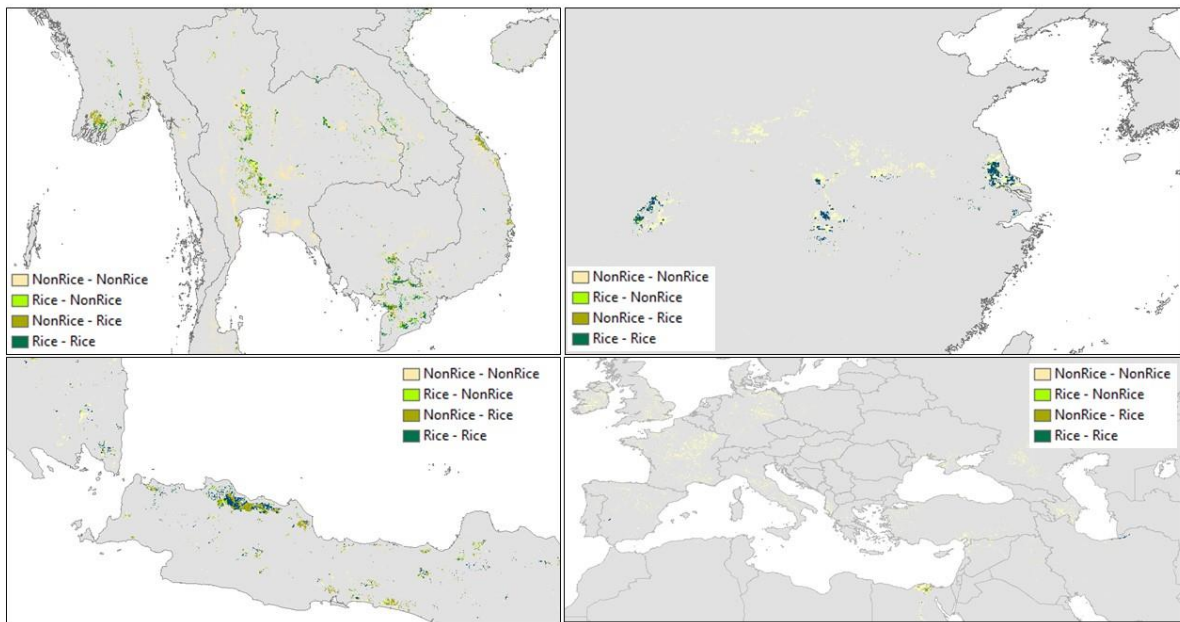


Figure 4-24. Double crop intensity of rice and non-rice cropping pattern in Southeast Asia, China and Europe

### Triple Cropping Pattern

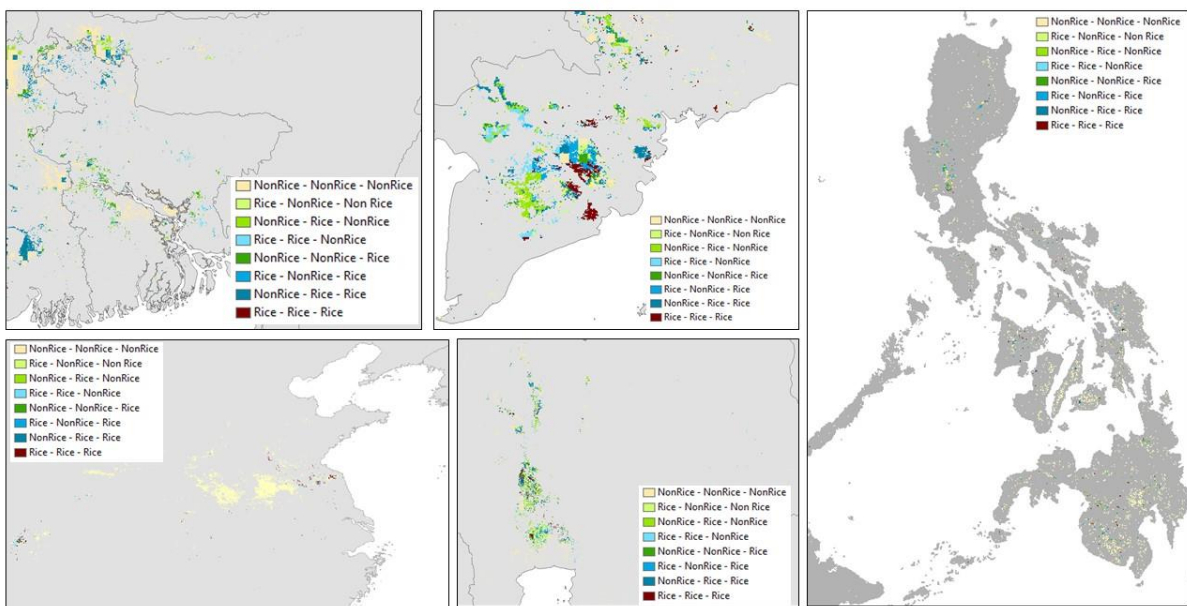


Figure 4-25. Triple crop intensity of rice and non-rice cropping pattern in Bangladesh, Vietnam, China, Thailand and Philippines.



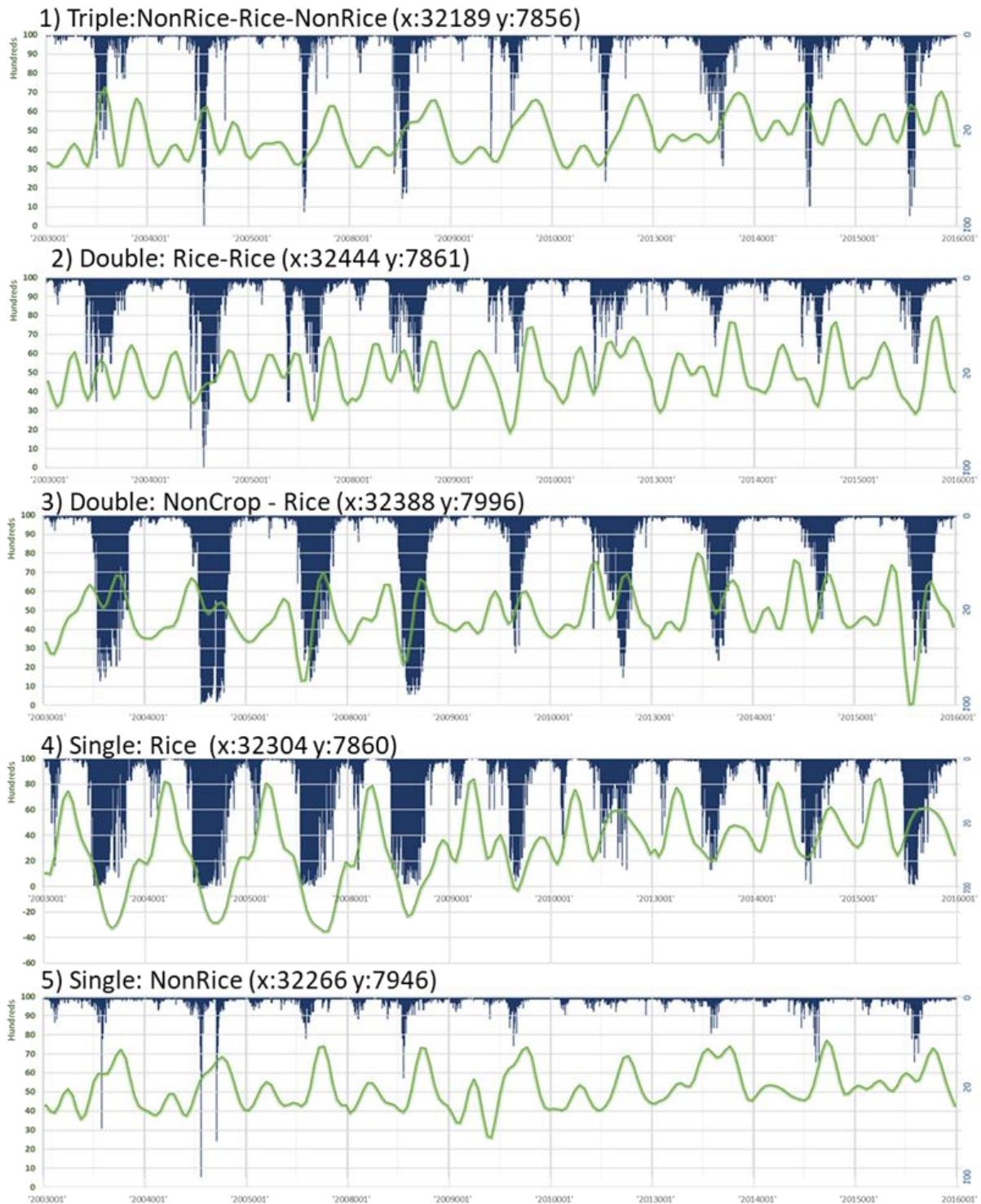


Figure 4-27. Integration strategy between time-series of 16 days composite DFT MODIS NDVI and daily AMSR LSWC several cropping pattern formations in Bangladesh

We applied the long-term time series DFT MODIS NDVI and LSWC AMSR-E/2 data analysis in five selected cropping pattern and simplify cropping pattern formation into rice and

non-rice crop type: 1. Triple: non-rice, rice, non-rice 2.) Double: rice and rice, 3) Double: non-rice and rice, 4). Single: Rice, 5) Single: non-rice (figure 4-27). This long-term time series data analysis investigated in nine years monitoring: 2003, 2004, 2005, 2008, 2009, 2010, 2013, 2014 and 2015.

In non-rice, rice, non-rice cropping pattern area, time series of MODIS NDVI shows has three peak dominants in each year and AMSR LSWC has one peak that located in the second peak of MODIS NDVI, this cropping pattern indicates that three cultivated sessions are identified where rice paddy plantation is located in second session.

## **4.5 Comparative Analysis**

In this section, the developed remote sensing products in this study are compared with previous research data product. The difficulty to find reference data from ground measurement that represents the actual data become main reasons we use comparative analysis rather than accuracy assessment approach. Some comparative analysis of studies conducted among others in this study are: 1. Comparison of the MODIS cropping intensity and SACRA product, 2. Comparison of cropping intensity change with HYDE V.3.2 irrigated rainfed change, and 3. Comparison of the MODIS-AMSR sowing month product with three previous sowing month products.

### **4.5.1 Comparison of Double and triple cropping area Estimates from the MODIS CI, SACRA and ZABEL with the Irrigated area FAO Data**

To evaluate cropping intensity area estimation results on the national and sub-national level, double and triple cropping intensity areas derived from the MODIS CI, SACRA CI and ZABEL CI products are compared to the irrigated area estimates from FAO-stat 2003, 2008 and 2010 as a statistical data reference. For national level we analyses 162 countries and for sub-national countries we select 51 states of U.S (Figure 4-28 and Figure 4-31).

Since there are no validated data of single, double and triple cropping intensity area in global scale, we proposed irrigated are as alternative reference data, since active cropping intensity area like double and triple area has tendency located in irrigated area. High amount source of water that located irrigated area could make cultivation period become two or three

time per year. For preliminary investigation we compare product of MODIS cropping intensity product with irrigated area distribution.

Table 4-2 shows research list of mapping cropland (irrigated and rainfed) and irrigated cropland fraction and table 4-3 shows research list of mapping cropland (irrigated and rainfed) and irrigated cropland fraction change. From the list of Irrigation mapping research, we used HYDE v 3.2 for preliminary investigation because this data can provide irrigated distribution map in multiyear analysis, which developed by combination of cropland - pasture statistic data, satellite information, specific allocation algorithms (which change over time), and weighting maps of the HYDE rules to create spatially explicit maps, which are fully consistent on a 5 longitude/ latitude grid resolution, and cover the period 10,000 bc to ad 2000. The input data for developing HYDE product include: Irrigated area statistic from FAO, monthly irrigated andrain-fed crop areas around the year 2000 (MIRCA2000), and Irrigated data from GMIA\_v5 [Siebert, 2008; Siebert et al.,2015].

Table 4-2. Research list of cropland (irrigated and rainfed) and irrigated cropland fraction

| No   | Data Source                                | Baseline Year | Spatial resolution | Source Data Download |
|--|--|---------------|--------------------|----------------------|
| <b>Cropland Fraction (Irrigated-Rainfed)</b> |  |               |                    |                      |
| 1  | Ramankutty and Foley, 1998                 | early 1990s   | 1 km               | Available            |
| 2  | Thenkabail et al., 2009 (GIAM)             | 2000          | ~10 km             | Available            |
| 3  | Goldewijk et al., 2009 (HYDE v1)           | -             | -                  | -                    |
| 4  | Portmann et al., 2010 (MIRCA2000)          | 2000          | 10 km              | Available            |
| 5  | Fritz et al., 2015 (IIASA Cropland Hybrid) | 2005          | 1 km               | Available            |
| <b>Irrigated Cropland Fraction</b>           |  |               |                    |                      |
| 1  | Siebert et al., 2006 (GMIA V.4)            | 2000          | ~10 km             | -                    |
| 2  | Thenkabail et al., 2009 (GIAM)             | 2000          | 10 km              | Available            |
| 3  | Siebert et al., 2013 (downscaled GMIA V.5) | 2000          | 10 km              | Statistic Data only  |
| 4  | Salmon et al., 2015 (GRIPCmap)             | 2005          | 500 m              | Available            |
| 5  | Thenkabail et al., 20016 (GFSAD1KCD)       | 2010          | 1km                | Available            |

Table 4-3. Research list of cropland (irrigated and rainfed) and irrigated cropland fraction change

| Research on Irrigated – Rainfed Fraction change |            |  |                                      |                            |                       |
|---|------------|--|--------------------------------------|----------------------------|-----------------------|
| Source  | Resolution | Baseline Product                                 | Year range                           | Product Data               | Data Availability     |
| Hanasaki et al., 2013                           | 50 km      | Siebert et al., 2006 (GMIA V.4)                  | 2000-2100                            | Irrigated Crop             | No Available          |
| Siebert et al., 2015                            | ~10 km     | Siebert et al., 2006 (GMIA V.4)                  | 1900-2005 *10 year interval          | Irrigated Crop             | Available             |
| Goldewijk et al., 2017) HYDE V.3.2              | ~10 km     | ESA CCI LC V.2.6 Siebert et al., 2006 (GMIA V.4) | 10 000 before Common Era (BCE) -2017 | Irrigated and Rainfed Crop | Available             |
| Maier et al, 2017 (on going discussion)         | ~1 km      | -  | 1999 to 2012                         | Irrigated                  | Available on request. |

Based on visual comparison some countries such as India, Thailand and Vietnam are countries with high correlation between irrigated area and active cropping intensity (double and triple) area (Figure 4-28), however not all country has this tendency, some countries like United States, China, and Japan are countries with low correlation between irrigated area and active cropping intensity (double and triple) area (Figure 4-29). The low correlation which shows in comparison between double-triple cropping and irrigated area, indicated that in some country, irrigated area still cannot boost food production with increasing intensity. the reasons behind this condition is because combination climate condition and physical land condition that make increasing intensity in irrigated area difficult.

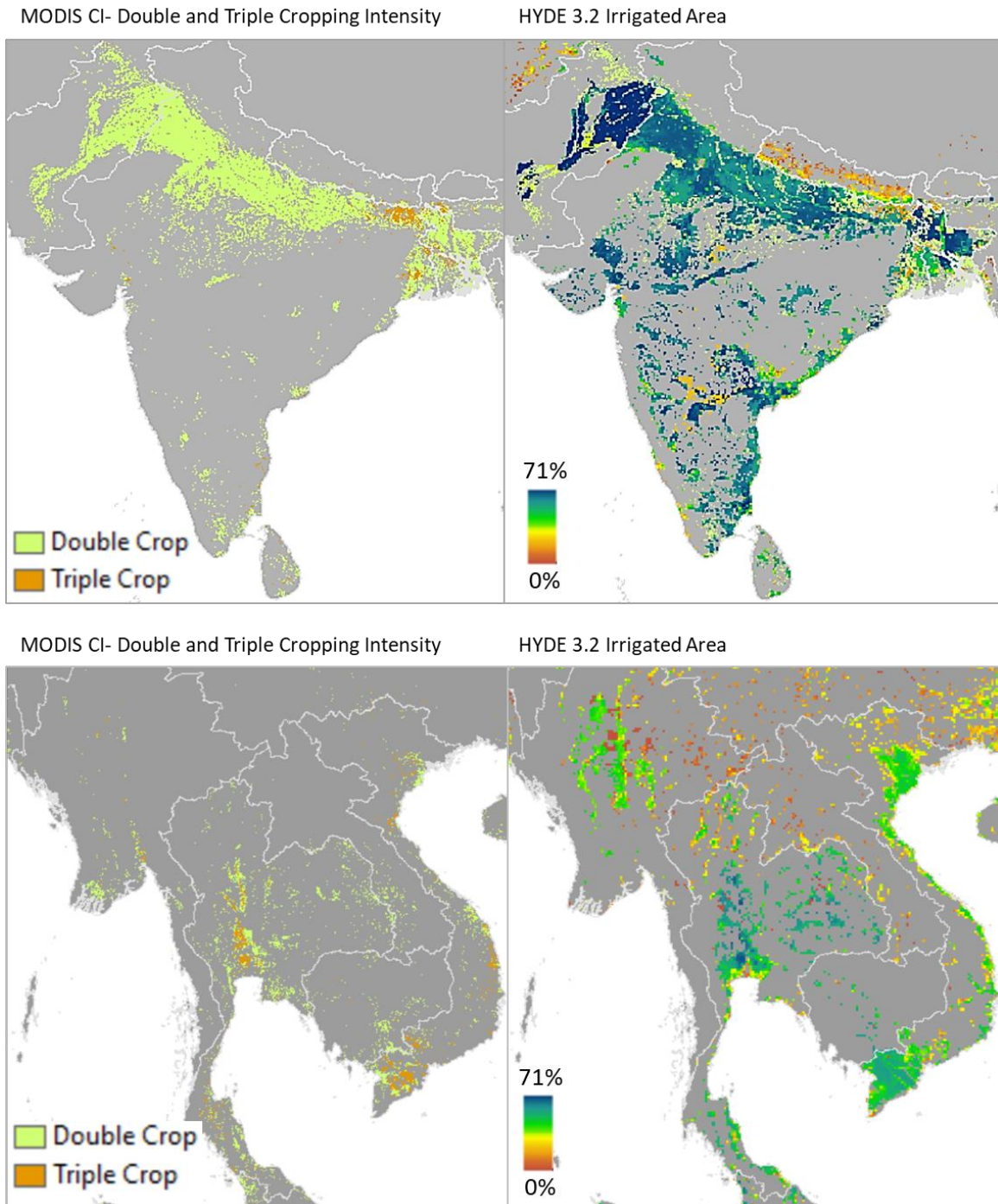
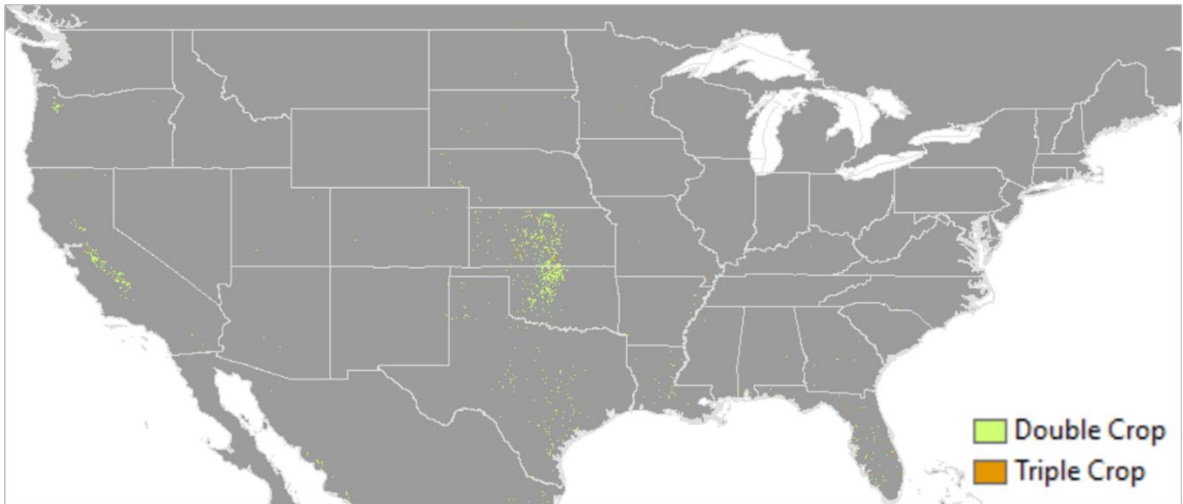
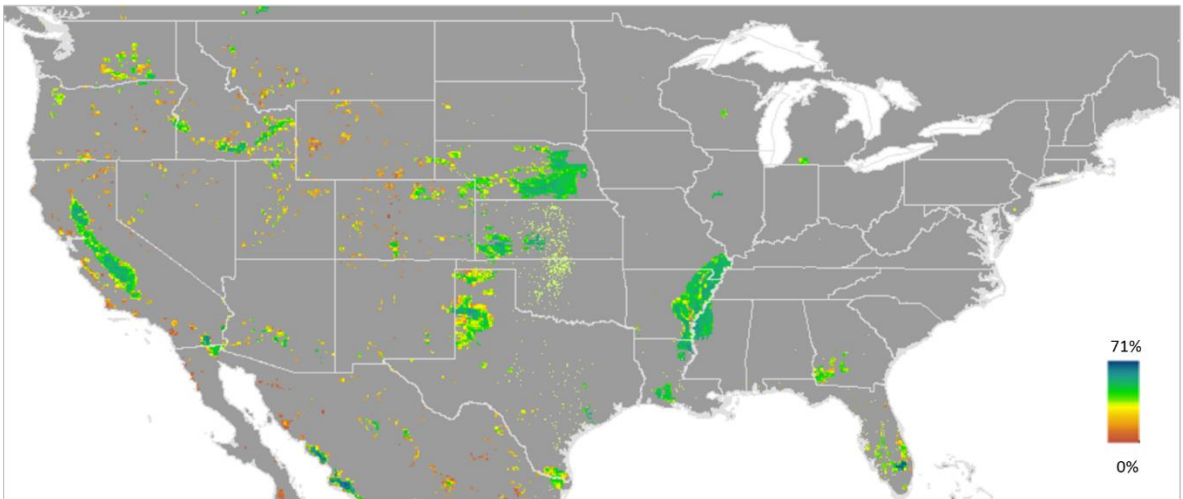


**Figure 4-28.** India, Thailand and Vietnam are countries with high correlation between irrigated area and active cropping intensity (double and triple) area

MODIS CI- Double and Triple Cropping Intensity



HYDE 3.2 Irrigated Area



MODIS CI- Double and Triple Cropping Intensity

HYDE 3.2 Irrigated Area

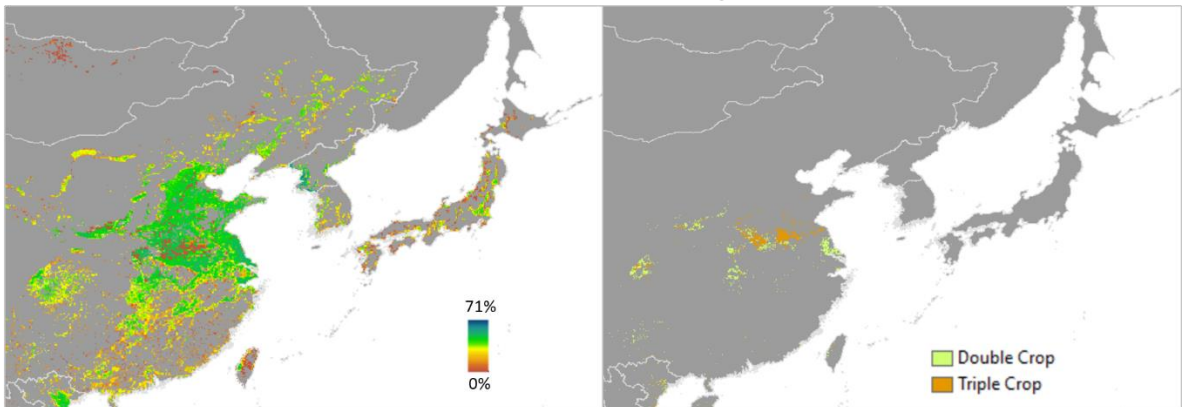


**Figure 4-29.** United States, China, and Japan are countries with low correlation between irrigated area and active cropping intensity (double and triple) area

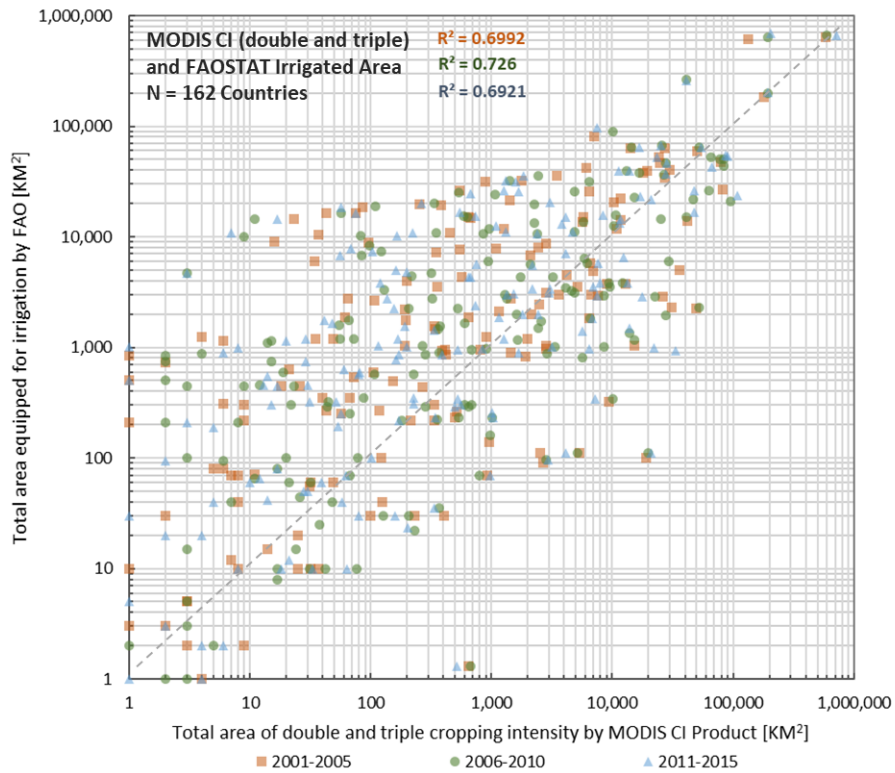


**Figure 4-30.** Comparison of modelled double and triple cropping area derived from MODIS CI product to FAO irrigated reported statistics [km<sup>2</sup>] per country (N = 162).

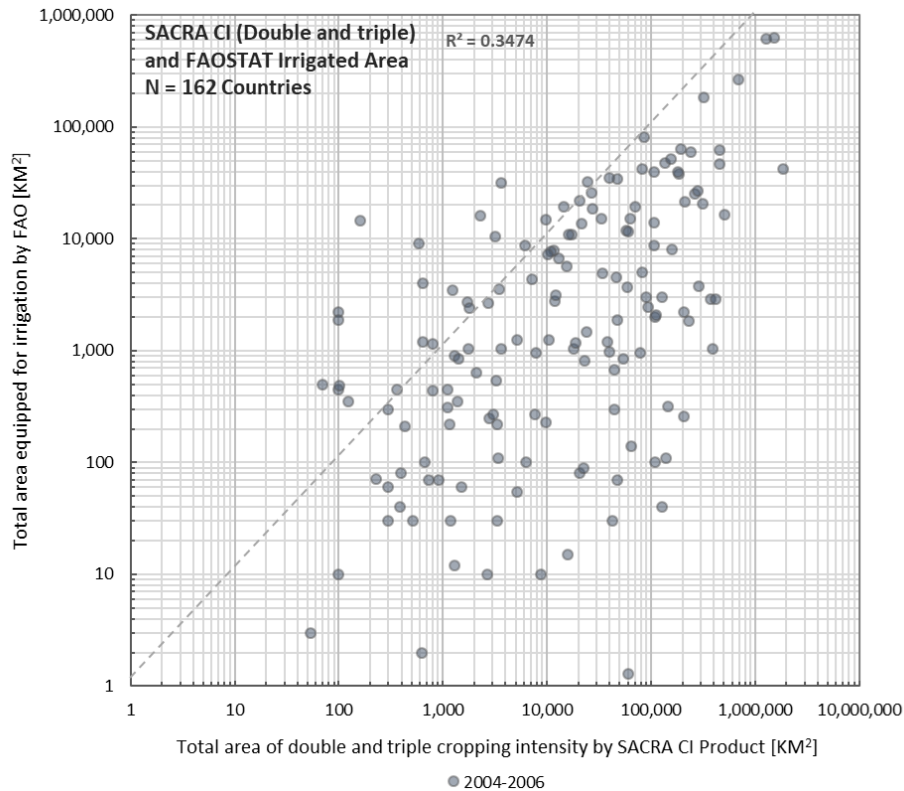


**Figure 4-31.** Comparison of modelled double and triple cropping area derived from SACRA CI product to FAO irrigated reported statistics [km<sup>2</sup>] per country (N = 162).

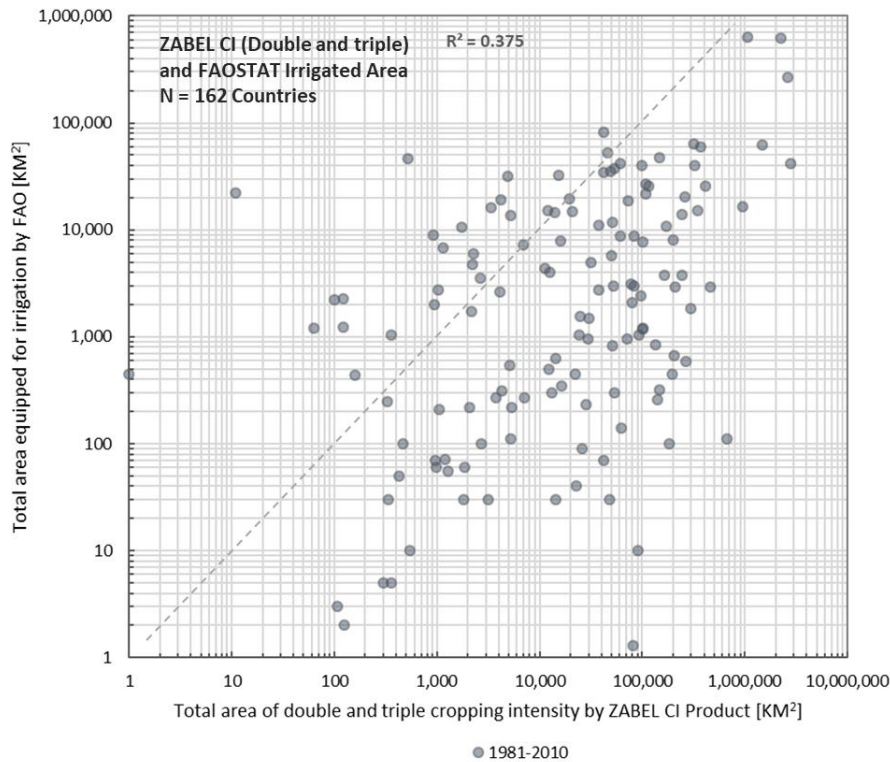


**Figure 4-32.** Comparison of modelled double and triple cropping area derived from ZABEL CI product to FAO irrigated reported statistics [km<sup>2</sup>] per country (N = 162).

The overall correlation is observed in global scale with total 162 countries for MODIS CI product of 2001-2005, 2006-2010 and 2011-2015 respectively and shows some proximity between the MODIS CI analysis and the FAO irrigated area with a 0.699, 0.726 and 0.692 regression value (Figure 4-28). We also analyze the accuracy of the two existing cropping intensity product SACRA and ZABEL product datasets to FAO statistics. In this framework, the regression value to the FAO have been observed as 0.34 for SACRA product (Figure 4-29) and 0.37 for ZABEL product (Figure 4-30). The comparison between MODIS double triple cropland area and irrigated area shows that double and triple crop area are underestimate compare with irrigated FAO data. In subnational data analysis we compare double-triple cropping intensity area with USDA statistic of irrigated area reported statistics in 51 states of United states.

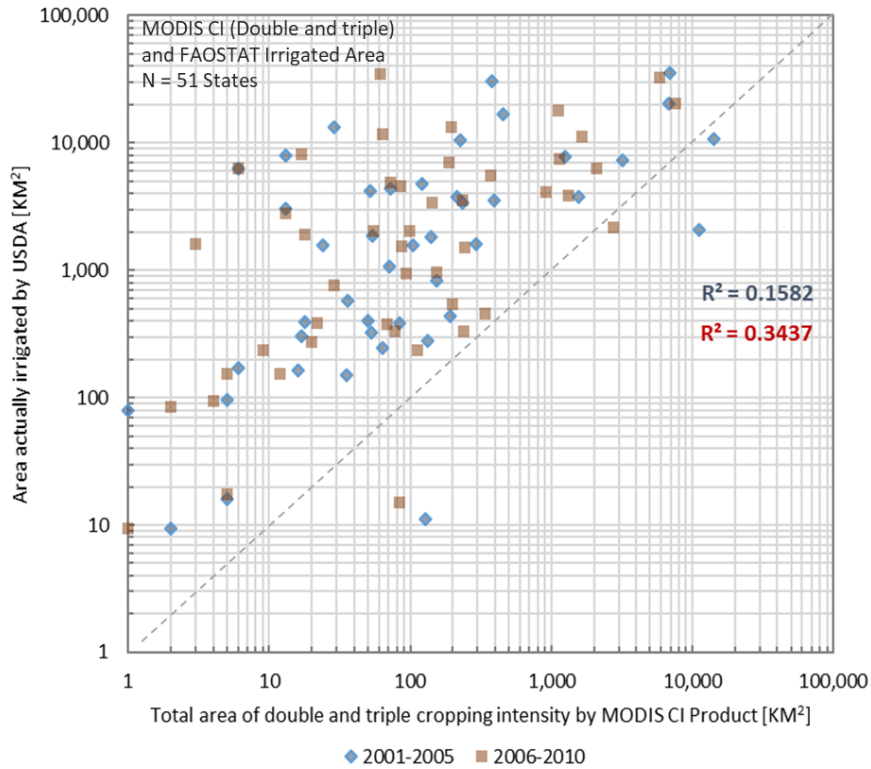


**Figure 4-34.** Comparison of modelled double and triple cropping area derived from MODIS CI product to USDA irrigated area reported statistics [km<sup>2</sup>] in 51 states of United States (US) (N = 162).

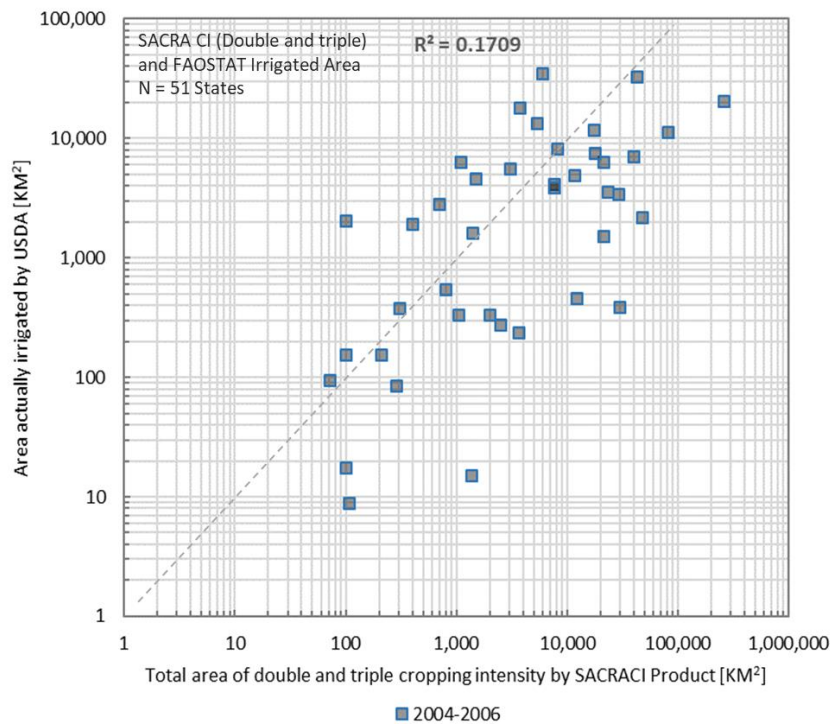


**Figure 4-35.** Comparison of modelled double and triple cropping area derived from SACRA CI product to USDA irrigated area reported statistics [km<sup>2</sup>] in 51 states of United States (US) (N = 162).

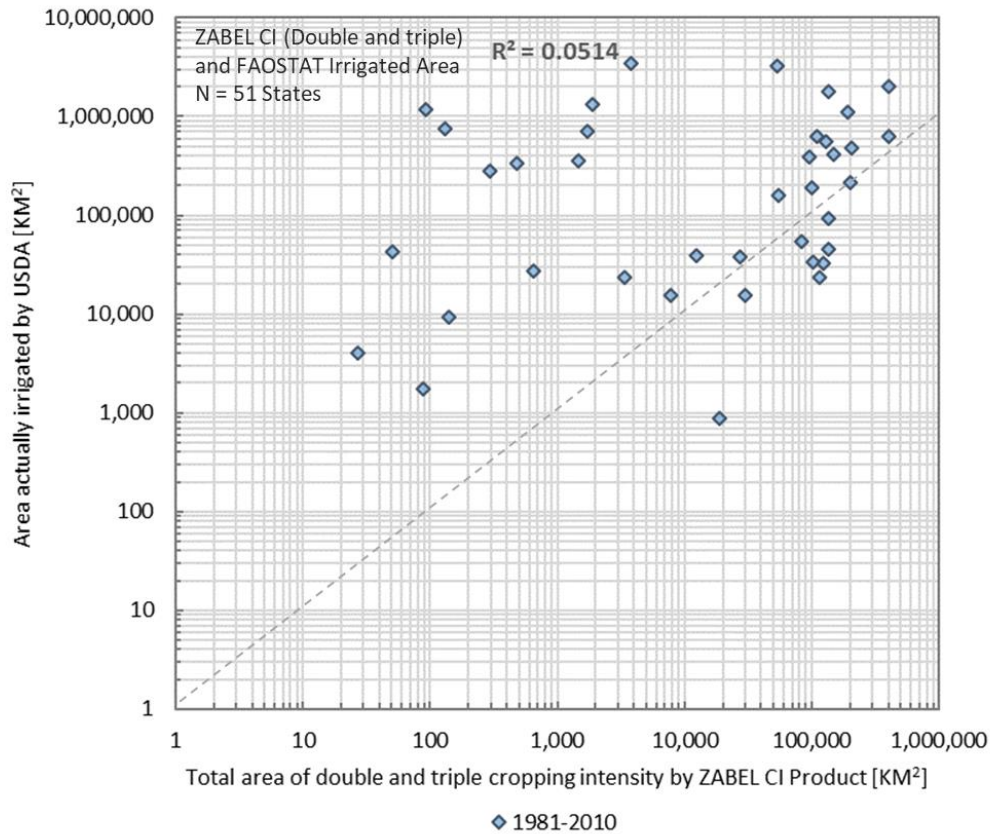


**Figure 4-36.** Comparison of modelled double and triple cropping area derived from ZABEL CI product to USDA irrigated area reported statistics [km<sup>2</sup>] in 51 states of United States (US) (N = 162).

The overall correlation is observed in global scale for USDA Irrigated area of 2001-2005 and 2006-2010 respectively and shows some proximity between the MODIS CI analysis and the USDA irrigated area with a 0.158 and 0.343 regression value (Figure 4-31). We also analyze the accuracy of the two existing cropping intensity product SACRA and ZABEL product datasets to USDA statistics. The regression value to the USDA have been observed as 0.17 for SACRA product (Figure 4-32) and 0.051 for ZABEL product (Figure 4-33).

The statistical result for both national and sub-national values promote the MODIS CI product as the most accurate dataset compared to FAO-stat within another two datasets in estimating active cropping intensity area (double and triple crop). Also, MODIS Double and triple area are the only product with underestimate result compare to Irrigated area, this condition follow the fact that not all irrigated area producing double and triple, hence the irrigated area should show larger total area value rather than total double and triple area.

Double and triple cropping intensity was modelled with the time series MODIS NDVI. Irrigated reported statistics at national level was obtained from the FAO-Stat database (<http://www.fao.org/nr/water/aquastat/main/index>). Based on the definition from FAO statistics, irrigated cropland is defined as “Total area equipped for irrigation” [Vancutsem et al., 2013]. However, irrigated reported statistics at subnational level in 51 states of US was obtained from the USDA database. We used logarithmic scale in scatterplot analysis to accommodate all countries irrigated area with high range from 1 km<sup>2</sup> to 200,000 km<sup>2</sup>. The dashed line represents the 1:1 slope.

Good correlation of the results to FAO statistics is still not enough for quality assessment of the product, accurate validation it is worth to compare the product with some more precise country level cropping intensity area (Single, double and triple) which have higher resolution. Globland30 [Chen et al., 2014] and Unified Cropland layer [Waldner et al., 2016] as one of the alternative for the analysis in next study. However, to provide more comprehensive analysis we develop agreement level product of cropping intensity for double and triple cropping intensity area.

#### 4.5.2 Agreement level analysis of the MODIS Cropping Intensity with SACRA and Zabel CI products

For cropping intensity analysis, we focus for comparing between MODIS and SACRA on double and triple cropping intensity. Figure 4-25 shows the agreement analysis result between MODIS, SACRA and Zabel cropping intensity product. In double cropping intensity area Pakistan, Egypt, Bangladesh and India are top four country which has high agreement between the two cropping intensity data. However, if the agreement level is compare globally. Some area that difficult to produce double intensity due to low irrigation infrastructure and low precipitation are detected has double crop intensity in large area such as in Africa region.

Based on the statistics result, table 4-1. Shows distribution of three agreement level of three cropping intensity product in double and triple cropping intensity product. SACRA CI product is overestimating in double cropping, because 76% of SACRA CI product is in agreement level 1. Zabel CI product is overestimating in triple cropping, because 98.5% of Zabel CI product is in agreement level 1. MODIS product is dominating in agreement level 2 and level 3: for double cropping (83.1%) and for triple cropping (64.4%). Based on the

distribution of level 2 and level 3, shows how MODIS is the most reliable product since has dominant pixel that located in higher agreement level of level 2 and level 3.

In triple cropping area, since triple crop are located in smaller area compare with double and single, higher pixel resolution of 1 km MODIS cropping intensity show promising result for detecting triple cropping compare with 10 km SACRA product, where India, Vietnam, China and Bangladesh has highest cropping intensity compare other country which has triple cropping area (Figure 4-29).

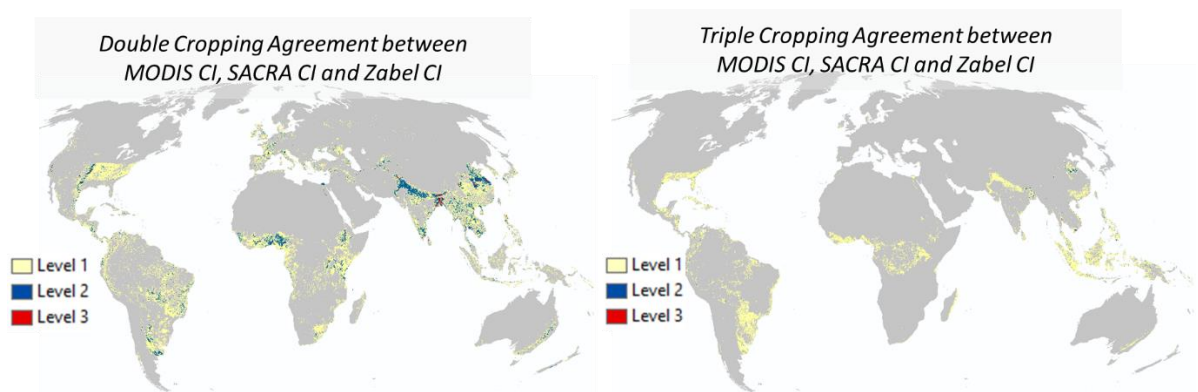


Figure 4-28. Agreement analysis between MODIS and SACRA cropping intensity in double (right) and triple cropping area (left)

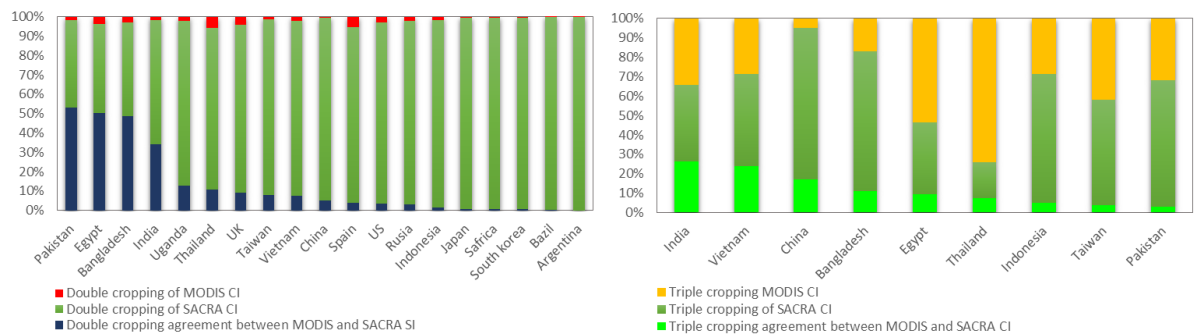


Figure 4-29. Country level analysis of agreement level between MODIS and SACRA Cropping Intensity products

Table 4-4. Analysis of three agreement level in double and triple cropping based on three cropping intensity data product of MODIS, SACRA and Zabel cropping intensity

| Cropping Intensity Data Products | Double Cropping Agreement (%) |         |         | Total Pixel Number | Triple Cropping Agreement (%) |         |         | Total Pixel Number |
|----------------------------------|-------------------------------|---------|---------|--------------------|-------------------------------|---------|---------|--------------------|
|                                  | Level 1                       | Level 2 | Level 3 |                    | Level 1                       | Level 2 | Level 3 |                    |
| MODIS CI 2001-2005               | 16.9                          | 69.8    | 13.3    | 1,590,956          | 35.6                          | 58.8    | 5.6     | 201,032            |
| SACRA CI 2004-2006               | 76.0                          | 23.8    | 0.2     | 15,109,469         | 76.4                          | 21.8    | 1.8     | 611,550            |
| Zabel CI 1981-2010               | 72.8                          | 25.3    | 1.9     | 11,114,799         | 98.5                          | 1.4     | 0.1     | 9,266,770          |

### 4.5.3 Comparison of Cropping Intensity Change with HYDE V.3.2 Annual Irrigated Rainfed

Another strategy to analyse the quality of MODIS cropping intensity product is by comparing product of MODIS cropping intensity change with HYDE irrigated rainfed area change, the reasons is because extending irrigated area has influence to increase intensity. We analyze the comparison by visual interpretation. HYDE is annual fraction of irrigated and rainfed product that use remote sensing product as base map and statistic approach for analysis the changes (figure 4-30).

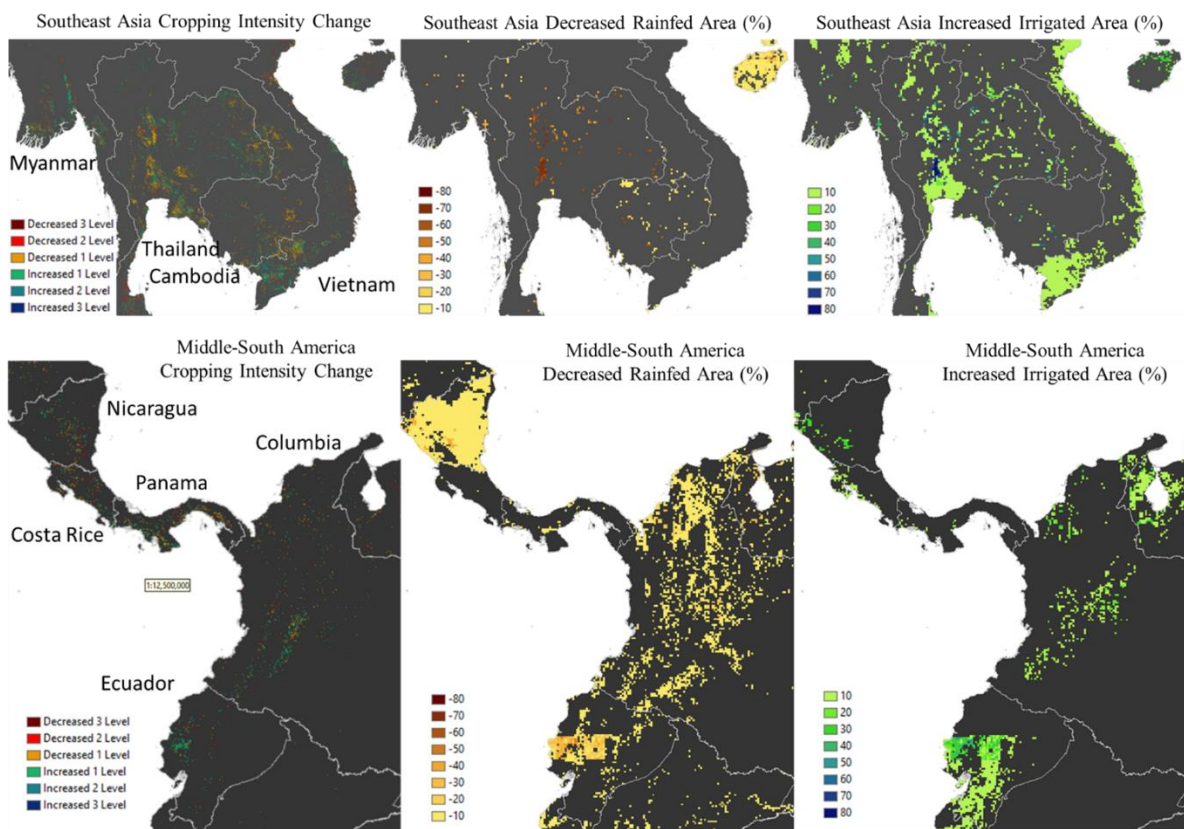


Figure 4-30. Comparison of MODIS cropping intensity product with HYDE Irrigated-rainfed area change from 2005-2015 in SEA and middle America regions

For making two product cropping intensity change and Irrigated-rainfed change in same level data, we using 2005 and 2015 data product for both datasets and produce MODIS Cropping intensity and HYDE irrigated rainfed change between 2005 to 2015.

The results show that intensity changes product which derived from MODIS has correlation with the change of irrigated and rainfed area which derived from HYDE product. However, the assumed dominant crop derived in 1 km MODIS cropping intensity product is

the major source of the difficulty to distinguish the change of rainfed and irrigated in cropping intensity product and source discrepancy in this analysis.

#### 4.5.4 Comparison of the MODIS-AMSR Product with other Sowing Month Products

Three existing data which represented three approaches: census based, modelling and remote sensing base, to be used for compared with MODIS-AMSR sowing month product. Since, our product released in unit of sowing month with aggregate 30 arc minute resolution (or 1 km in center earth). All three previous sowing month products have harmonized process to re-produce the data in same level with MODIS-AMSR sowing month product.

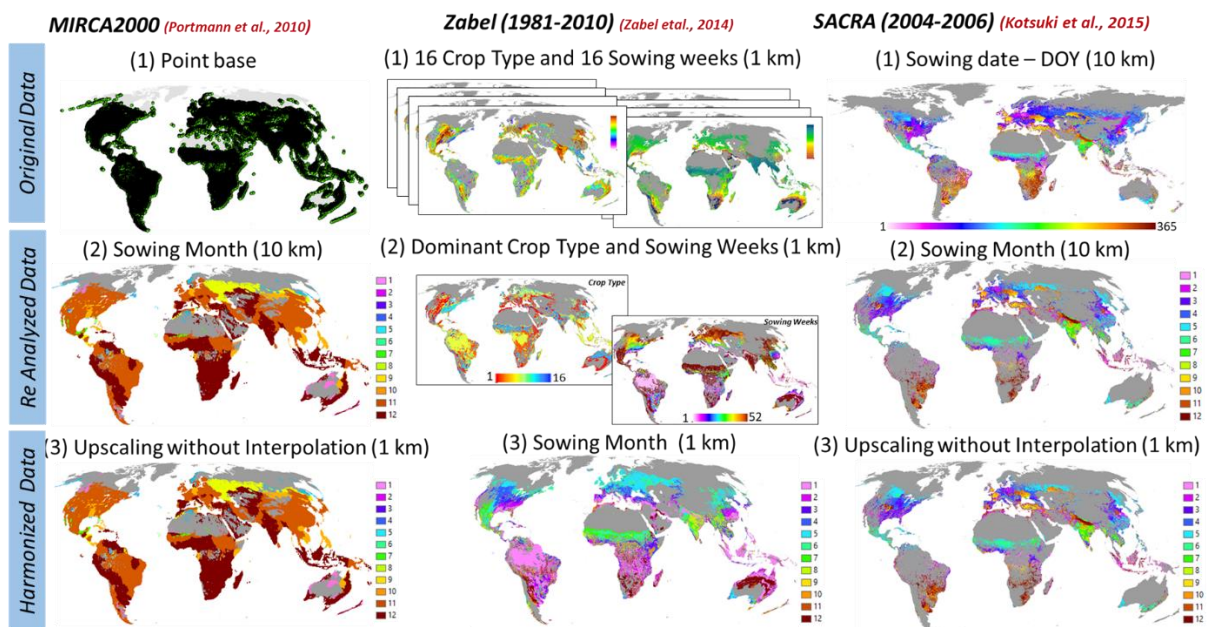


Figure 4-31. Three steps of harmonization process of previous sowing month product

Figure 4-31 show three previous product in three level data: 1). original product, 2). re-analysed and 3). final harmonized product. Where all previous product we convert from DOY (SACRA) or Sowing weeks (ZABEL) into sowing month unit. Since the unit target is sowing month, for increasing pixel resolution from 50 km (MIRCA2000) or 10 km (SACRA) into 1 km pixel resolution we applied upscaling without interpolation approach (figure 4-32).

The last procedure is comparison between MODIS-SOWING month product with harmonized product of MIRCA, ZABEL and SACRA sowing month product. The comparison product has to be converter by cycling mode to simplify sowing month different analysis. Before cycling mode, the different between two sowing month product can be -11 to +11

(Planting earlier 11 month or late 11 month), after cycling mode process the sowing month different between two sowing month product can be 0 to 6, it is mean the different of each pixel can be 0 month (same month) to 6 months (Figure 4-33). Figure 4-34. Shows the visual comparison among four harmonized sowing month product of MODIS-AMSR, MIRCA2000, Sacra and Zabel, which zoom in in southern and south east part of Asia.

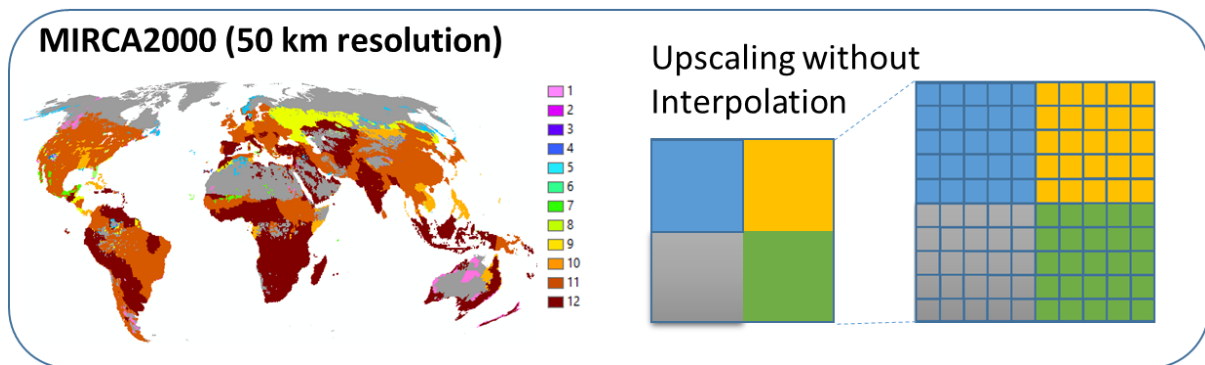


Figure 4-32. The process of upscaling without interpolation for 50 km and 1 km pixel resolution to 1 km

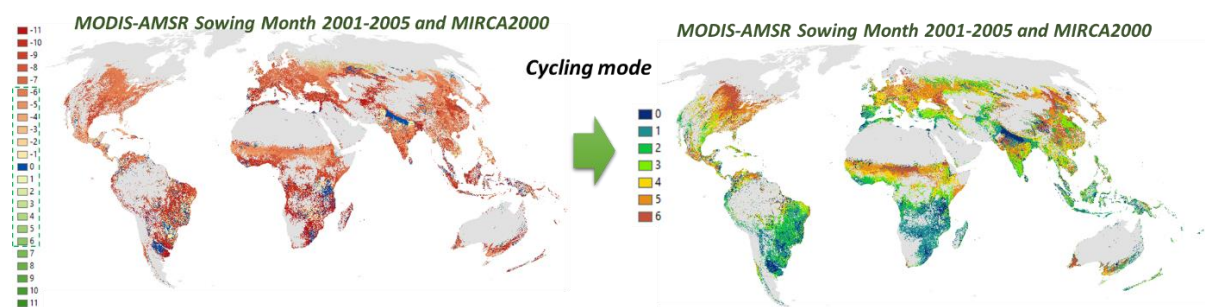


Figure 4-33. Cycling mode approach to simplify sowing month different analysis

The figures compare sowing dates averaged over the pixel based units. In this comparison we only used single cropping grids to compute the averaged sowing date for MODIS-AMSR Sowing month. The result of comparison analysis between MODIS-AMSR sowing month 2001-2005 product with previous three sowing month products shows that MODIS-AMSR sowing month product has a similar pattern with SACRA product (2005-year baseline) however MODIS-AMSR sowing month product has a big difference with MIRCA2000 (2000-year baseline) (Figure 4-35).

Figure 4-34 shows the sowing month different between MODIS-AMSR sowing month product and three previous sowing month MIRCA, ZABEL and SACRA. Comparison between

MODIS-AMSR and MIRCA are dominantly has five months different. Compare with SACRA and ZABEL which have dominant in one month different. In sowing month different distribution, by implementing 1<sup>st</sup> and 2<sup>nd</sup> adjustment in MODIS-AMSR can reduce six months different in comparison analysis with SACRA and ZABEL products (figure 4-35).

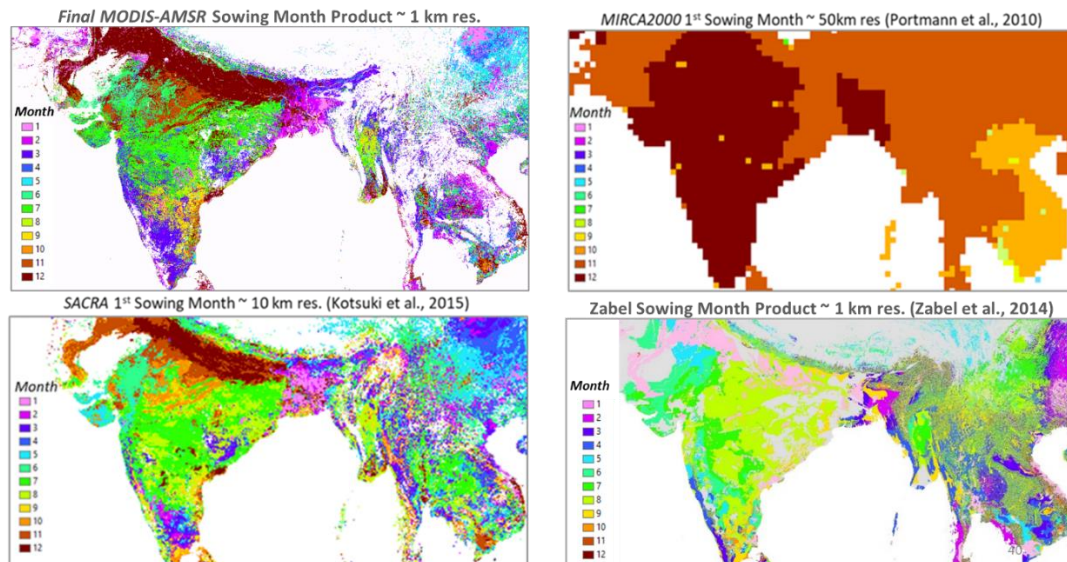


Figure 4-34. Comparison of the MODIS-AMSR sowing month product (2001-2005) with three previous sowing month product of MIRCA2000, SACRA and Zabel.

We highlight the comparison of two countries Bangladesh and Japan. Figure 4-36, shows the product of cropping intensity and sowing month of the two countries are compare with USDA crop calendar. The product crop calendar from derived from USDA shows crop calendar which derived from top five crop type in both countries. In Bangladesh top five crop dominant are Rice (Aman), Rice (Aus), Rice (Boro), Shorgum and Wheat, where dominant sowing month are on January, March and December. However in Japan, the top five are Barley, Rice (Central-south), Rice (Nort, Hokaido), Soybeans and Wheat, where dominant sowing month on April, May and June. MODIS-AMSR Sowing month product in Bangladesh has similar result with USDA crop Calendar, however in Japan MODIS-AMSR also detecting December and January in some pixel. This different reflect how complexity in detecting sowing month in pixel based analysis.

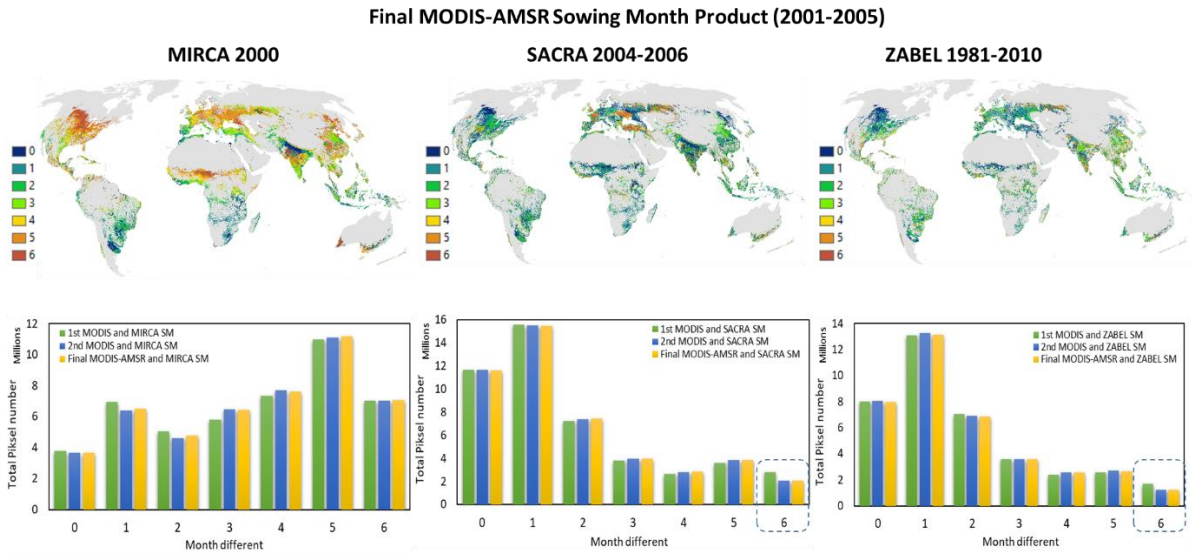


Figure 4-35. Comparison of final MODIS-AMSR product with MIRCA, SACRA and ZABEL sowing month products

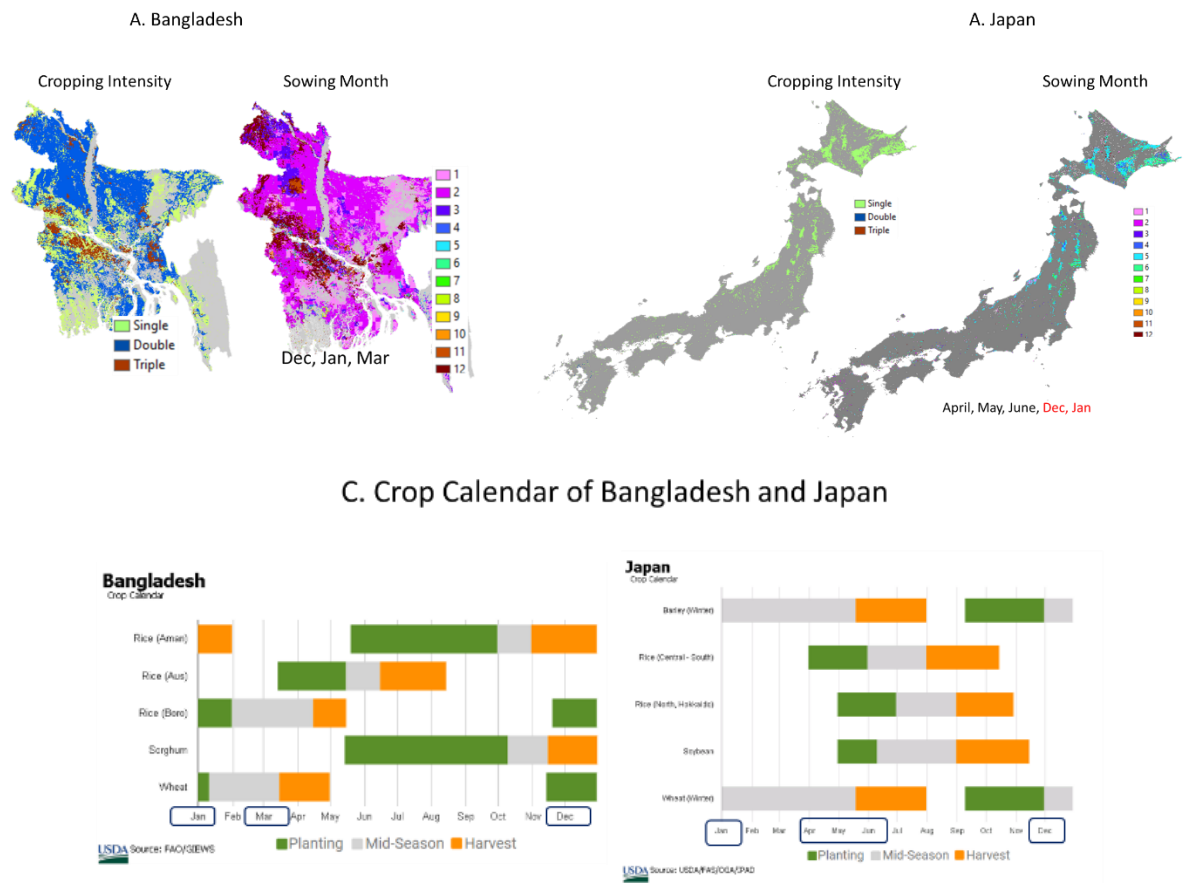


Figure 4-36. Sowing month comparison between Bangladesh and Japan

Based on combination of three sowing month different analysis, we produce Sowing month agreement product (figure 4-37). Pixel with low agreement value indicated that in that

pixel has high agreement among MODIS-AMSR compare with these MIRCA, SACRA and ZABEL products. Accuracy of MODIS-AMSR depends on the accuracy of the MODIS NDVI and AMSR LSWC data sets. A major discrepancy in crop calendars between MODIS-AMSR and other products (MIRCA, ZABEL, and SACRA) can be due to the selection of one dominant crop in each pixel unit. The disadvantages of the approach may be reduced with future improvements based on finer satellite sensors such as Landsat, Sentinel or GCOM-C to avoid mixture of phenology. The model-based method like Zabel can also result in a variety of sowing month. However, it is difficult to demonstrate that the variability is correct around the globe without knowledge of local sowing month information.

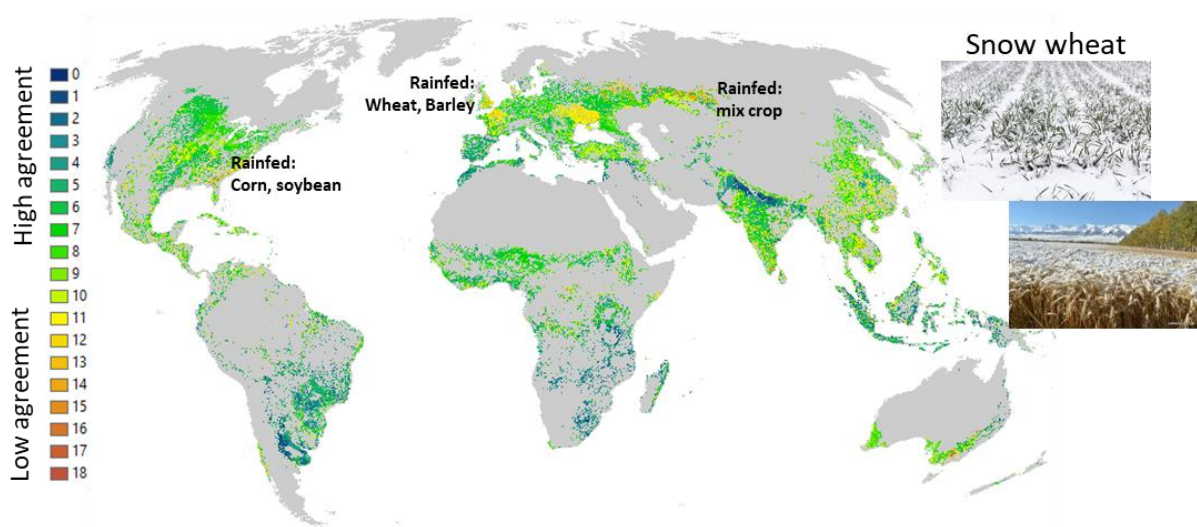


Figure 4-37. Sowing month agreement level product and investigation result of dominant crop based on GFSAD product

Figure 4-37 shows the product of sowing month agreement based on combination previous sowing month different. To analyze deeply the product of sowing month agreement, we compare it with The GFSAD Crop Dominance product, the result shows that rainfed snow-wheat has most inconsistent sowing month among four sowing month product (figure 4-37). The difficulty for estimating the sowing date for snow-wheat also discussed in SACRA product [Kotsuki et al, 2015]. For countries with large irrigated such as India, Vietnam, US and China, high sowing month agreement are dominantly located in irrigated area. However, countries with small irrigated area such as Argentina, UK, Russia and South Africa, high and low sowing month agreement are randomly distributed in both irrigated and rainfed area (figure 4-38).

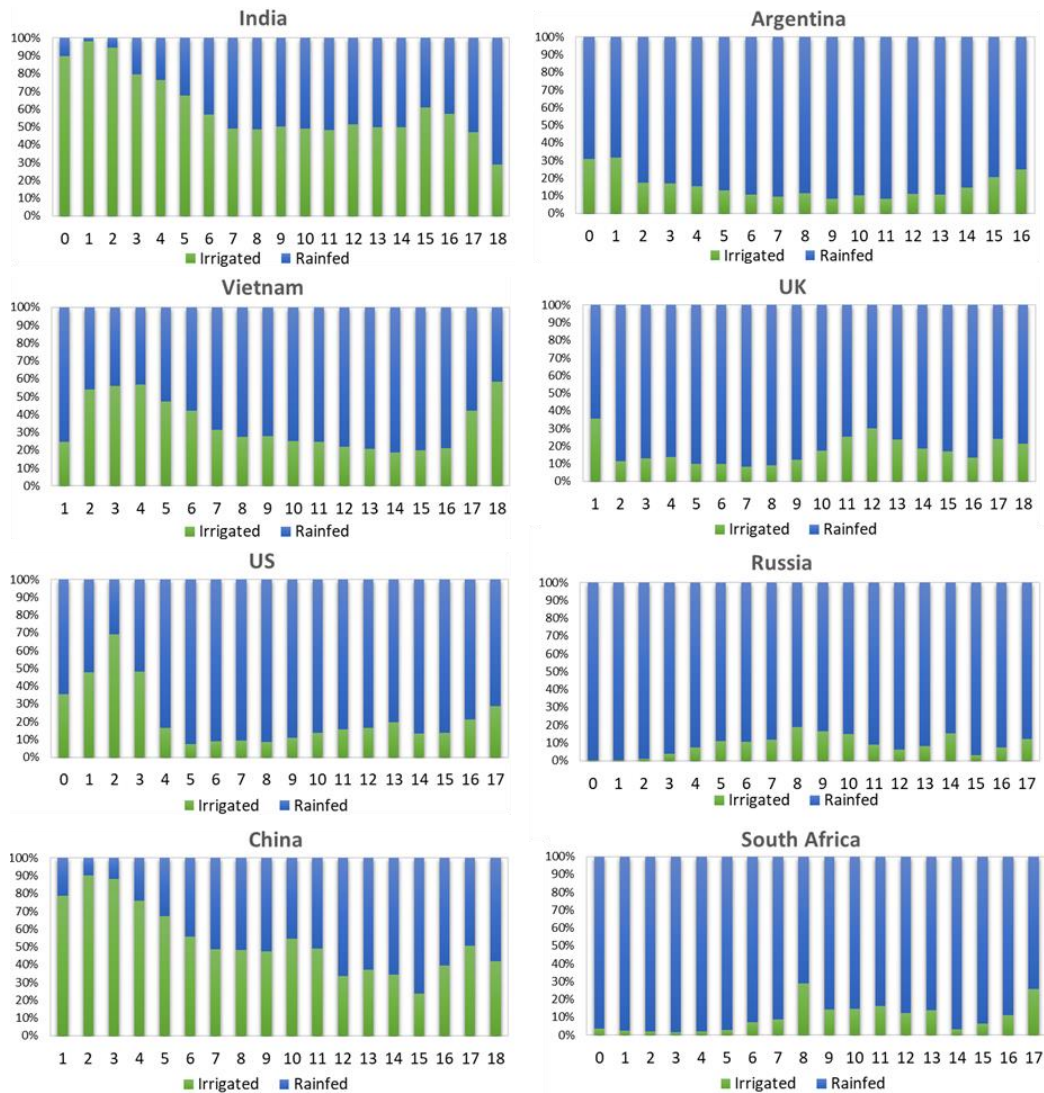


Figure 4-38. Eight countries analysis of Sowing month agreement

#### 4.5.5 Comparison of the MODIS-AMSR Rice Paddy Distribution Product with FAO-Stat in country level analysis

One of integration product between MODIS NDVI and AMSR LSWC is to detecting Rice Cropping pattern in multi cropping intensity, however the ground data information of this cropping pattern are very limited. In previous section how Bangladesh Government can provide the rice paddy cropping pattern in 2001 based on census based approaches. Since the cropping pattern ground data are very limited in this analysis we only concern on rice paddy area in general. FAO-Stat rice paddy area are used for reference data. We are combine rice cropping pattern especially in multi crop to produce a single product rice and non-rice by combining cropping pattern which contain at least rice paddy cultivation in one seasons. For reflect the

mix problem, we used HYDE rice paddy fraction and integrate it in MODIS-AMSR rice paddy distribution. Figure 4-39 shows the combination of rice cropping pattern to produce rice and non-rice distribution, combined with rice paddy fraction of HYDE product.

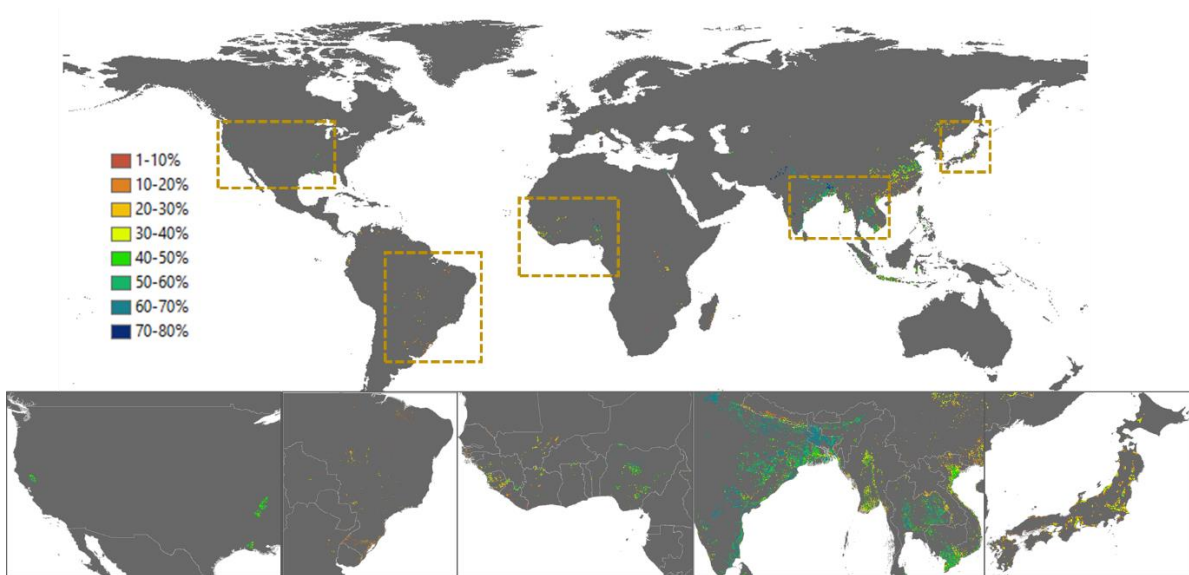


Figure 4-39. Integration of Rice Paddy (MODIS – AMSR) with HYDE Rice Fraction

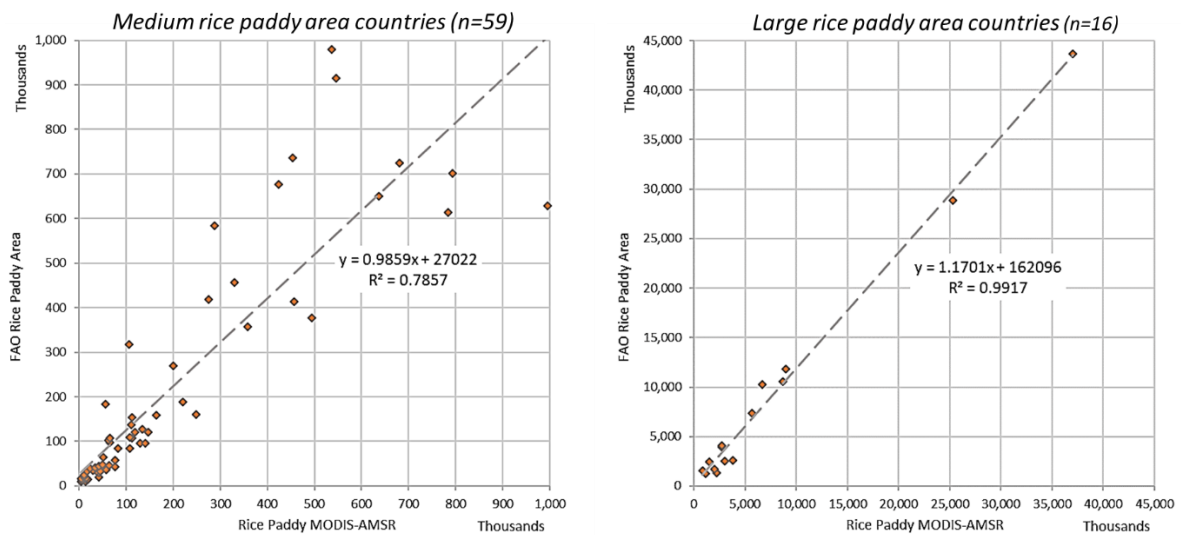


Figure 4-40. Comparison between Rice Paddy (MODIS – AMSR) and FAO rice Paddy area

As the result we calculate 75 countries and divided in two group which represent countries with medium and large rice paddy area. The regression value in group of medium rice paddy area are 0.7857 however in large rice paddy area up to 0.9917 we multiplying

number of fraction become two time since the HYDE rice paddy fraction are developed in 10 km pixel resolution, however the MODIS-AMSR Rice paddy has 1 km pixel resolution.

#### **4.6 Conclusion**

The MODIS-AMSR sowing month and Cropping pattern products are the first satellite-based products which derived from integration of vegetation and water index phenology that can analyze 15 years' dynamic change of crop activity 1 km pixel resolution. The advantage of the MODIS-AMSR sowing month product are the capability to detect short period crop cultivation and to distinguish rice and non-rice crop type. The assumed dominant crop and cloud contamination are the major source of discrepancy of MODIS-AMSR crop intensity and Sowing month product. Low agreement between MODIS-AMSR and previous sowing month products are dominantly located in rainfed area especially rainfed snow-wheat.

Future study will focus on analyze the trend of intensity change and compare it to country level agriculture investment variables such as Development Flows to Agriculture (DFA) and Gross Fixed Capital Formation (GFCF) to investigate the relationship between country investment and food production trend.

## Chapter 5 DEVELOPMENT OF CROP COEFFICIENT USING CROPWAT EMPIRICAL MODEL

### 6.1 Background

Crop coefficient is important for studying plant responses to available water particularly under nonstandard irrigation practices such as intermittent irrigation. Moreover, it is needed for estimating crop evapotranspiration, which represents the main route of water loss from both plant and soil surfaces and is a main component of water consumption in cropland. Crop coefficients  $k_c$  depend on the growing stage of the crop [Doorenbos and Kassam, 1979]. Developing high accuracy crop coefficient data is vital for irrigation scheduling and water resource allocation, management and planning [Jensen et al., 1990]. The crop coefficient ( $K_c$ ) takes into account the crop type and crop development to adjust the potential evapotranspiration ( $ET_o$ ) for that specific crop. Commonly, crop coefficient is derived empirically by using a lysimetric and is computed as the ratio of crop evapotranspiration to reference evapotranspiration based on weather data [Vu et al., 2005; Mohan and Arumugam, 1994; Tyagi et al., 2000] under Food and Agriculture Organization (FAO) standard conditions with continuous flooding irrigation. However, this method is time consuming and expensive, especially for equipment preparation.

There may be several crop coefficients used for a single crop throughout an irrigation season depending on the crop's stage of development. Crop coefficients may also vary depending on how the evapotranspiration data has been calculated or obtained. In this study we considering the long-term dynamic of global cropping intensity, sowing month and rice non-rice cropping pattern as novel strategy to estimate accurately water demand in agriculture. Since, those input parameters are essential inputs for estimating food production, water demand and emissions [Takeuchi, 2009; See, 2013].

The purposes of this study to develop global crop coefficient in three group of year where the evaluation and discussion of the agricultural water requirements will conduct under different cropping patterns.

## 6.2 Material

To achieve the product target, we include previous crop data product such as MODIS-Cropping intensity, MODIS-AMSR sowing month and dominant cropping pattern with CROPWAT empirical model to develop global crop coefficient in three group of year. Figure 5-1 shows the four developed parameter to develop crop coefficient (Kc)

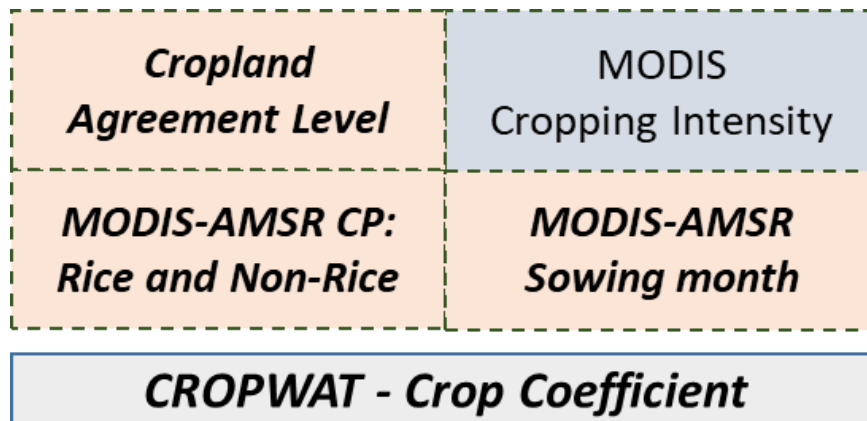


Figure 5-1. Four parameters to develop Crop Coefficient (Kc)

## 6.3 Methods

### 6.3.1 CROPWAT Empirical Model

The CROPWAT is empirical model that widely used to calculate crop related data in each decade of a month, such as: (1) crop coefficient, (2) crop leaf index, (3) crop evapotranspiration, (4) percolation, (5) effective rainfall, and (6) crop water requirements. In CROPWAT model, crop growth periods can be divided into four distinct growth stages; initial, crop development, mid-season and late season (Figure 5-2). CROPWAT model can define the length of each of these stages based on previous research of combining local observations data and then determine the growth stage of the crop and which Kc values to use. This Kc also derived from study of impact of the climate, latitude, elevation and planting date to crop coefficient value.

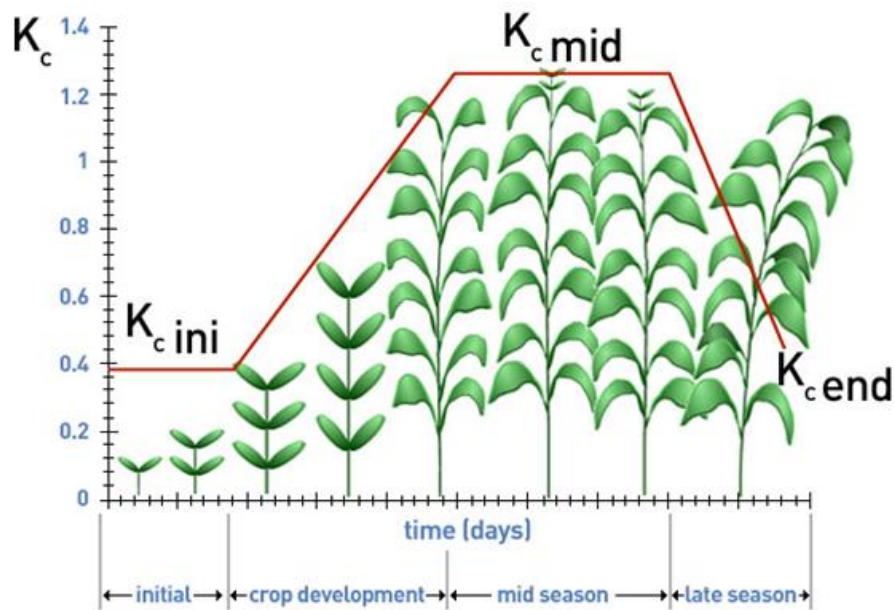


Figure 5-2. Kc values are based on plant growth schema

## 6.4 Result and Discussion

### 6.4.1 CROPWAT Crop Coefficient Product

Rice is very important crop with specific planting characteristic and has highest water demand. Based on CROPWAT crop coefficient [FAO, 2009] shows rice has higher crop coefficient compare with non-rice crop type. Hence, understanding rice paddy phenology to separate rice and non-rice crop type can improve the accuracy of sowing month estimation and irrigation water demand as well.

Figure 5-3. Provides a description of the sorghum and rice paddy plant growth stages derived from CROPWAT empirical model. These stages can be used to select an appropriate crop coefficient to distinguish rice and non-rice crop type. We combine four global dominant crop there are maize, potato, Sorghum, and wheat and calculate the average of those crop coefficient in each growth stage, and we compare it with rice paddy crop coefficient product (figure 5-4). The average values of crop coefficient for each time step are estimated by linear interpolation between the Kc values for each crop development stage.

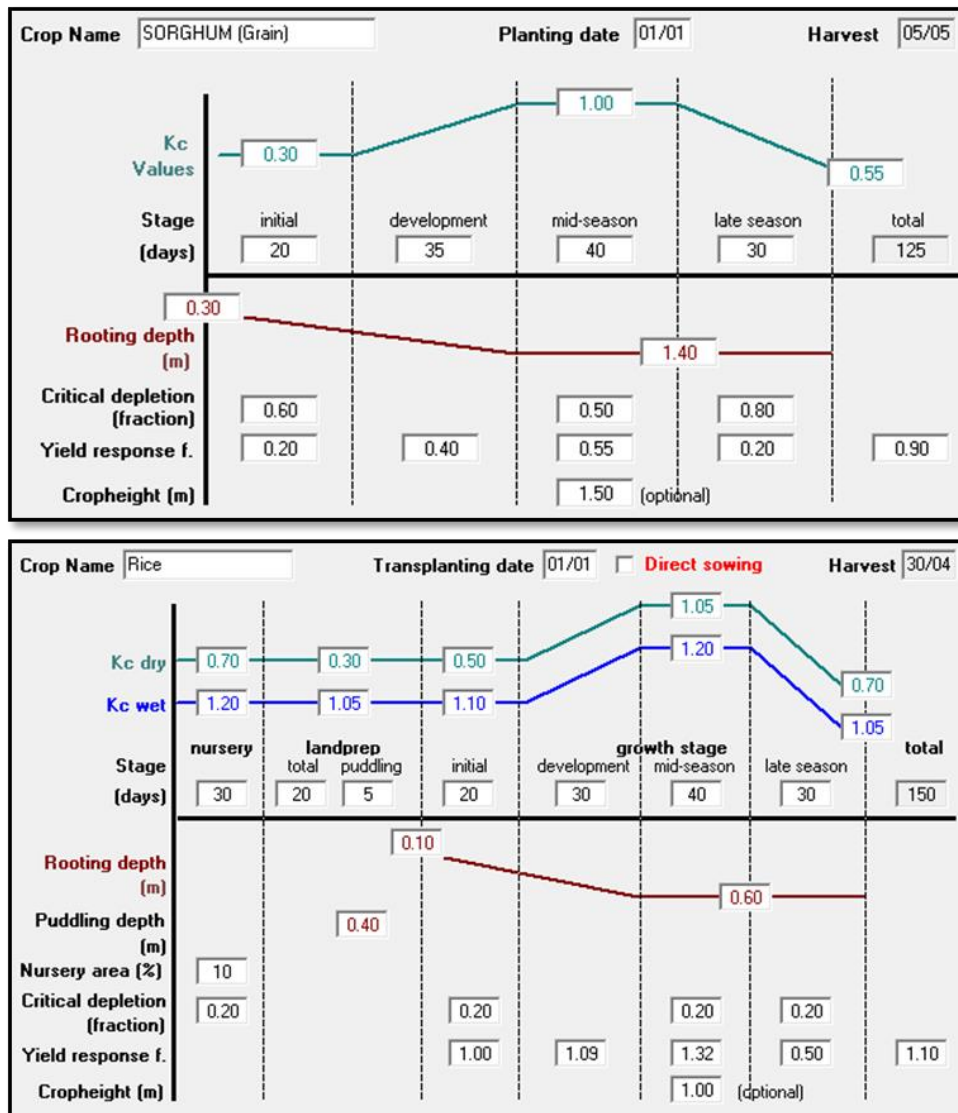


Figure 5-3. Kc value derived by using CROPWAT empirical model

| Decade            | 1st month |         |              | 2nd month    |              |            | 3rd month  |            |            | 4 month     |             |             |             |      |
|-------------------|-----------|---------|--------------|--------------|--------------|------------|------------|------------|------------|-------------|-------------|-------------|-------------|------|
|                   | 1         | 2       | 3            | 1            | 2            | 3          | 1          | 2          | 3          | 1           | 2           | 3           | 1           |      |
| Stage             | Initial   | Initial | Develop ment | Develop ment | Develop ment | Mid-season | Mid-season | Mid-season | Mid-season | Late-season | Late-season | Late-season | Late-season |      |
| Kc coeff          | Maize     | 0.3     | 0.3          | 0.45         | 0.72         | 0.97       | 1.17       | 1.19       | 1.19       | 1.19        | 1.15        | 0.89        | 0.62        | 0.41 |
|                   | Potato    | 0.5     | 0.5          | 0.54         | 0.75         | 0.96       | 1.12       | 1.14       | 1.14       | 1.14        | 1.14        | 1.07        | 0.93        | 0.8  |
|                   | Shorgum   | 0.3     | 0.3          | 0.42         | 0.62         | 0.82       | 0.97       | 0.99       | 0.99       | 0.99        | 0.97        | 0.83        | 0.68        | 0.56 |
|                   | Wheat     | 0.3     | 0.3          | 0.3          | 0.48         | 0.76       | 1.01       | 1.14       | 1.14       | 1.14        | 1.14        | 0.98        | 0.71        | 0.43 |
| Non-Rice Kc coeff | 0.3       |         |              | 0.75         |              |            | 1.14       |            |            | 0.815       |             |             |             |      |

| Decade                | 1st month |                |                | 2nd month |         |              | 3rd month    |              |            | 4th month  |            |            | 5th month   |             |             |      |
|-----------------------|-----------|----------------|----------------|-----------|---------|--------------|--------------|--------------|------------|------------|------------|------------|-------------|-------------|-------------|------|
|                       | 1         | 2              | 3              | 1         | 2       | 3            | 1            | 2            | 3          | 1          | 2          | 3          | 1           | 2           | 3           |      |
| Stage                 | Nursery   | Nurs/ LandPrep | Nurs/ LandPrep | Initial   | Initial | Develop ment | Develop ment | Develop ment | Mid-season | Mid-season | Mid-season | Mid-season | Late-season | Late-season | Late-season |      |
| Rice Kc coeff         | 1.2       | 1.08           | 1.06           | 1.1       | 1.1     | 1.12         | 1.15         | 1.18         | 1.19       | 1.19       | 1.19       | 1.19       | 1.19        | 1.16        | 1.11        | 1.06 |
| Avr Non-Rice Kc coeff | 1.11      |                |                | 1.11      |         |              | 1.17         |              |            | 1.19       |            |            | 1.11        |             |             |      |

Figure 5-4. Estimation Kc values of rice and non-rice derived from CROPWAT empirical model for standard Kc Development

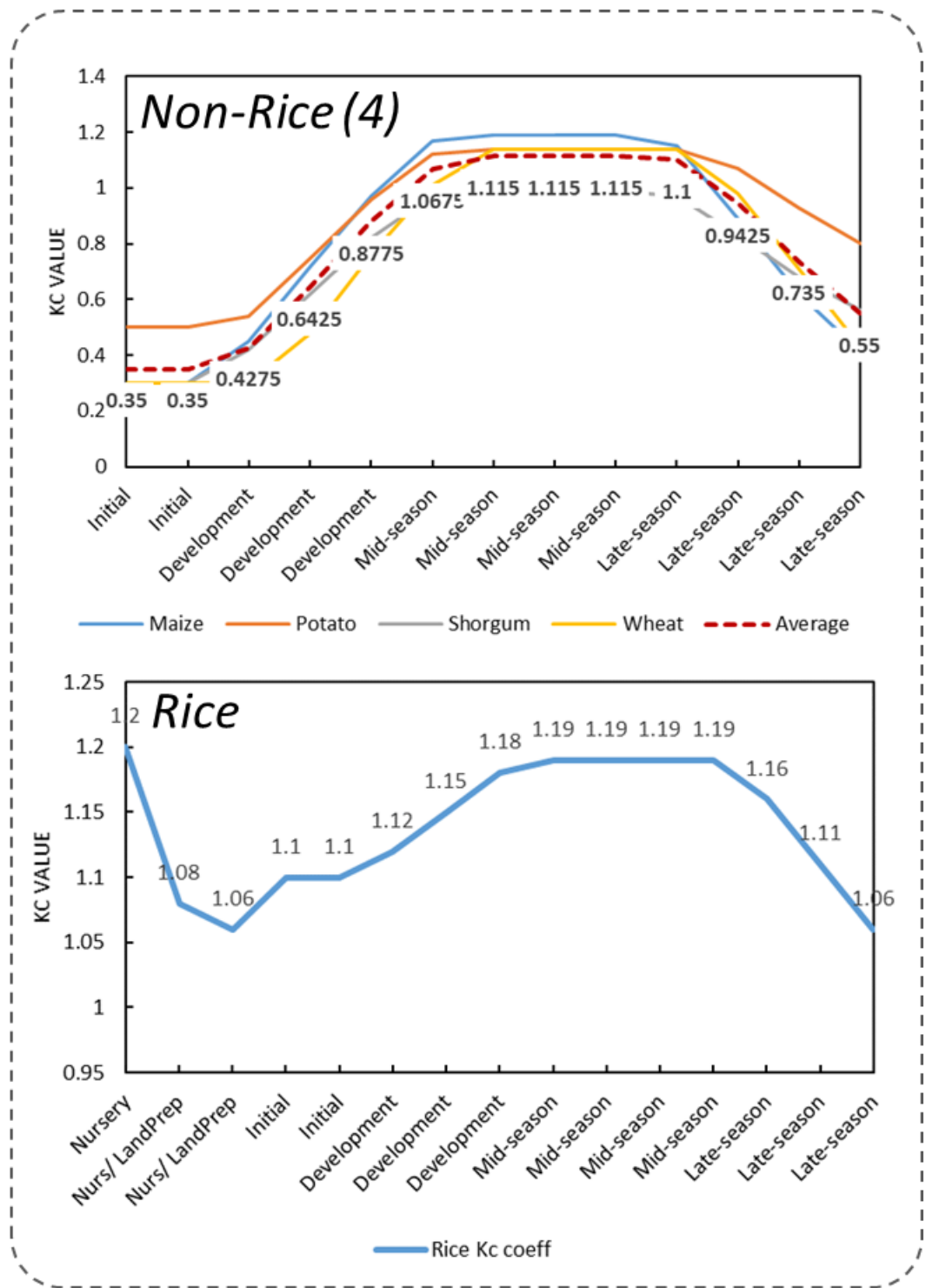


Figure 5-5. Development of standard Kc Value derived from four dominant crop type.

Since this Kc value are the key factor to convert previous crop activity od cropping intensity, sowing month, and rice cropping pattern, the definition of Kc estimation will reflect into final converting this crop activity into water demand estimation. Here, we proposed two kind of Kc model, first developed for standard Kc calculation where we used four Kc from four

dominant crop type, and the second product we developed for error estimation, where we used in total 15 crop type that reflect the range of KC in each level growth condition. After that we pick up the lowest and highest Kc value in the Kc phenology and develop Kc product based on lowest and highest Kc range from 15 crop type. Figure 5-5 shows the value of single cultivation period derived from average four dominant crop type for standard Kc development. Figure 5-6 show the range between the lowest and highest Kc which derived from 15 crop type in single crop cultivation period.

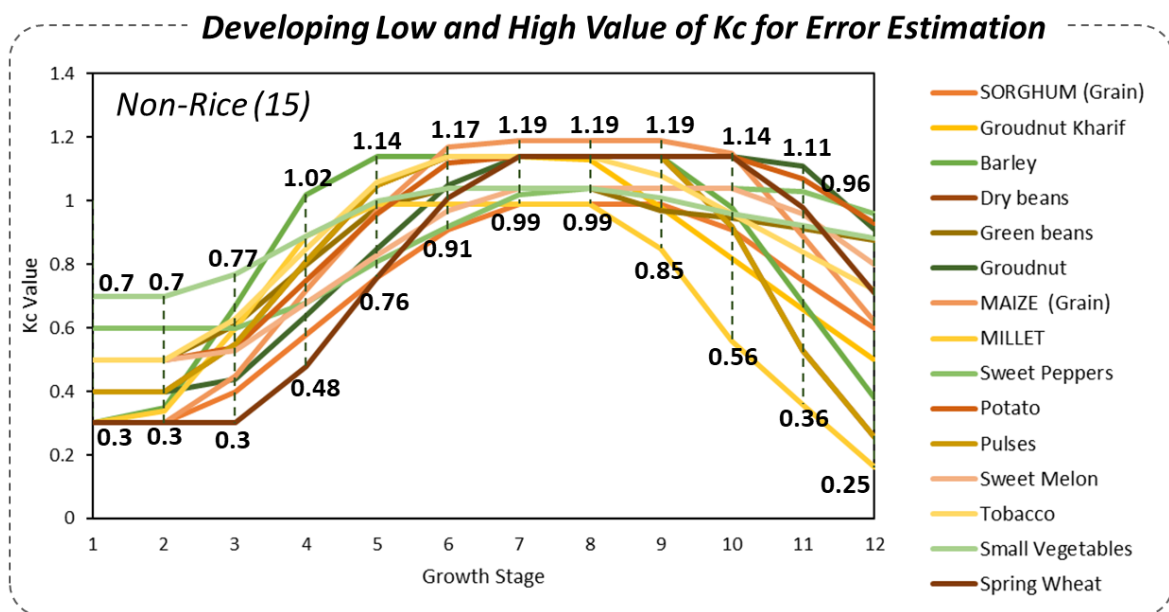


Figure 5-6. Development of lowest and highest kc Value for error estimation

#### 6.4.2 Monthly Gridded Crop Coefficient Product

The CROPWAT crop coefficient (Kc) method of the Food and Agricultural Organization (FAO) Irrigation and Drainage is intended to improve monthly simulation of crop ET by considering spatial contribution of evaporation from soil. Considering the same climatic data for all the crops at the same region, the crop coefficient plays the essential role to determine the irrigation water demand (IWD).

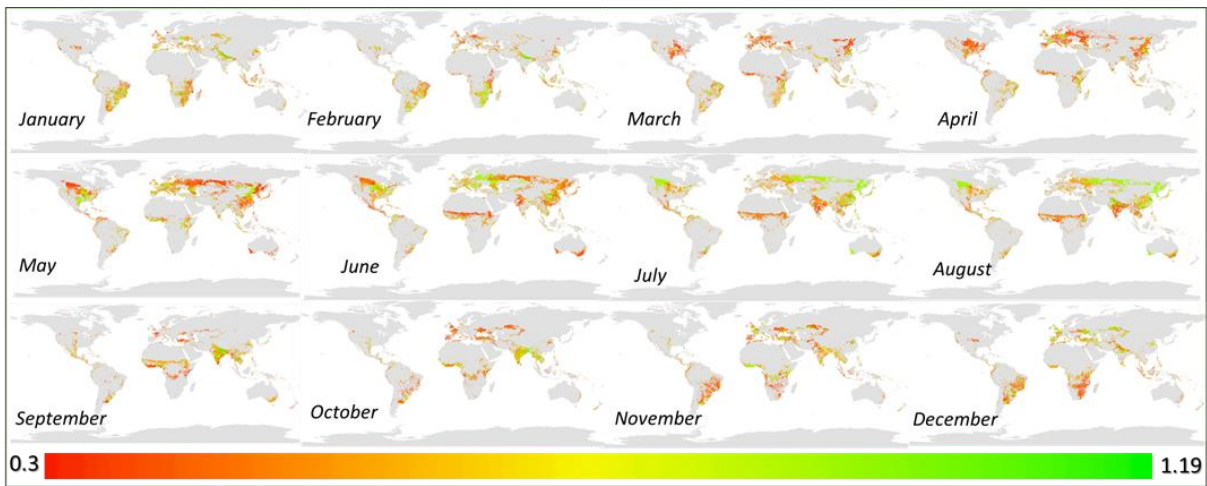


Figure 5-7. Result of monthly Kc in global scale

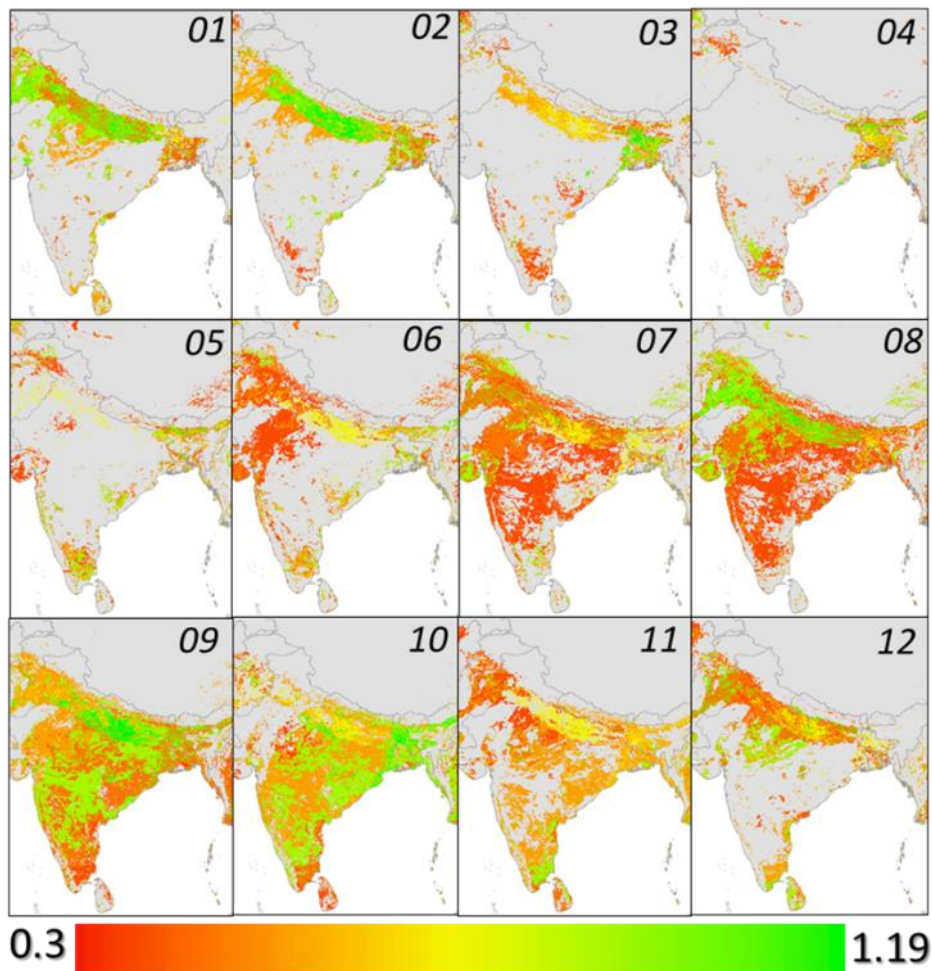


Figure 5-8. Crop Coefficient (kc) value in south Asia region

As shown in figure 5-7 for global and figure 5-8 for South Asia monthly crop coefficient. July, August and September has largest active and highest crop coefficient along one year it ranges between 0.3 to 1.15. The highest value of crop coefficient can be simulated as the end of development stage or the midseason. Kc values for initial, mid and late growth stages of annual and seasonal crops are used. In the case of perennial crops, same Kc value is used for the growth period. Crop coefficient are used in determining each crop`s actual evapotranspiration.

## **6.5 Conclusion**

The average values of crop coefficient for each time step are estimated by linear interpolation between the Kc values for each crop development stage. The result of analysis that conducted from this CROPWAT empirical model approach can be used to construct a simulation of crop active level for achieving higher accuracy of IWD product. The advantages of CROPWAT empirical model is can be applied to estimate the irrigation schedule for each crop with 5 different options: (1) each irrigation defined by irrigation manager, (2) irrigation at below or above critical soil depletion (% RAM), (3) irrigation at fixed interval per crop growing stage, (4) deficit irrigation, and (5) no irrigation. Afterwards, the CROPWAT model can simulate the on-farm crop water balance, including: (1) irrigation times, dates and depths, (2) soil moisture depletion, (3) amount of percolation, (4) actual crop evapotranspiration, and (5) crop yield.

## Chapter 6

# DEVELOPMENT OF IRRIGATION WATER DEMAND

### 7.1 Background

Freshwater scarcity is the second most important environmental issue of the 21st century [UNEP, 2002]. In this context, Irrigated agriculture have to be considerably extended in the future in order to feed growing populations. It is not yet known whether there will be enough water available for the necessary extension. Hence, Necessary to model the “water requirement” of irrigated agriculture. The trend of widespread abandonment agricultural land and shrinking cropland area due to urbanization, makes extensification strategy become not preferred to mitigate the unavoidable increase of agricultural production demand [Wua et al., 2018]. Several countries tried to Irrigated their own crop and intensify land-use on already cultivated lands. Irrigation pointed as the highest global water consumption compare with other sector and contribute the biggest water loss problem [FAO, 2012]. Increasing water-use efficiency in irrigated area is one of the important keys to achieve SDGs targets. Irrigation Water Demand (IWD), which defines as the amount of water that must be applied to the crop, is an essential input for numerical Irrigation efficiency estimations [Doll and Siebert., 2002]. This study aims to estimate the monthly IWD from 2001 to 2015 by dividing the analysis into three group of year (2001-2005, 2006-2010, 2011-2015) at a spatial resolution of 1 km in the global scale.

### 7.2 Material and Methods

Crop water demand for rice and non-rice are estimated by using combination crop coefficient product with climate datasets. Crop coefficient values (Kc) are taken from available previous data product. These values vary based on the four previous long-term crop activity products: cropland agreement level, cropping intensity, sowing month, and dominant cropping pattern of rice and non-rice. For climate data we used MODIS potential evapotranspiration product (MOD16A2) and GSMaP precipitation data.

### 7.2.1 MODIS Potential Evapotranspiration Product (MOD16A2)

Evapotranspiration is the one of most important element of the hydrological cycle and listed as one priorities of water societal benefit area. The reasons of the importance are crucial for the transportation of minerals and nutrients required for plant growth also because need large amounts of energy during the conversion of liquid water to vapour. Accurate estimates of the evapotranspiration, Hence improved quantification of the catchment water balance and sustainable water resource management.

One of remote sensing product of global estimates of ET is MOD16Q1 with spatial resolution of 1 km and is available on an eight-day, monthly and yearly basis. Developed by University of Montana's Numerical Terradynamic Simulation group. In MOD16 ET product [Mu et al. , Cleugh et al.] used Penman-Monteith derived model:

$$ET_o = \frac{0.408\Delta(R_n - G) + \gamma \frac{900}{T + 273} u_2 (e_s - e_a)}{\Delta + \gamma(1 + 0.34u_2)} \quad (1)$$

where  $ET_o$  = reference evapotranspiration  $[\text{mm} \cdot \text{day}^{-1}]$ ,  $R_n$  = net radiation at the crop surface  $[\text{MJ} \cdot \text{m}^{-2} \cdot \text{day}^{-1}]$ ,

$G$  = soil heat flux density  $[\text{MJ} \cdot \text{m}^{-2} \cdot \text{day}^{-1}]$ ,

$T$  = average temperature  $[\text{°C}]$ ,

$u_2$  = wind speed at 2 m height  $[\text{m} \cdot \text{s}^{-1}]$ ,

$e_s$  = saturation vapour pressure  $[\text{kPa}]$ ,

$e_a$  = actual vapour pressure  $[\text{kPa}]$ ,

$(e_s - e_a)$  = saturation vapour pressure deficit  $[\text{kPa}]$ ,

$\Delta$  = slope vapour pressure curve  $[\text{kPa} \cdot \text{°C}^{-1}]$ ,

$\gamma$  = psychrometric constant  $[\text{kPa} \cdot \text{°C}^{-1}]$ .

From previous studies, Cleugh et al. [2007], Mu et al. [2007], Kim et al. [2012], Jia et al. [2012] and Rameole et al. [2014], validated spatiotemporal MODIS ET product using Asiaflux stations in several studies and found inaccuracies were observed between the flux

tower and MOD16 ET estimates. Errors to be caused by: 1 Input data of the Penman-Monteith  
2. flux tower measurement error, 3. Flux tower footprint vs. MODIS pixel, 3. the limitations  
of the algorithm.

The main input data for the MODIS MOD16Q1 are MODIS land cover, Albedo, leaf  
area index (LAI), fraction of photosynthetic absorbed radiation (FPAR), meteorological data.  
The Coarse scale products, generally poorly or not validated in the semi-arid conditions of  
South Africa. Generate significant ET prediction errors. MODIS global land cover  
(MOD12Q1) (1 km) is inadequately captures savannah. MODIS based LAI or FPAR products  
have not been validated in Southern Africa.

## 7.2.2 Crop Water Balance Approach

We generate global IWD change by combining various multi-source earth observation  
data and FAO-CROPWAT model. By following Doll and Siebert [2002] approach we  
distinguished rice and non-rice crop type, since rice has the highest water demand compared  
with another crop. After that we develop Crop Coefficient (KC) by combining the satellite-  
based crop calendar and intensity products with CROPWAT model. The final analysis is  
applying Doll and Siebert approach [2009] by multiplying MODIS potential evapotranspiration  
product (MOD16A2) with the developed KC. We include GSMaP precipitation and HYDE 3.2  
Irrigated-Rainfed crop fraction in 2005, 2010 and 2015 to produce final product of long-term  
global IWD. Figure 6-1. Shows the crop water balance concept that used for water demand  
estimation in cropland area. Figure 6-2 show the overall concept derived from Doll and Siebert  
[2002] to estimate irrigation water demand.

$$\text{Irrigation Water Demand} = \left\{ \sum_{i=1}^n \left( \left[ \sum_{j=1}^m (CWR - P_{eff}(\text{Green water}))_j \right] \cdot [\% \text{ of Area}]_i \right) \right\} \quad (1)$$

$$\text{Crop Water Demand} = \left\{ \sum_{i=1}^n \left( \left[ \sum_{j=1}^m (Kc \cdot Epot)_j \right] \cdot [\% \text{ of Area}]_i \right) \right\} \quad (2)$$

$$\text{Effective Precipitation (a)} = \left\{ \sum_{i=1}^n \left( \left[ \sum_{j=1}^m (P(4.17 - 0.2P)/417)_{j_i} \right] \right) \right\} \text{ for } P < 8.3 \text{ mm/d} \quad (3)$$

$$\text{Effective Precipitation (b)} = \left\{ \sum_{i=1}^n \left( \left[ \sum_{j=1}^m (4.17 + 0.1P)_{j_i} \right] \right) \right\} \text{ for } P < 8.3 \text{ mm/d} \quad (4)$$

Where:

n: number of crops grown within the grid cell

m: the number of months of the year (12)

Epot: potential evapotranspiration [mm/month]

kc: crop coefficient [dimensionless]

Peff: Effective Precipitation [mm/month]

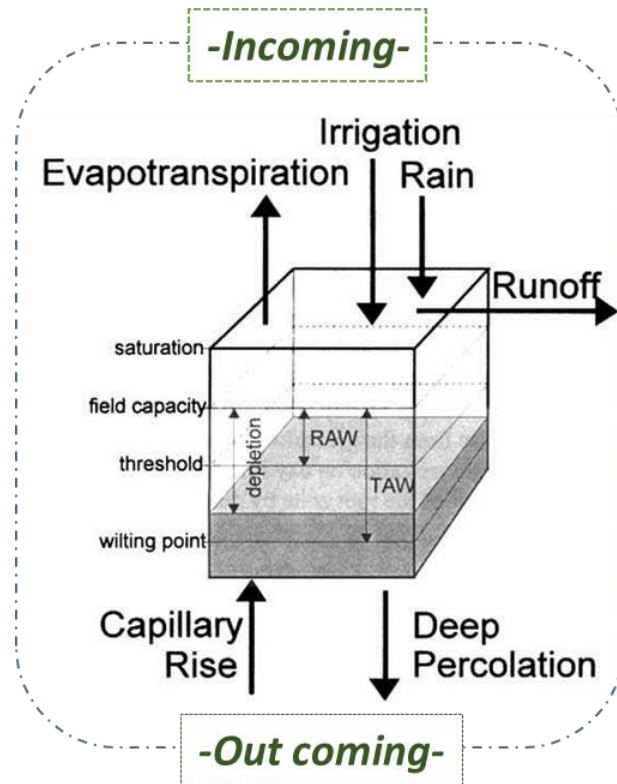


Figure 6-1. Water balance of the root zone (Image source: [FAO, 2002])

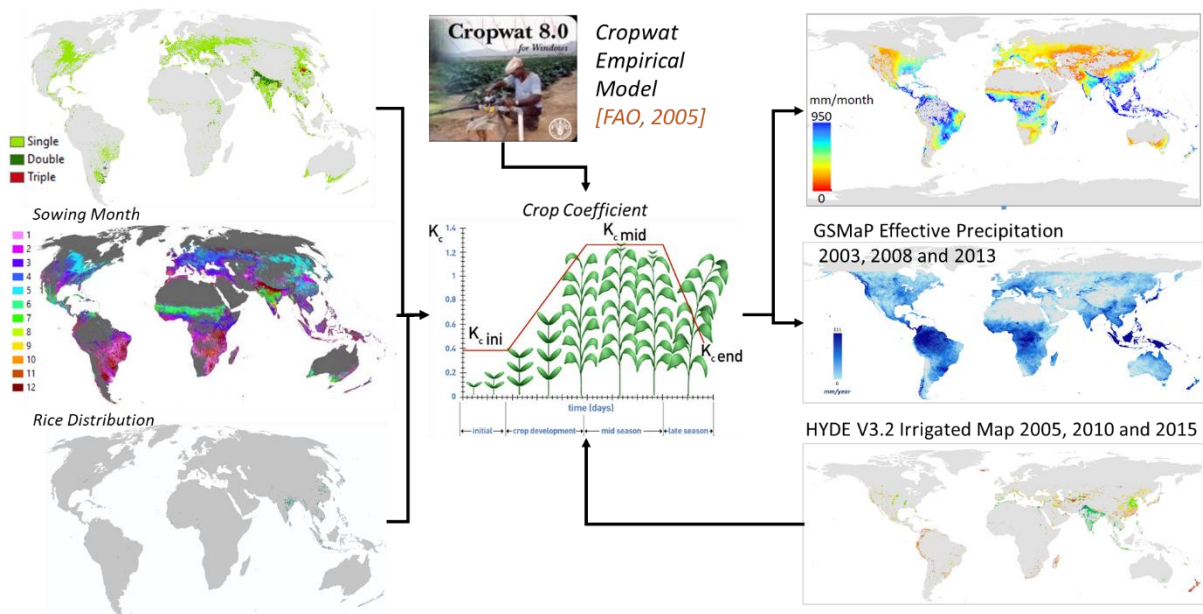


Figure 6-2. overall data and methodology to estimate irrigation water demand

## 7.3 Result and Discussion

### 7.3.1 Effective Precipitation (Green Water) Product

Water in the soil moisture that transpires through crops and vegetation is termed “green water” since this water is available for crop productivity and vegetation. Siebert and Döll [2009] proposed an effective precipitation to compute green water use of crops, where effective rainfall refers to that portion of rainfall that can effectively be used by plants. For estimating monthly effective precipitation data, we used two high resolution precipitation data product there are GSMaP 2010 (10 km pixel resolution) and WorldClim 1960-1990 (1 km data product) precipitation data product.

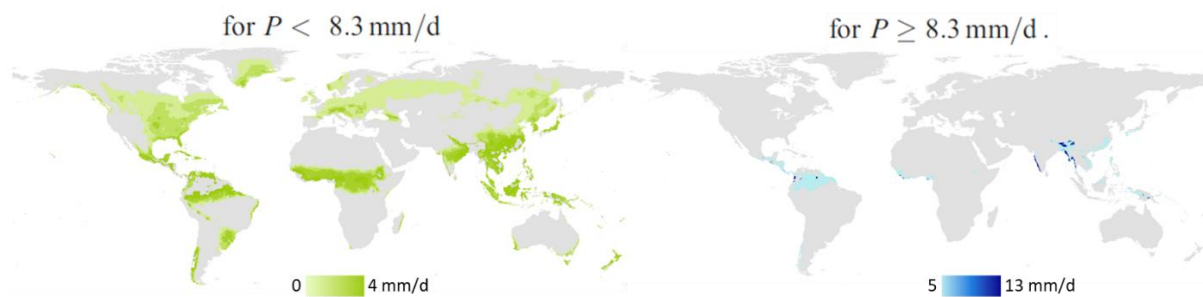


Figure 6-3. Effective precipitation value from two group: Lower than 8.3 mm/day and higher than 8.3 mm/day (in January)

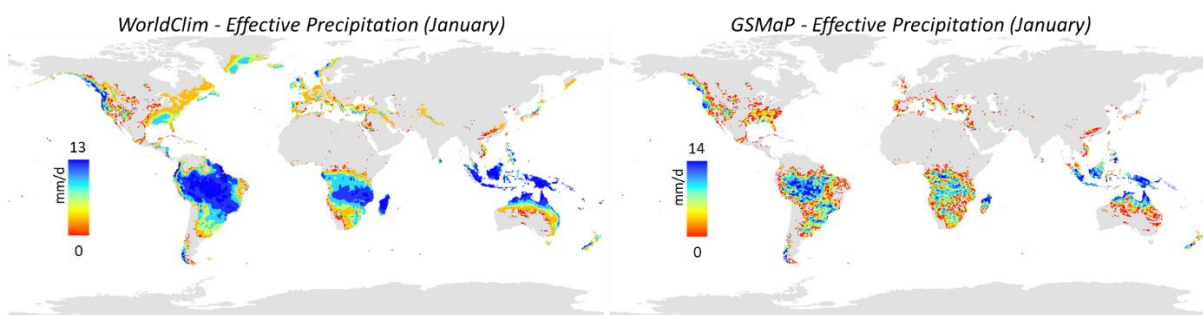


Figure 6-4. Comparison of effective precipitation on January between Worldclim (left) and GSMaP (right) precipitation data products

To estimate effective precipitation, we have to separate two group of precipitation that are area with precipitation lower 8.3 mm/day and area with precipitation higher 8.3 mm/day. Figure 6-3. Effective precipitation value from two group: Lower than 8.3 mm/day and higher than 8.3 mm/day (in January). Figure 6-4. Comparison of effective precipitation on January

between Worldclim (left) and GSMaP (right) precipitation data products. Figure 6-5. Total annual effective precipitation derived from GSMaP precipitation data product.

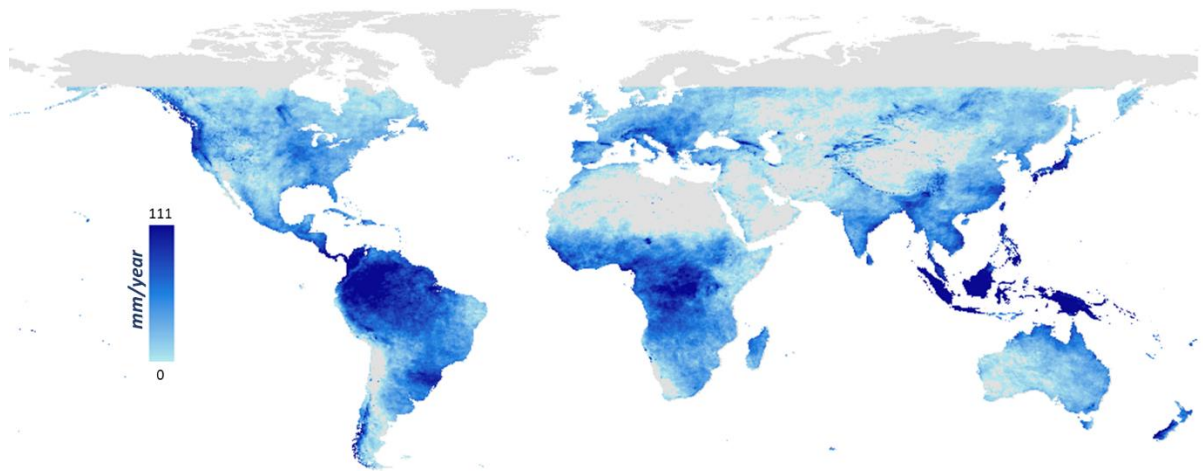


Figure 6-5. Total annual effective precipitation derived from GSMaP precipitation data product

### 7.3.2 Long-term Crop Water Demand

The “Crop Kc” values are calculated as  $K_c \times \text{Crop Area}$ , so if the crop covers only 50% of the area, the “Crop Kc” values will be half of the Kc values in the crop coefficient data sets. For annual crops, during the crop’s germination and establishment, most of the ET occurs as evaporation from the soil surface. As the foliage develops evaporation from the soil surface decreases and transpiration increases. For perennial crops a similar pattern may occur as the plant starts to leaf out, grow new shoots and develop fruit. The percentage of canopy cover will determine the rate of evapotranspiration (ET). Maximum ET occurs when the canopy cover is about 60-70% for tree crops and 70- 80% for field and row crops.

The maximum canopy cover often coincides with the time of year that sun radiation and air temperature are at their greatest. The maximum ET therefore occurs during mid-season. During the crop development stage there are no set Kc values. If irrigating during this period, choose a Kc value that is between Kcini and Kcmid. A similar approach should be taken for the time period between Kcmid and Kcend. However, this time period may be much shorter and a jump directly from Kcmid to Kcend could be taken. Figure 6-6, 6-7, 6-8 shows global monthly crop water demand product in mm/day unit.

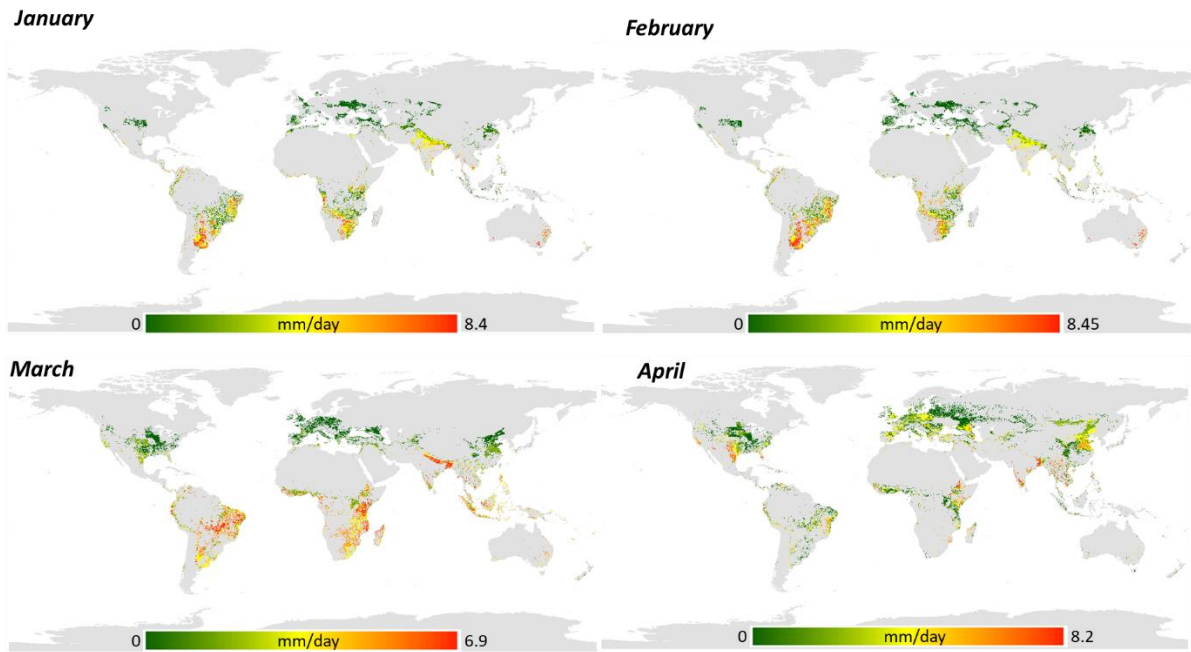


Figure 6-6. Global Crop water demand product on January, February, March and April in mm/day unit

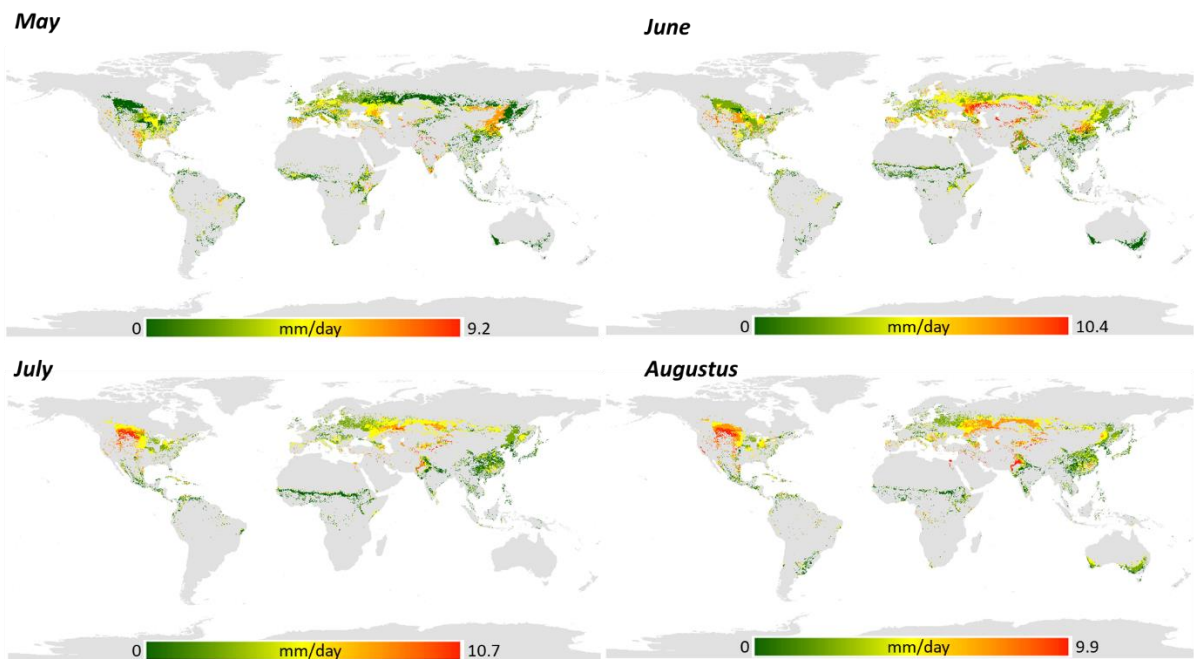


Figure 6-7. Global Crop water demand product on May, June, July and August in mm/day unit

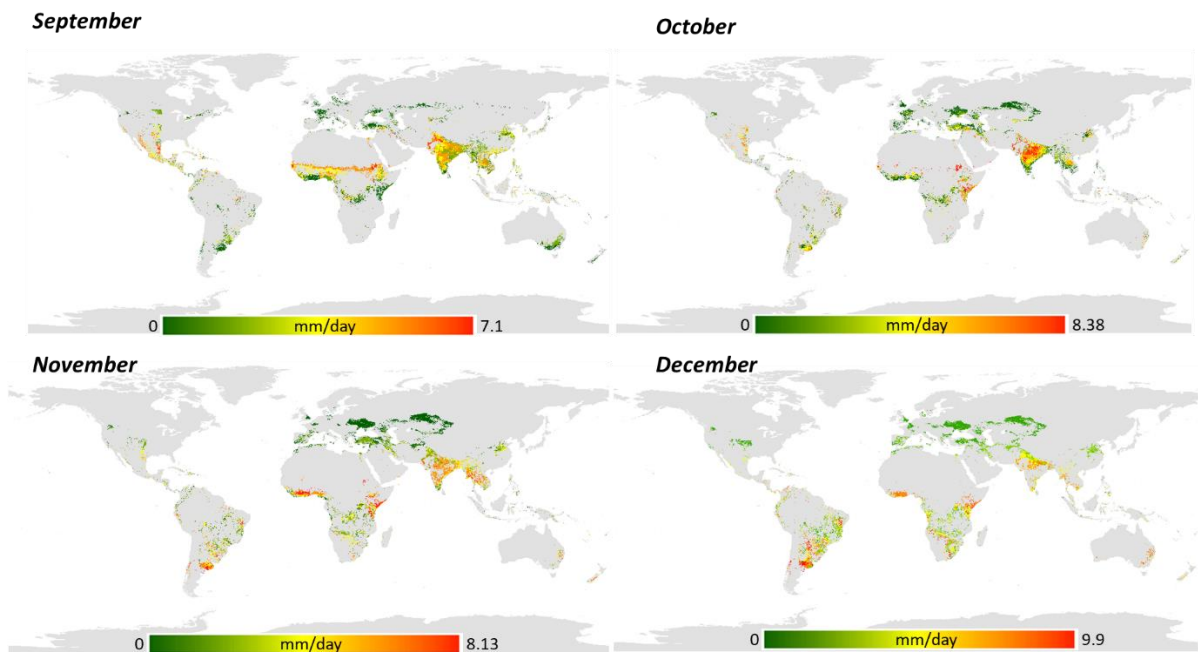


Figure 6-8. Global Crop water demand product on September, October, November and December in mm/day unit

The final product of crop water demand is the reflection of two product crop coefficient which derived by combination of cropping Intensity, sowing month and rice cropping pattern with the product of MODIS Potential Evapotranspiration. Hence, this crop water demand is reflect with the limitation from input data itself.

The limitations of the algorithm of MODQ1 product which explained by Mu et al. [2011] argued that physical factors (micro-climate, plant biophysics and landscape heterogeneity) influence the soil surface evaporation and plant transpiration. The MOD16 ET does not account for disturbance history or species composition and stand age hence, the algorithm makes the assumption that the stomata close during the night this makes underestimation of daily ET because of the bias imposed by night time vegetation transpiration.

Important issues such as FPAR and LAI are also assessed and validated in the local context only, this help determine error propagation within the MOD16 and support integrated water management system. Sensitivity analyses are required to identify the variables which influence the potential evapotranspiration output.

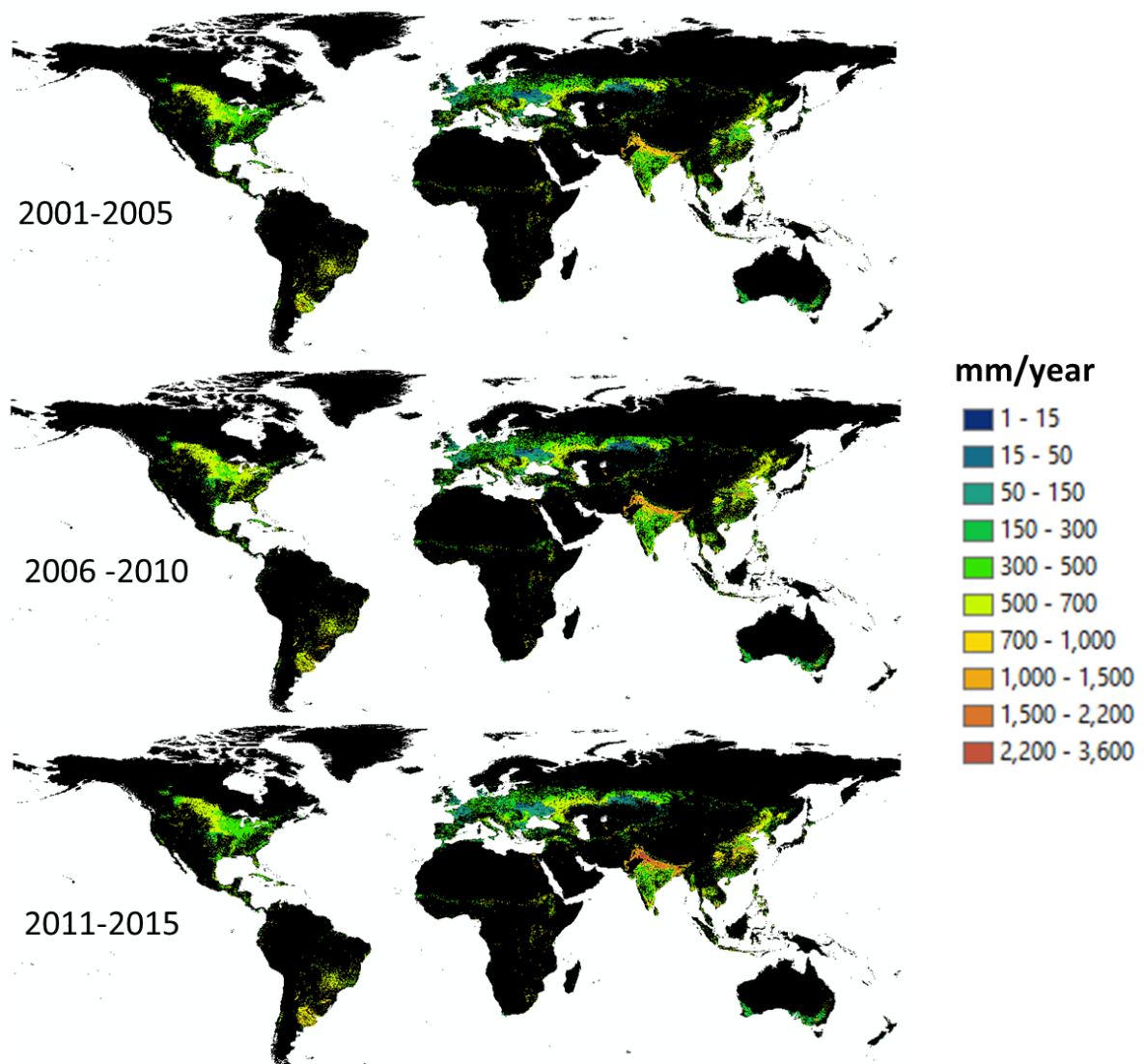


Figure 6-9. Global crop water demand in three group of year: 2001-2005, 2006-2010, 2011-2015

Based on monthly CWD product we found that in tropical area, water demand still active in a whole year, compared with the northern area where CWR is high in March to September, and southern area in September to May. Some area has rapid increase of CWR between (2001-2005) and (2011-2015) (figure 6-10). Those areas are: Gurwana district India, with the escalation of up to 2212 mm/year, Deng district China, with the escalation of up to 1828 mm/year. Some other country facing rapid decreasing, such as: Sumbas district, Turkey with the reduction up to -1284 mm/y and Jakobabad district, Pakistan with the reduction of up to -1988 mm/y. We are comparing these areas with long-term NDVI to analyze the correlation

between the reduction and the escalation of water consumption with vegetation index pattern in 15 years (figure 4-7).

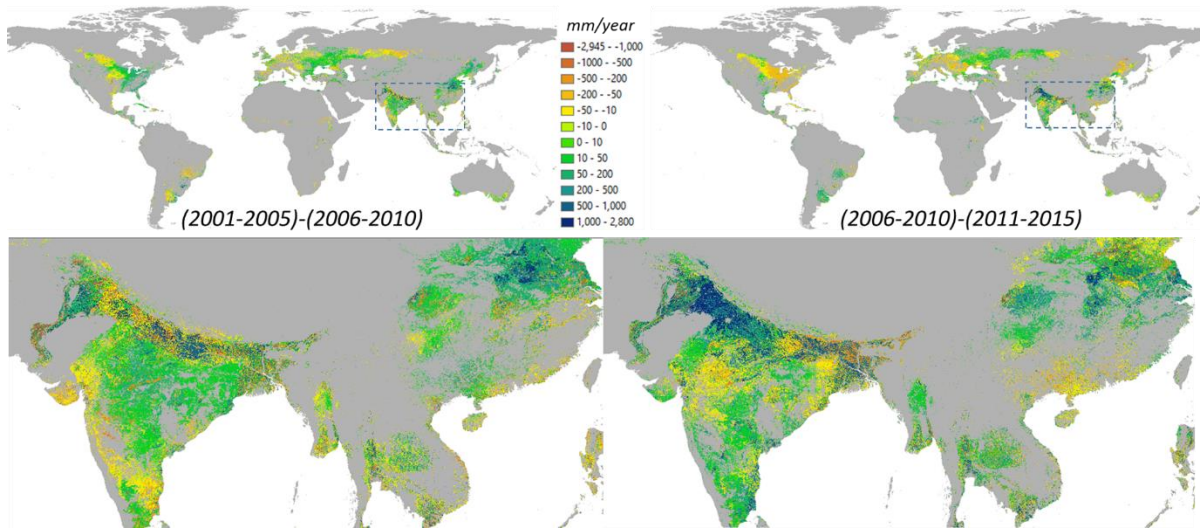


Figure 6-10 Global Crop Water Demand change :2001-2005 - 2006-2010 and 2006-2010 - 20101-2015.

### 7.3.3 Irrigation Water Demand

The next process is to calculate Irrigation water demand (IWD) by comparing product of monthly effective precipitation with crop water demand (crop potential evapotranspiration). In this study we are using two precipitation data for analyzing impact of different climate data to irrigation water demand estimation product. Figure 6-11 shows comparison of IWD product derived from two precipitation datasets Wordclim and GSMaP.

We used FAO independent data of consumptive irrigation water use based on 2008-2010 statistic data processing to compare country level IWD estimation from two precipitation data products. Figure 6-11 shows comparison analysis of country level IWD estimation derived from two precipitation datasets with FAO independent data of consumptive irrigation water use in large and medium irrigated area country. Since, our next target is to calculate long-term irrigation water demand, single data of worldclim data product cannot be used to achieve this purpose. Hence, GSMaP data that produce monthly in 15 years can be main precipitation data that can used for analyzing long-term IWD product. Figure 6-12 shows total of global net irrigation water demand (IWD) in 2006-2010.

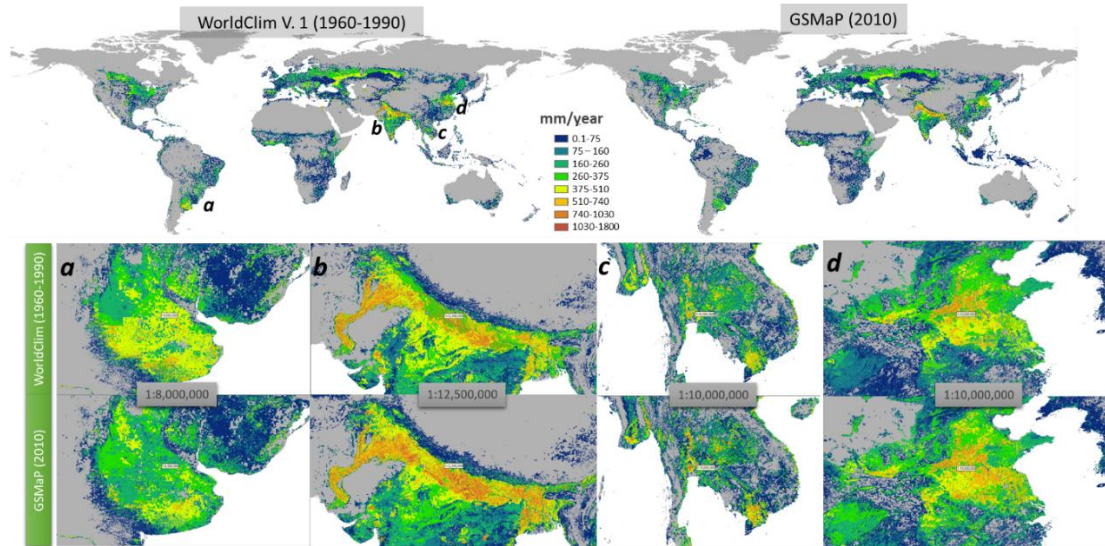


Figure 6-11. Comparison of IWD product derived from two precipitation datasets: Wordclim and GSMaP

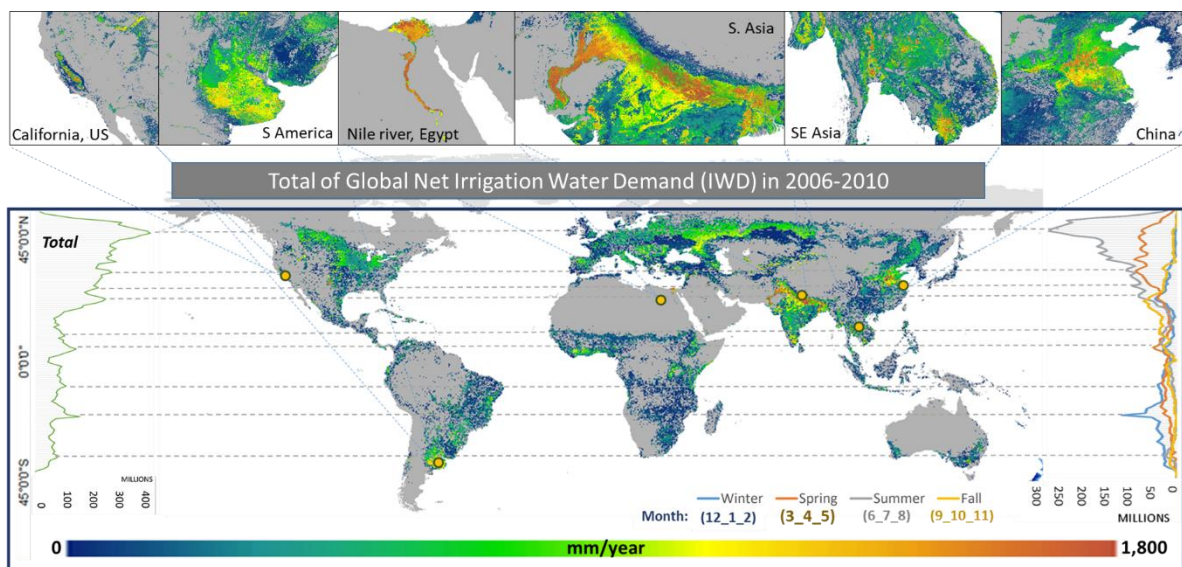


Figure 6-12. Total of global net irrigation water demand (IWD) in 2006-2010

We investigate also based on climate condition for supplementary analysis in since climate condition are reflecting level of evapotranspiration and precipitation as well. In hot arid and semi-arid regions, IWD value is more than 1000 mm/ year ( $1 \text{ m}^3$  of water per  $1 \text{ m}^2$  of irrigated area). However, colder areas like in European region or in the humid tropics, values of less than 100 mm/ year. In dry and hot years. IWD is higher than under average climatic conditions. This condition shows how climate are very influence the value of IWD, hence climate change become issues that can give big impact into how human need to prepare water for cultivation activities in future. From sessional analysis we also found how climatic

condition are reflecting into level of cultivation activity during one-year monitoring. Figure 6-14 shows seasonal analysis of average 2006-2010 IWD product. Precipitation, and in particular its effective portion, provides part of the water crops need to satisfy their transpiration requirements. The soil, acting as a buffer, stores part of the precipitation water and returns it to the crops in times of deficit. In humid climates, this mechanism is sufficient to ensure satisfactory growth in rainfed agriculture. In arid climates or during extended dry seasons, irrigation is necessary to compensate for the evapotranspiration (crop transpiration and soil evaporation) deficit due to insufficient or erratic precipitation.

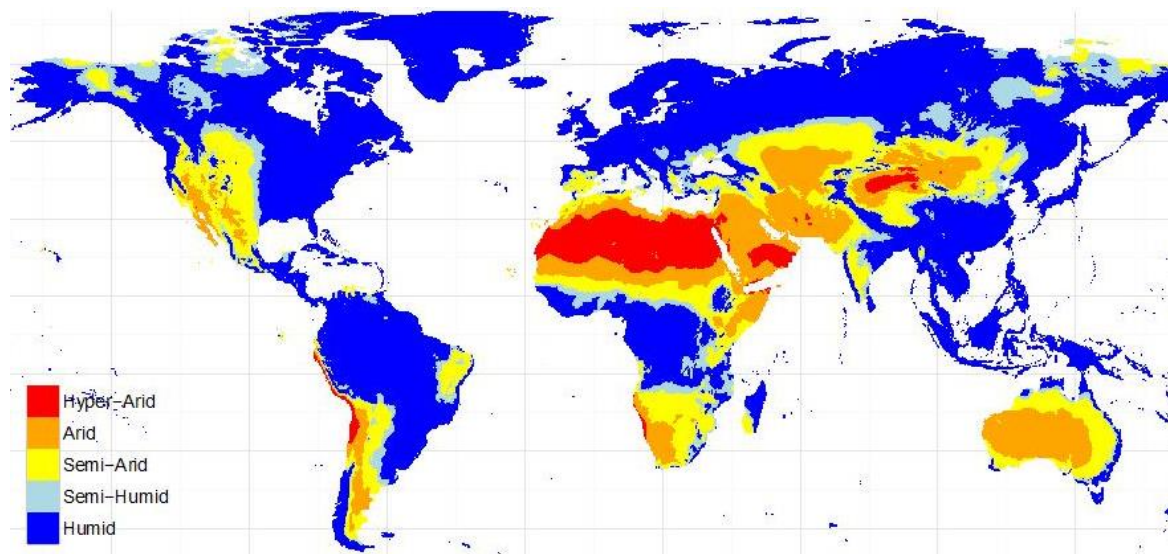


Figure 6-13. Distribution of humid and arid region

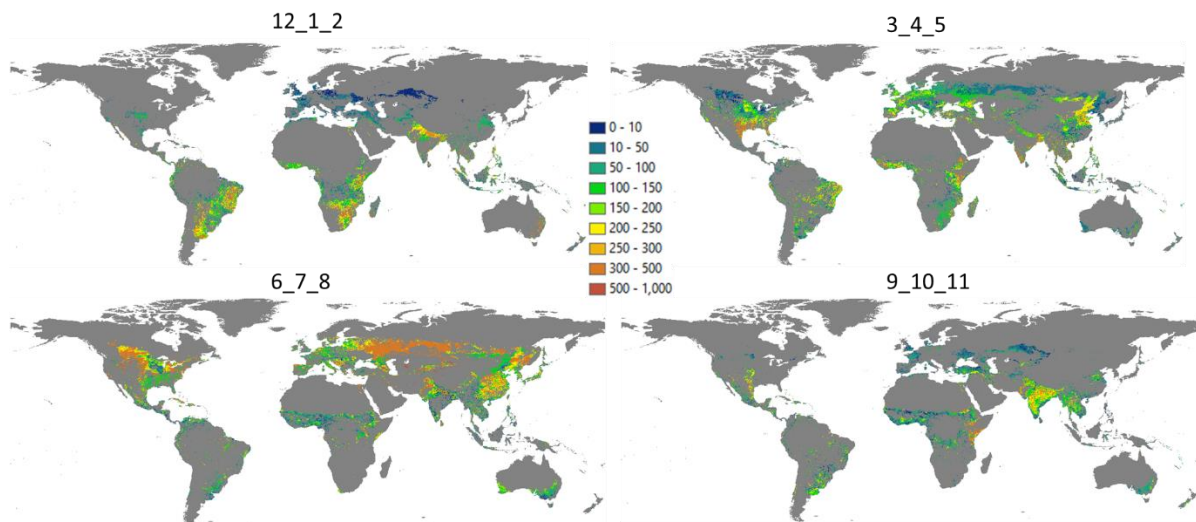


Figure 6-14. Seasonal analysis of average 2006-2010 IWD product

Figure 6-15 shows the result of IWD product in three group of year 2001-2005, 2006-2010, 2011-2015. The total water use by irrigated and rainfed are 6,137 km<sup>3</sup>/ year in 2001-2005, 5,834 km<sup>3</sup>/ year in 2006-2010, and 7,491 km<sup>3</sup>/ year in 2006-2010 (figure 6-16). This calculation derived from three water use estimation categories: 1) total blue water use (irrigation) by irrigated crop, 2) total green water use (precipitation) by irrigated crop and 3). Green water use by rainfed crops.

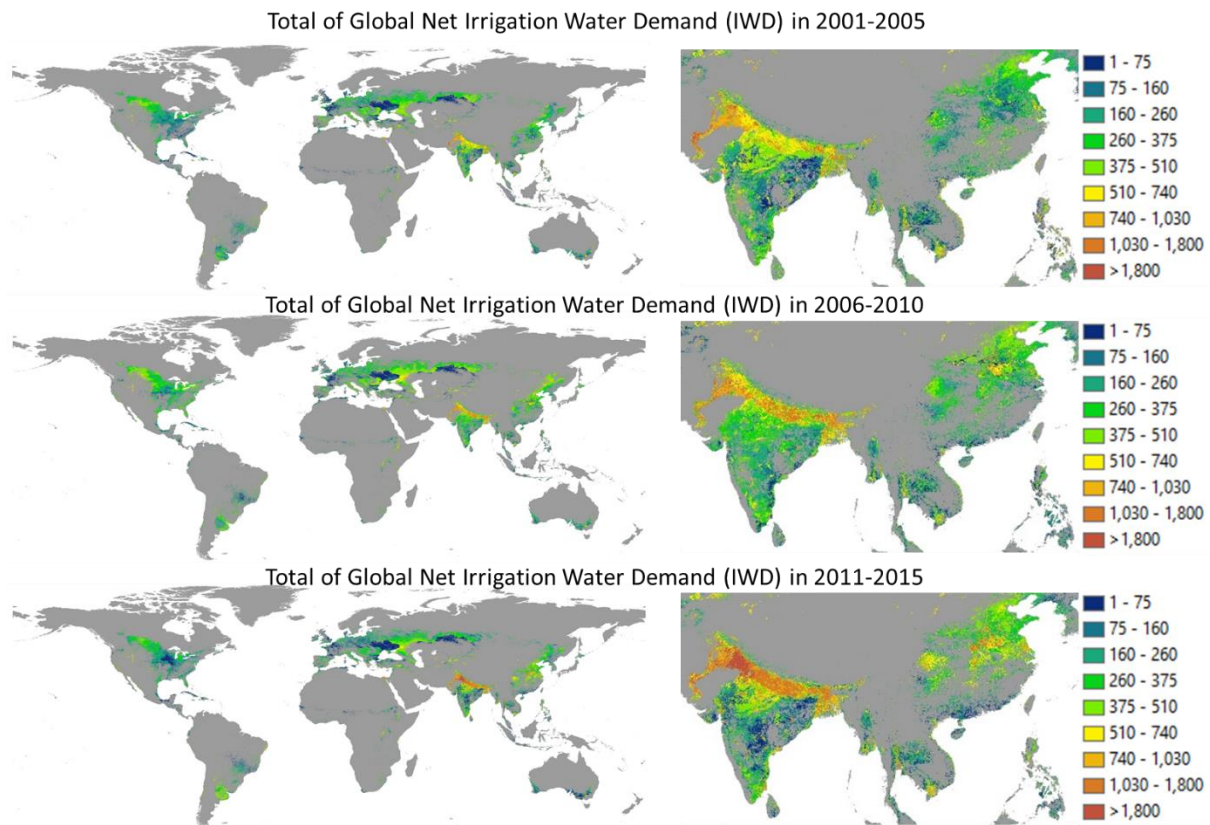


Figure 6-15. Result of IWD product in three group of year 2001-2005, 2006-2010, 2011-2015

Total global water demand is increasing, mainly due to economic and population growth in developing countries that reflect to increasing water demand in food sector. By applying low and high Kc value (Figure 5-6), Based on 2005 data processing: The range of different value in lowest Kc it's from 12 to 60 Km<sup>3</sup> per month the range of different value in highest Kc it's from 29 to 99 Km<sup>3</sup> per month. we identified the error value of Total IWD per year by around 402 km<sup>3</sup> for low Kc and 650 km<sup>3</sup> for high Kc compared with from Standard Kc value (Figure 6-17).

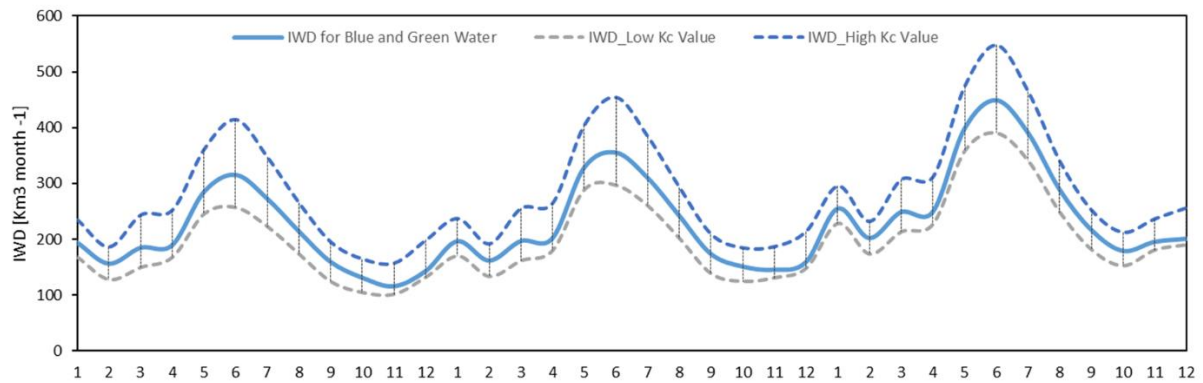


Figure 6-16. Seasonal IWD for Blue (irrigation) and Green Water (Effective precipitation) Contribution in the three group of year derived with Standard, Lowest and highest Kc

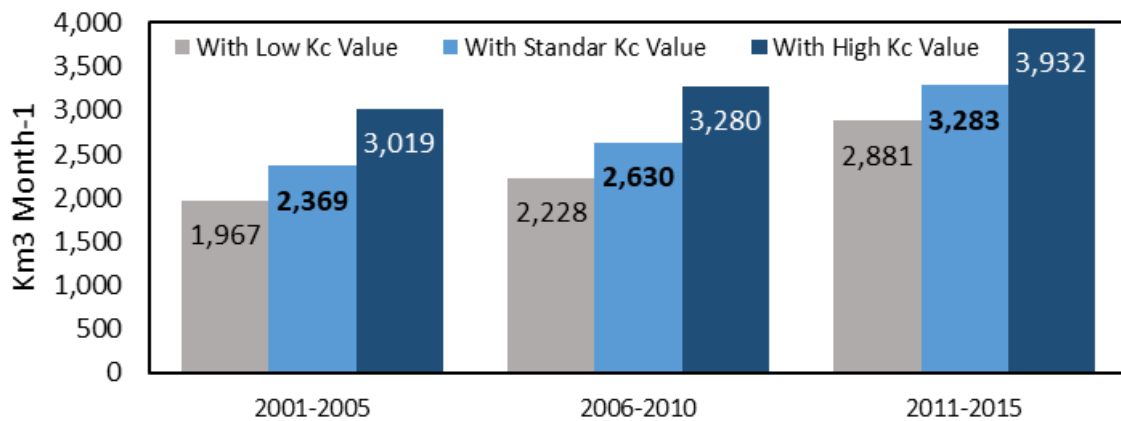


Figure 6-17. Total IWD in the three group of year derived with Standard, Lowest and highest Kc

#### 7.3.4 Contribution of Blue and Green for Irrigation Water Demand in Regional Analysis

For detailed investigation we select eight regional for sessional analysis. Figure 6-18. Shows distribution of eight regional analyses in this study: 1. Southern Asia, 2. Eastern Asia, 3. South-east Asia, 4. North America, 5. South America, 6. Europe, 7. Africa, and 8. Oceania. We divided Asia into three sub regions since Asia has very high value of water demand which distributed mainly in southern part, eastern part and southeast part of Asia.

Figure 6-19 shows the final analysis about sseasonal value of irrigation water demand for blue (irrigation) and green (effective precipitation) water contribution. From statistic data result shows how Southern Asia region is the highest blue and green water consumption region for irrigation (2,865 and 1,047 Km<sup>3</sup> respectively), followed by Eastern Asia (1,533 and 986

Km<sup>3</sup> respectively) and North America (326 and 274 Km<sup>3</sup> respectively). Interesting finding shows how South East Asia is the only region that has higher green water contribution compare with blue water contribution (272/239 km<sup>3</sup>) and also in Africa region demand of Blue water is very high compare with green water consumption (135/26 km<sup>3</sup>) (Figure 6-20), this condition make the two regions could have significantly affected with climate change impact if there are not sustainable irrigation system.

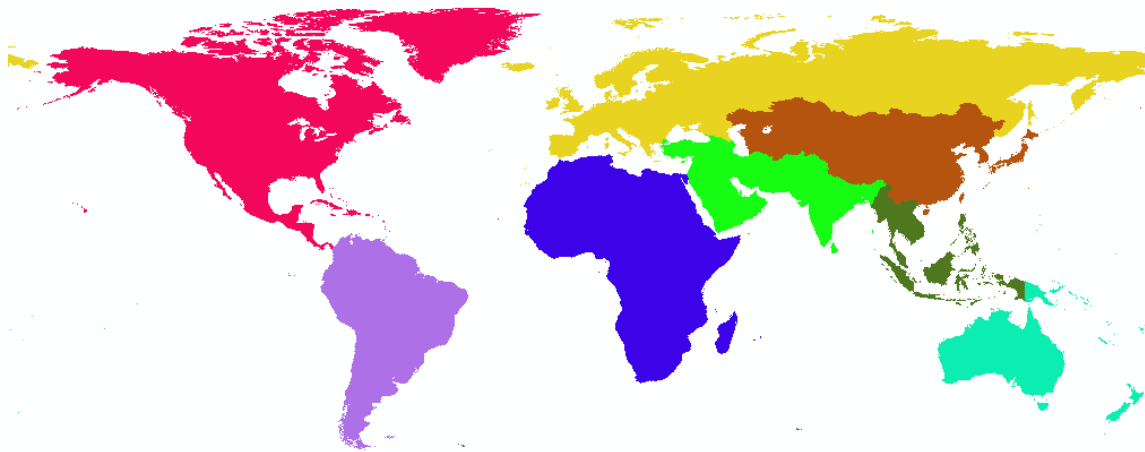


Figure 6-18. Distribution of eight regional analyses: 1. Southern Asia, 2. Eastern Asia, 3. South-east Asia, 4. North America, 5. South America, 6. Europe, 7. Africa, and 8. Oceania

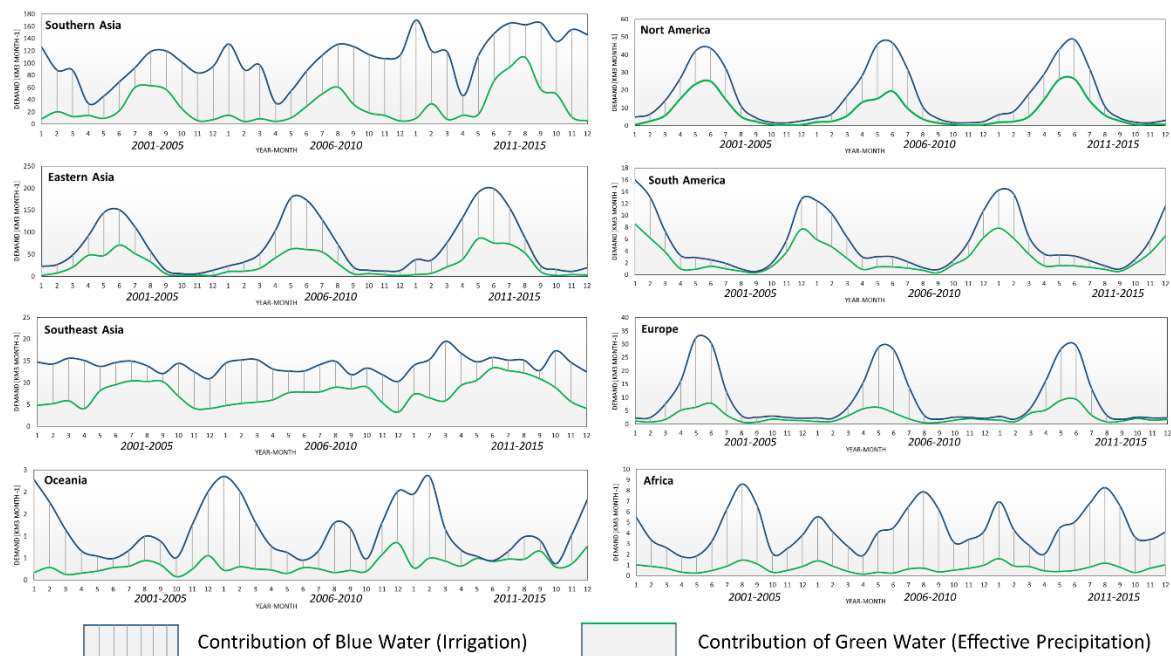


Figure 6-19. Seasonal Irrigation Water Demand of Blue (Irrigation) and Green Water (Effective Precipitation) Contribution in the three group of year

| Regional           | Water Sources                   | Total Irrigation Water Demand Contribution [km <sup>3</sup> month <sup>-1</sup> ] |           |           |       |
|--------------------|---------------------------------|---|-----------|-----------|-------|
|                    |                                 | 2001-2005   | 2006-2010 | 2011-2015 | Total |
| Southern Asia      | Green (Effective Precipitation) | 309   | 257       | 481       | 1047  |
|                    | Blue (Irrigation)               | 755   | 944       | 1166      | 2865  |
| Eastern Asia       | Green (Effective Precipitation) | 296   | 310       | 380       | 986   |
|                    | Blue (Irrigation)               | 402   | 519       | 612       | 1533  |
| Nort America       | Green (Effective Precipitation) | 97  | 75        | 102       | 274   |
|                    | Blue (Irrigation)               | 95  | 126       | 105       | 326   |
| South-Eastern Asia | Green (Effective Precipitation) | 84  | 80        | 108       | 272   |
|                    | Blue (Irrigation)               | 83  | 79        | 76        | 239   |
| Europe             | Green (Effective Precipitation) | 34  | 31        | 42        | 106   |
|                    | Blue (Irrigation)               | 84  | 80        | 70        | 234   |
| South America      | Green (Effective Precipitation) | 37  | 30        | 37        | 104   |
|                    | Blue (Irrigation)               | 32  | 31        | 32        | 96    |
| Africa             | Green (Effective Precipitation) | 9   | 7         | 10        | 26    |
|                    | Blue (Irrigation)               | 39  | 47        | 49        | 135   |
| Oceania            | Green (Effective Precipitation) | 3   | 4         | 5         | 12    |
|                    | Blue (Irrigation)               | 10  | 11        | 7         | 28    |

Figure 6-20. Contribution of Blue (irrigation) and Green (Effective precipitation) for estimating total irrigation water demand in irrigated area in eight regional analysis

The final goal of this study is specifically estimates blue or irrigation source water contribution in the three group of year 2001-2005, 2006-2010 and 2011-2015 (Figure 6-21). This result is tried to investigate the evolution of the IWD at the eight regional in monthly based analysis.

The growth of IWD volume takes place unevenly among the world's regions. South Asia has become a major of increasing IWD in irrigated are from irrigation water source contribution. Some specific countries play a very important role in the global IWD. Reflection of the dramatic increase in the underlying food trade. This increasing in several region has correlation with trade activities, reflecting of American internal trade (US-Mexico) and North American exports to Asia t. (NA Free Trade Agreement) hat implemented in last fifteen years, can increased GDP per capita of mostly in all countries in south America [GDPPC multiplied by 5.1 from 1986 to 2000]. However, exports from NA to Europe have shrunk indicated the reasons behind dynamic change in several regions. Most to the trade volume increase between 1986 and 2007 Exports from South America to Asia contributed the (30%) internal trade in North America (11%). Irrigation Water demand decreases in OECD countries might be due to rapid changes in technology in irrigation technology.

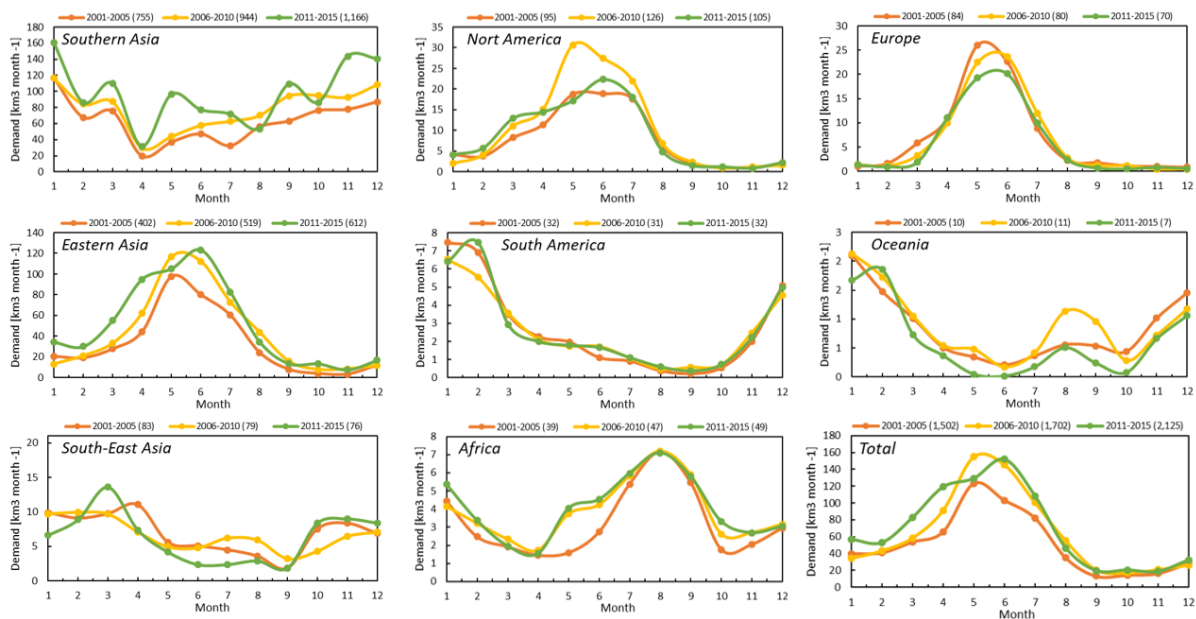


Figure 6-21. Seasonal Irrigation Water Demand of Blue Water (Irrigation) Contribution in the three group of year

### 7.3.5 Comparative analysis of Irrigation Water Demand product with current statistic data

Since the high accuracy ground data of Irrigation water demand are very limited. We used two parameter of water use statistic data; 1). Consumptive irrigation water used or Irrigation water demand and 3). Irrigation water withdrawal from Aqua-stat.

**Irrigation consumptive water use or Irrigation water demand** indicated the volume of water needed to compensate for the deficit between potential evapotranspiration on the one side and effective precipitation over the crop growing period and change in soil moisture content on the other side [FAO, 2005]. In this study, the irrigation consumptive water use is computed for each country on the basis of the irrigated crop calendar for a specific year (from 1995 to 2015 depend on country report), The irrigation water requirement computed in this study is available by country under the variable "Irrigation water requirement" [code 4260] in the AQUASTAT database

**Agricultural water withdrawal** indicated total water used for cultivation process, it is normally far exceeds the net irrigation water demand because of water lost in its distribution from its source to the crops. For 118 out of the 175 countries and territories information on

water withdrawal is available from national sources (i.e. not estimated). In order to fill the data gaps regarding the 47 countries for which this information is not available (or only estimated), a ratio of the estimated irrigation water requirement to the actual irrigation water withdrawal is calculated for countries for which such data is available.

For Irrigation water demand analysis, first we compare two IWD estimation products derived from two precipitation datasets (GSMaP and WordClim) with FAO independent data of consumptive irrigation water use in two groups of large irrigated area countries (from 40 to 160 km<sup>3</sup>/year) and medium irrigated area countries (from 0.5 to 15 km<sup>3</sup>/year).

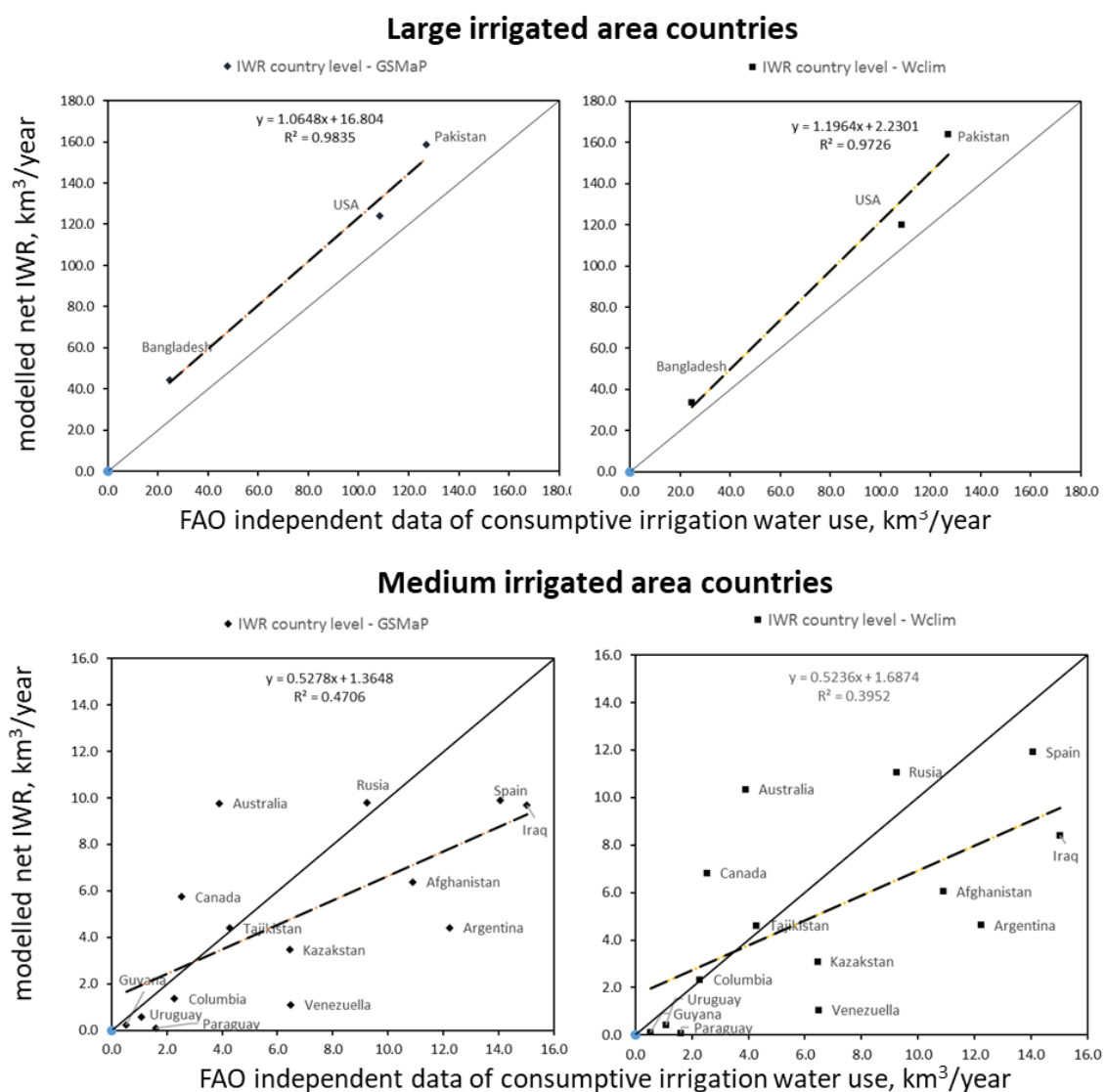


**Figure 6-21.** Comparison of country level IWD estimation derived from two precipitation datasets with FAO independent data of consumptive irrigation water use

The regression value of comparison two group Irrigation water demand with consumptive irrigation water use based GSMaP precipitation data shows the regression value of FAO statistics data and simulated IWD is 0.47 and 0.983 for medium and large irrigated area respectively (Figure 6-21). Compared with WorldClim precipitation datasets The regression value is 0.39 and 0.975 (Figure 6-21). Indicated GSMaP precipitation data can estimate in more accurate for estimating Irrigation Water Demand.

For further analysis, the product result of IWD in country level are compared with two water use data statistics: Irrigation Water Demand and Agriculture Water Withdrawal. We used logarithmic scale in scatterplot analysis to accommodate high range of IWD countries values with range from 0.002 km<sup>3</sup>/year (Saint Kitts and Nevis) to 688 km<sup>3</sup>/year (India). The dashed line represents the 1:1 slope.

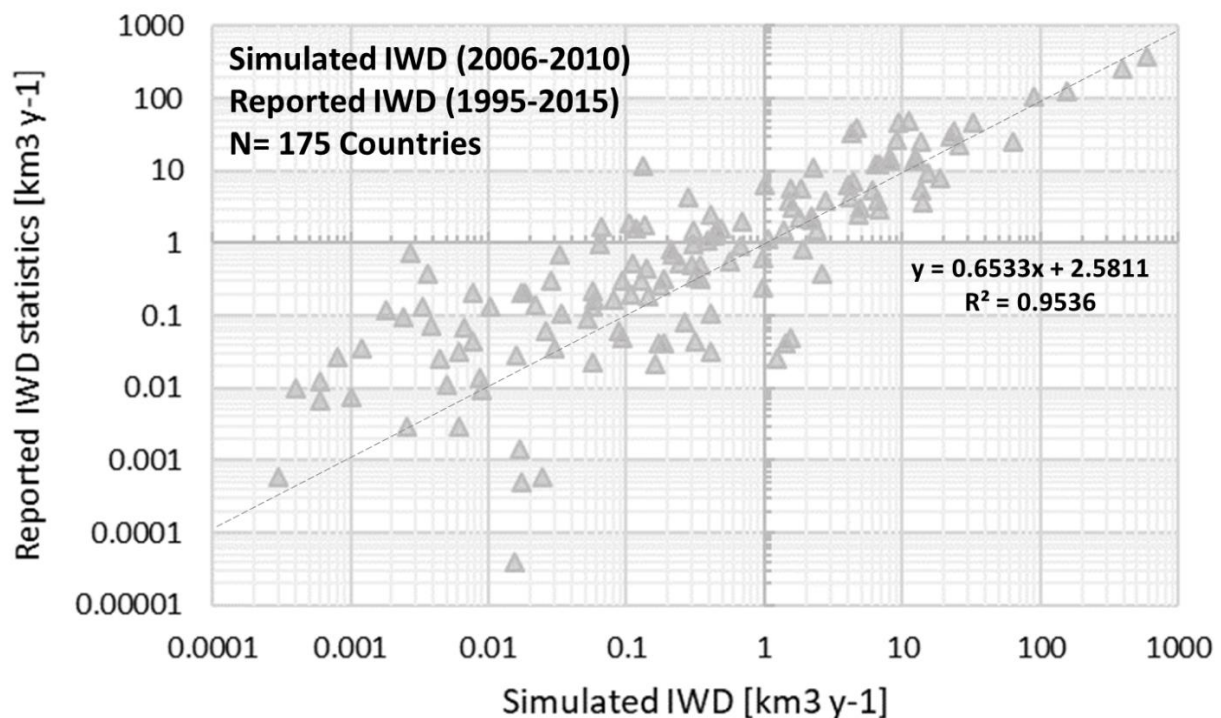


**Figure 6-22.** Comparison of simulated IWD to reported IWD statistics [km<sup>3</sup> yr<sup>-1</sup>] per country (N = 175).

IWD was modelled with the MODIS Cropping Intensity, MODIS-AMSR Sowing Month, MODIS-AMSR rice paddy cropping pattern, and FAO-Cropwat simulated model respectively. IWD Reported statistics was obtained from the FAO AQUASTAT database (<http://www.fao.org/nr/water/aquastat/main/index>). The overall correlation between IWD product derived from remote sensing (2006-2010 data product) and the Aqua-Stat Irrigation

Water Demand (1995-2015 data product) is observed in global scale with total 172 countries. The result show regression value is 0.953 (Figure 6-22) indicated the simulated and reported value of Irrigation water demand has good relation.

We indicate there are more overestimate estimation value compare with Aqua-stat value. The reasons of overestimated are; 1. Fraction of the irrigated crops is actually grown in the winter, while the temperature criterion in the model leads to a summer growing season. 2. Ortiz [1998] noted that for the calculation, the basic plant water requirement was adjusted to actual good irrigation practices.

We also analyze the accuracy of the two variable of Irrigation water demand (IWD) and Agriculture water withdrawal (AWW) product. In this framework, the regression value to the Aqua-stat have been observed as 0.941 (Figure 6-23). The comparison of IWD shows underestimate value compare to and AWW Aqua-stat data.

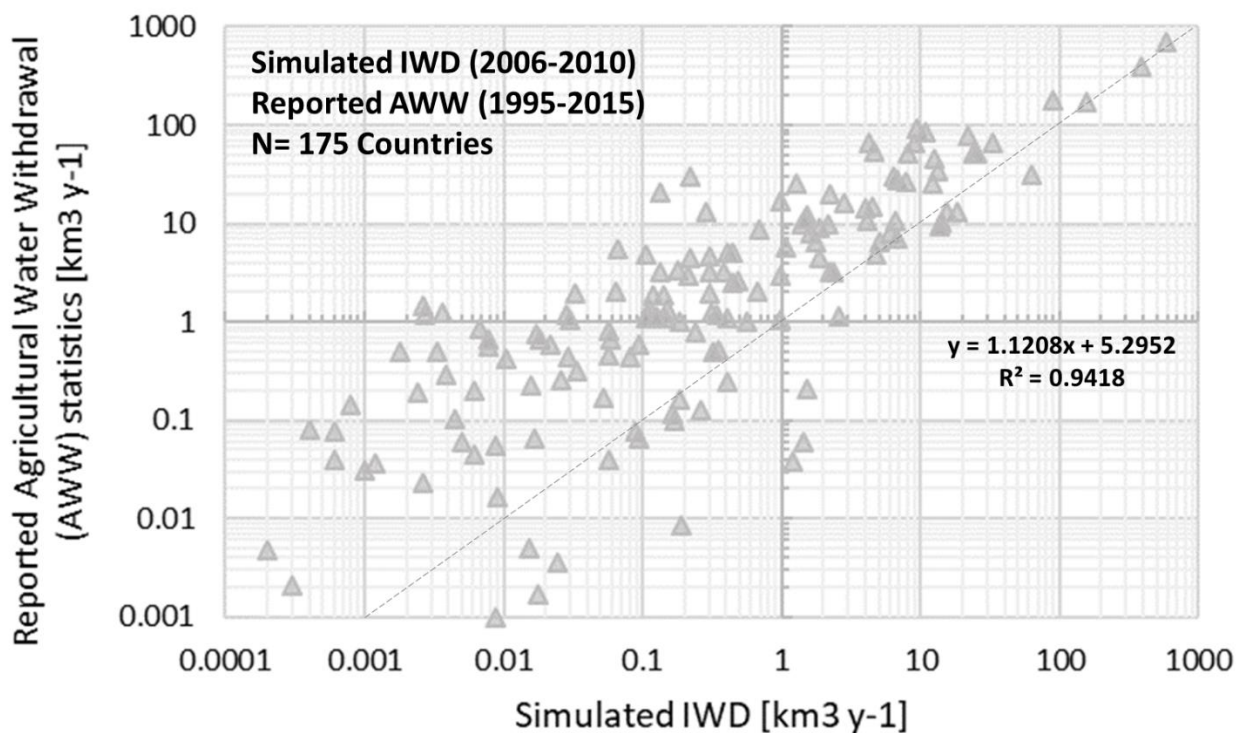


**Figure 6-23.** Comparison of simulated IWD to reported AWW statistics [km<sup>3</sup> yr<sup>-1</sup>] per country (N = 175).

The comparison product between “Irrigation water demand” and “Agriculture water withdrawal” can often referred to as "water use efficiency" [FAO, 2012] in agriculture or "irrigation efficiency". However, the use of the expression is subject of debate [Perry and Kite,

2003]. The word "efficiency" implies that that water is being wasted when the efficiency is low. This is not necessarily so. The recoverable fraction of the non-consumed water can be used further down-stream in the irrigation scheme, it can flow back to the river or it can contribute to the recharge of aquifers. It is for this reason that in this study the term "water requirement ratio" is employed when referring to the ratio between irrigation water requirement and the amount of water withdrawn for irrigation.

The average of the water demand ratio calculated at national level enables, in combination with the irrigation water demand calculated in the previous step, the estimation of irrigation water withdrawal for countries with missing data. In addition, it also permits to cross-check data and thus their correction. Assessing the impact of irrigation on water resources requires an estimate of the water effectively withdrawn for irrigation, i.e. the volume of water extracted from rivers, lakes and aquifers for irrigation purposes. Irrigation water withdrawal

The limitation of this statistics dataset are not all countries are reported the water used data, also not in all year there are available data for comparison, some countries reported based 1995 data and another country report the updated data until 2015. It also appears by country in figure 6-23 and figure 6-24, comparing the product of IWD with reported IWD and reported irrigation water withdrawal (IWW).

### 7.3.6 Comparative analysis of Irrigation Water Demand product with Previous Product of Irrigation water demand.

In total there are sixteen product IWD estimation where three products are produce in this study (Table 6-1). Since all estimated product are produced using different input data, Direct comparisons do not make sense. This comparison can be used as Indicator the possible range of irrigation water demand range estimation in the 21st century.

This studies have close to the IWD estimation of Siebert and Doll [2009] and Wada et al. [2011]. Discussing model feasibility is quite difficult under the current regression modelling framework. Changes are shown for individual IWD product in each product estimation, potential irrigation water demand increase globally, except for IWD product estimated by Sursel et al [2010] and Pokhrel et al. [2012].

Increasing of total blue water use by irrigated crop, in three group of year: 1,502 km<sup>3</sup>/ year in 2001-2005, 1,702 km<sup>3</sup>/ year in 2006-2010 and 2,125 km<sup>3</sup>/ year in 2011-2015 that located in specific area indicated the increasing intensification in 15 years is happened. This condition is support by the increasing of total green water use by irrigated crop as well; 860 km<sup>3</sup>/ year in 2006-2010, 926 km<sup>3</sup>/ year in 2006-2010 and 1,158 km<sup>3</sup>/ year in 2011-2015. This condition shows how precipitation could supply half of water demand in agriculture.

Based on analysis of green water use by rainfed crops, decreasing green water happen in between 2001-2005 to 2006-2010 from 6,137 to 5,839 km<sup>3</sup>/ year, and increase again in 2011-2015 estimation by reach 6,494 km<sup>3</sup>/ year. The decreasing of green water in rainfed area and increasing green water in irrigated area has hypothesis that shifting from rainfed to irrigated in large area globally are happen in between 2001-2010.

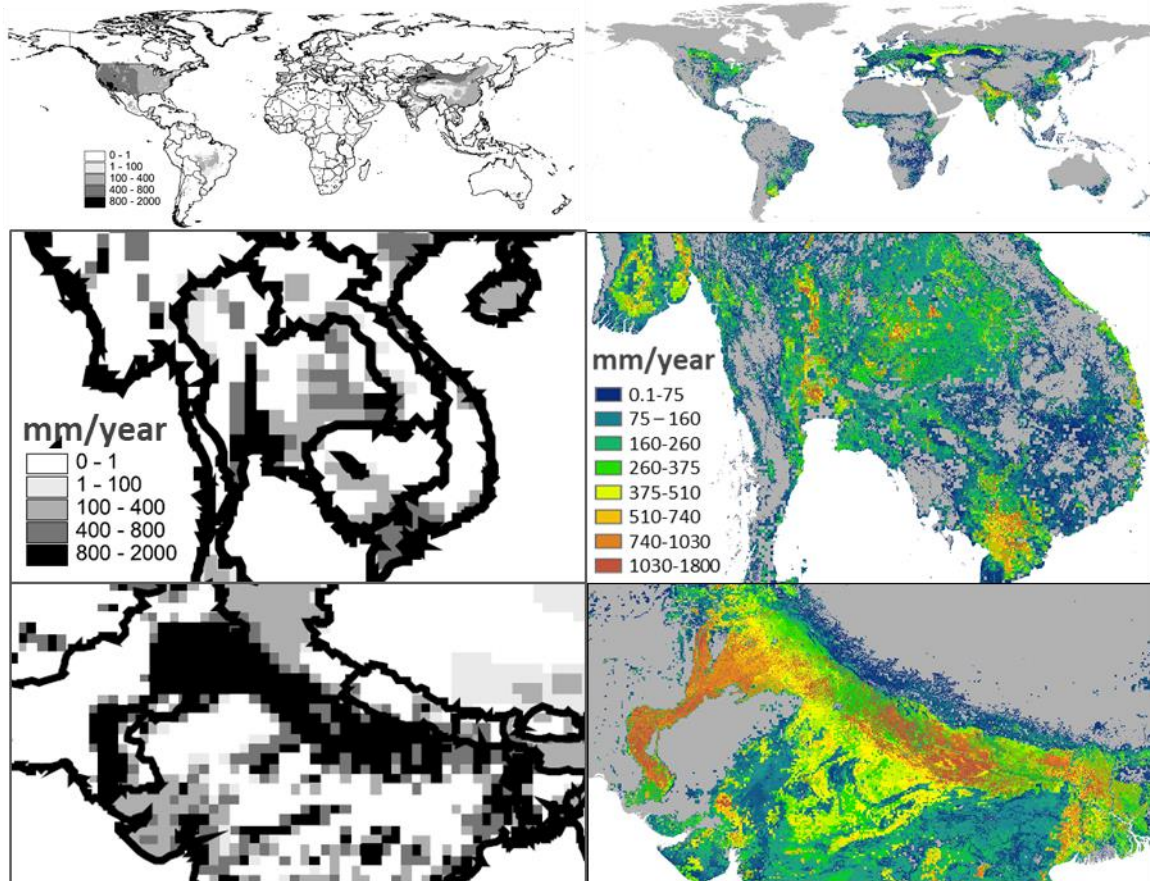


Figure 6-24. Visual comparison of 50 km pixel resolution derived from model simulation [Doll and Siebert, 2002] and 1 km resolution derived from remote sensing data integration in this study

**Table 6-2.** Total water use by irrigated-rainfed crop estimation derived from this study and previous studies.

| References              | Year baseline  | Blue Water use by Irrigated Crop km <sup>3</sup> /yr | Green water use by Irrigated crop km <sup>3</sup> /yr | Blue and Green water use by Irrigated crop km <sup>3</sup> /yr | Green water use by rainfed crops km <sup>3</sup> /yr | Total water use by Irrigated-rainfed crop km <sup>3</sup> /yr | Spatial resolution n |
|-------------------------|----------------|--|---|--|--|---|----------------------|
| Hanasaki et al. [2006]  | Avg. 1987–1988 |  |   | 2,254  |  |   | 0.5°                 |
| Doll and Siebert [2002] | Avg. 1961–1990 |  |   | 2,452  |  | 7,500   | 0.5°                 |
| Postel [1998]           | 1995           |  |   |  |  |   | -                    |
| Hanasaki et al. [2010]  | Avg. 1985–1999 |  |   | 1,530  |  |   | 0.5°                 |
| Falkenmark [2006]       | 1950-2000      | 1,800  |   |  | 5,000  | 6,800   | 0.5°                 |
| Rost et al. (2008)      | Avg. 1971–2000 |  |   | 2,555  |  |   | 0.5°                 |
| Sulser et al. [2010]    | 2000           |  |   | 3,128  |  |   | -                    |
| Pokhrel et al. [2012]   | 2000           |  |   | 2,462  |  |   | 1°                   |
| Wada et al. [2011]      | Avg. 1958–2001 |  |   | 2,057  |  |   | 0.5°                 |
| Siebert and Doll [2009] | Avg. 1998–2002 | 1,180  | 919   | 2,099  | 4,586  | 6,685   | 0.083°               |
| In this study           | 2001-2005      | 1,502  | 860   | 2,362  | 3,775  | 8,499   | 0.0083°              |
| Pokhrel et al. [2012]   | 1983–2007      |  |   | 2,158  |  |   | 0.5°                 |
| In this study           | 2006-2010      | 1,702  | 926   | 2,628  | 3,211  | 8,457   | 0.0083°              |
| In this study           | 2011-2015      | 2,125  | 1,158   | 3,283  | 4,208  | 10,774  | 0.0083°              |
| Sulser et al. [2010]    | 2025           |  |   | 4,060  |  |   | -                    |
| Sulser et al. [2010]    | 2050           |  |   | 4,396  |  |   | -                    |

The issues of different input data can be a major source of the different result between this study and other study. The growing period of crops and water requirement during the crop period varied on a grid-basis. Hanasaki et al. [2010] assumed that the crop-specific growing period and daily water requirement are uniform globally. The advantage of the IWD product compare with previous studies are capability to estimate two source of water (green and blue water) for both irrigated and rainfed crop type. Higher pixel resolution also can improve country level analysis of water demand in crop sector. Figure 6-24 shows comparison 50 km and 1 km pixel resolution derived from model simulation and remote sensing data integration. In this study increasing spatial resolution might be the advantages of Global irrigation water demand product which derived from remote sensing datasets compare with previous study which derived from model simulation based approaches. The increase in spatial resolution from previous studies using simulation model in 50 km resolution [Doll and Siebert, 2002; Hanasaki et al., 2010] to 1 km in this study improves analysis at country level. This improvement can help to provide a more comprehensive analysis since each country has their complexity of problems in trying to achieve the Sustainable Development Goals (SDGs) [FAO, 2015].

#### **7.4 Conclusion**

The final result of global irrigation water demand (IWD) products are the first satellite-based products that can analyze 15 years' dynamic change of water demand in cropland area. The total water use by irrigated and rainfed are 6,137 km<sup>3</sup>/ year in 2001-2005, 5,834 km<sup>3</sup>/ year in 2006-2010, and 7,491 km<sup>3</sup>/ year in 2006-2010. This calculation derived from three water use estimation categories: 1) total blue water (irrigation) used by irrigated crop, 2) total green water (precipitation) used by irrigated crop and 3). Green water used by rainfed crops. The total water use by irrigated are 2,362 km<sup>3</sup>/ year in 2001-2005, 2,628 km<sup>3</sup>/ year in 2006-2010, and 3,283 km<sup>3</sup>/ year in 2010-2015.

By applying low and high Kc value, we identified the error value of Total IWD per year by around 402 km<sup>2</sup> for low Kc and 650 km<sup>3</sup> for high Kc compared with from Standard Kc value. The regression value of FAO statistics data and simulated IWD is 0.47 and 0.98 for medium and large irrigated area respectively. The long-term global IWD products are projected

to simulate global surface water cycle in agriculture area in more realistic way by considering climate and crop activities which derived from actual, consistent and latest remote sensing datasets. This high resolution IWD product will support to achieve SDGs target in regional and country level analysis.

## Chapter 7 CONCLUSIONS AND RECOMMENDATIONS

### 8.1 Conclusions

The 1 km Global Irrigation Water demand product are the first satellite-based products which derived from integration of vegetation and water index phenology that can analyze 15 years' dynamic change of water demand. The advantage of the combination MODIS-AMSR products are the capability to detect short period of crop cultivation and distinguish rice and non-rice crop type. The Increasing pixel resolution and consistency dataset are some advantages in the IWD product, hence increasing time resolution will become key to improve IWD product and for Verification propose. The assumed dominant crop and cloud contamination are the major source of discrepancy of MODIS-AMSR crop intensity and Sowing month product.

The results of cropland agreement level (CAL) analysis proposed four agreement levels, and the correlation factor obtained from the CAL product and IIASA crop fraction comparison had successfully estimated the percentage of cropland area from four agreement levels. The cropland estimate results from the CAL analysis were observed along with FAO data statistics and showed the highest accuracy, with a 0.70 and 0.71 regression value for 2005 and 2010 respectively. The presented MODIS-AMSR sowing month and cropping pattern products, to our knowledge are the first satellite-based products which derived from integration of vegetation and water index phenology from optic and microwave satellite sensor, that can analyze dynamic change of crop activities as one of essential input for estimating irrigation water demand. The advantages of the MODIS-AMSR sowing month product are capable to detect short period crop cultivation, distinguish rice and non-rice crop type and analyze trend of sowing month change from 15 years' data monitoring.

The final result of global irrigation water demand (IWD) products are the first satellite-based products that can analyze 15 years' dynamic change of water demand in cropland area. The total water use by irrigated and rainfed are 6,137 km<sup>3</sup>/ year in 2001-2005, 5,834 km<sup>3</sup>/ year in 2006-2010, and 7,491 km<sup>3</sup>/ year in 2006-2010. This calculation derived from three water use estimation categories: 1) total blue water (irrigation) used by irrigated crop, 2) total green water (precipitation) used by irrigated crop and 3). Green water used by rainfed crops. The long-term global IWD products are projected to simulate global surface water cycle in agriculture area in

more realistic way by considering climate and crop activities which derived from actual, consistent and latest remote sensing datasets. This high resolution IWD product will support to achieve SDGs target in regional and country level analysis.

## **8.2 Recommendations**

One of the limitation on this product is we not include yet the product of dominant cropping pattern of rice and non-rice and it is change in long-term analysis in multi cropping intensity area. Hence, based on current IWD product, some area should be facing over estimation especially in triple cropping rice paddy area. Since bases on cropping pattern product in this study, large area of triple rice only found in Mekong delta, Vietnam. Also, in this analysis, we do not include yet the calculation of water volume that applied in flooding season in the beginning of rice paddy plantation. From previous discussion we propose three improve ment strategy that can tackle the limitation of current product. First, the product of 15-year dominant cropping pattern should be address in developing Crop Coefficient ( $K_c$ ), Second, Investigate the general volume of water that applied in flooding session of rice paddy, and involve the value into water balance approach estimation, and third, improving the 15 year IWD product in higher time resolution from monthly data processing to 10 days' data analysis.

## **8.3 Future Works**

Future research will conduct the updating the developed  $K_c$  based on integration of three group of year the MODIS cropping intensity product, MODIS-AMSR sowing month, and dominant cropping pattern of rice and non-rice in higher time spatial resolution (10 days' data analysis). Hence, the developed new product of monthly IWD in the three group of year 2001-2005, 2006-2010 and 2011-2015 will conduct. The 15-year investigation impact of cropping intensity, sowing month and cropping pattern change impact to the long-term monthly IWD product also will analyze combined with existing additional data especially gridded socio-economic dataset. Another important issues that should be tackle is pixel by pixel comparison analysis of IWD product with published IWD Doll Siebert product which derived from WaterGAP model.

## **ACKNOWLEDGMENT**

First of all, my gratitude goes to Japan Government for having afford me an opportunity to pursue my master study at the Graduate School of Engineering, The University of Tokyo. The same manner, I acknowledge the support from Global Leader Program for Social Design and Management (GSDM) by the Ministry of Education, Culture, Sport, Science and Technology Japan.

I would like to express my sincere gratitude to my academic supervisor Dr. Wataru Takeuchi for his valuable direction and technical guidance that is very meaningful to enhance my knowledge in Remote Sensing and during construction of this thesis. Without his support and guidance this research may not carried out.

I would like to say thanks to my lab friends in RSED laboratory. for the advice and critics that were given during laboratory seminar.

I would like to express sincerely thanks to my parents, beloved wife, baby azfar, brother and sisters for their endless support and encouragements. Finally, all praise to Allah SWT for his grace and favour beginning until the end of the completion of this thesis. I ask him to reward this humble effort and to make it useful to everyone.

## BIBLIOGRAPHY

- Altchenko, Y., and Villholth, K. G. (2015) Mapping irrigation potential from renewable groundwater in Africa – a quantitative hydrological approach. *Hydrol. Earth Syst. Sci.*, 19, 1-13, Doi: 10.5194/hessd-19-1-2015
- As-syakur, A. R. (2011) Perubahan penggunaan lahan di provinsi Bali [Land Use Land Cover change in Bali]. *Ecotrophic*, vol. 6, no.1, pp.1 7.
- Bai, Y., Feng, M., Jiang, H., Wang, J., Zhu, Y., and Liu, Y. (2014) Assessing Consistency of Five Global Land Cover Data Sets in China. *Remote Sens.*, vol. 6, no. 9, pp. 8739–8759.
- Bartholomé, E. and Belward, A. S. (2005) GLC2000: a new approach to global land cover mapping from Earth observation data. *Int. J. Remote Sens.*, vol. 26:9, pp. 1959–1977.
- Bontemps, S., Defourny, P., Van Bogaert, E., Arino, O., Kalogirou, V., and Perez, J. R. (2009) GLOBCOVER 2009 Products description and report. Toulouse, France.
- Carlson, K. M., Gerber, J. S., Mueller, N. D., Herrero., MacDonald, G. K., West. P.C. (2016) Greenhouse gas emission intensity of Global Croplands. *Nature Climate Change*. November. DOI:10.1039/NCLIMATE3158
- CCI-LC. (2014) Land cover CCI: Product user guide version 2. Louvain-la-Neuve, Belgium.
- Chen, J., Ban, Y., Li, S. (2014) China: Open access to Earth land-cover map. *Nature*, 514(7523): 434-434. DOI:10.1038/514434c.
- Cleugh, H. A., Leuning, R., Nu, A (2007) Regional evapotranspiration estimated from flux tower and MODIS Satellite Data. *Remote Sensing of Environment*, 206, 285-304.
- Dalin C., Konar, M., Hanasaki., Rinaldo, A., Iturbe, I, R. (2012) Evolution of Global Virtual Water Trade Network. *Proceedings of National Academy of Science of The United State of America*.
- Di Gregorio, A. Land cover classification system: Classification concepts. Software version 3. (2016).
- Doll, P., and Fiedler, K. (2008) Global-scale modelling of groundwater recharge, *Hydrol. Earth Syst. Sci.* 12, 863–885 pp
- Doll, P. and Siebert, S. (2002) Global Modeling of Irrigation Water Requirements. *Water Resour. Res.*, vol. 38, no. 4.

- Doll, P. and Siebert, S. (2002) Global Modeling of Irrigation Water Requirements. *Water Resources Research*, 38
- Falkenmark, M.; Rockström, J. (2006) The New Blue and Green Water paradigm: Breaking new ground for water resources planning and management. *J. Water Res. Plan. Manag.* 132, 1–15.
- FAO. (2012). Irrigation water requirement and water withdrawal by country. FAO AQUASTAT Reports. FAO, Rome
- FAO, IFAD, and WFP. (2015) The state of food insecurity in the world 2015. Meeting the 2015 international hunger target: taking stock of uneven progress. Rome, FAO.
- FAO. (2016) The state of food and agriculture. Climate change, agriculture and food Security. Rome, FAO.
- FAO., 2009. CROPWAT 8: A Computer Program for Irrigation Planning and Management. Rome, Italy.
- Foster, S. and Perry, C. (2010) Improving groundwater resource accounting in irrigated areas: a prerequisite for promoting sustainable use, *Hydrogeol. J.*, 18, 291–294.
- Friedl, M. A., Sulla-Menashe, D., Tan, B., Schneider, A., Ramankutty, N., Sibley, A., and Huang, X. (2010) MODIS Collection 5 global land cover: Algorithm refinements and characterization of new datasets. *Remote Sens. Environ.*, vol. 114, no. 1, pp. 168–182.
- Fritz, S. and See, L. (2005) Comparison of land cover maps using fuzzy agreement. *Int. J. Geogr. Inf. Sci.*, vol. 19, no. 7, pp. 787–807.
- Fritz, S., See, L., Mccallum, I., You, L., Bun, A., Moltchanova, E., Duerauer, M., Albrecht, F., Schill, C., Perger, C., Havlik, P., Mosnier, A., Thornton, P., Wood-Sichra, U., Herrero, M., Becker-Reshef, I., Justice, Hansen, M., Gong, P., Abdel, A. S., Cipriani, A., Cumani, R., Cecchi, G., Conchedda, G., Ferreira, S.C., Gomez, A., Haffani, M., Kayitakire, F., Malanding, J., Mueller, R., Newby, T., Nonguierma, A., Olusegun, A., Ortner, S., Rajak, D. R., Rocha, J., Schepaschenko, D., Schepaschenko, M., Terekhov, A., Tiangwa, A., Vancutsem, C., Vintrou, E., Wenbin, W., van der Velde, M., Dunwoody, A., Kraxner, F., and Obersteiner, M. (2015) Mapping global cropland and field size. *Glob. Chang. Biol.*, vol. 21, pp. 1980–1992.
- Fritz, S., Mccallum, I., Schill, C., Perger, C., Grillmayer, R., Achard, F., Kraxner, F., and Obersteiner, M. (2009) Geo-Wiki.Org: The use of crowdsourcing to improve global land

- cover. *Remote Sens.*, pp. 345–354.
- Fritz, S. and See, L. (2008) “Identifying and quantifying uncertainty and spatial disagreement in the comparison of Global Land Cover for different applications,” *Glob. Chang. Biol.*, vol. 14, no. 5, pp. 1057–1075.
- Giri, C., Zhu, Z., and Reed, B. (2005) A comparative analysis of the Global Land Cover 2000 and MODIS land cover data sets. *Remote Sens. Environ.*, vol. 94, no. 1, pp. 123–132.
- Gordon, L.J.; Peterson, G.D.; Bennett, E. (2008) Agricultural modifications of hydrological flows create ecological surprises. *Trends Ecol. Evolut.* 23, 211–219
- Grekoussis, G., Mountrakis, G., and Kavouras, M. (2015) An overview of 21 global and 43 regional land- cover mapping products. *Int. J. Remote Sens.*, vol. 36, no. 21, pp. 5309–5335.
- Hanasaki, N., Kanae, S., and Oki, T. (2005) A reservoir operation scheme for global river routing models, *J. Hydrol.*, 327, 22–41, doi:10.1016/j.jhydrol.2005.11.011, 2006.
- Hanasaki, N., Kanae, S., Oki, T., Masuda, K., Motoya, K., Shirakawa, N., Shen, Y., and Tanaka, K. (2008) An integrated model for the assessment of global water resources – Part 1: Model description and input meteorological forcing, *Hydrol. Earth Syst. Sci.*, 12, 1007–1025, doi:10.5194/hess-12-1007-2008
- Hanasaki, N., Kanae, S., Oki, T., Masuda, K., Motoya, K., Shirakawa, N., Shen, Y., and Tanaka, K. (2008) An integrated model for the assessment of global water resources – Part 2: Applications and assessments, *Hydrol. Earth Syst. Sci.*, 12, 1027–1037, doi:10.5194/hess-12-1027-2008, 2008b.
- Hanasaki, N., Inuzuka, T., Kanae, S., and Oki, T. (2010) An estimation of global virtual water flow and sources of water withdrawal for major crops and livestock products using a global hydrological model, *J. Hydrol.*, 384, 232–244
- Hanasaki, N., Inuzuka, T., Shinjiro, k., Oki, T. (2010) An Estimation of global virtual water flow and source of water withdrawal for major crops and livestock product using a global hydrological model. *Journal of Hydrology.* 384, 232-244.
- Hanasaki, N., Fujimori, S. Yamamoto, T., Yoshikawa, S., Masaki, Y., Kanae, S. (2013) A Global Water Scarcity assessment under shared socio-economic pathways - Part 1: Water use. *Hydrology and Earth System Science.* 17, 2375-2391.
- Hanasaki, N., Fujimori, S. Yamamoto, T., Yoshikawa, S., Masaki, Y., Kanae, S. (2013) A Global Water Scarcity assessment under shared socio-economic pathways - Part 2: Water availability

and scarcity. *Hydrology and Earth System Science*. 17, 2393-2413.

Hansen, M. C., Defries, R. S., Townshend, J. R. G., and Sohlberg, R. (2000) Global land cover classification at 1 km spatial resolution using a classification tree approach. *Int. J. Remote Sens.*, vol. 21:6-7, pp. 1331–1364.

Hansen, M. C. and Reed, B. (2000) A comparison of the IGBP DISCover and University of Maryland 1 km global land cover products. *Int. J. Remote Sens.*, vol. 21, no. 7, pp. 1365–1373.

Herold, M., Woodcock, C. E., Di Gregorio, A., Mayaux, P., Belward, A. S., Latham, J., and Schmullius, C. C. (2006) A joint initiative for harmonization and validation of land cover datasets. *IEEE Trans. Geosci. Remote Sens.*, vol. 44, no. 7, pp. 1719–1727.

Herold, M., Mayaux, P., Woodcock, C. E., Baccini, A., Schmullius, C. (2008) Some Challenges in Global Land Cover Mapping: An Assessment of Agreement and Accuracy in Existing 1 km Datasets. *Remote Sens. Environ.*, vol. 112, no. 5, pp. 2538–2556.

Jewitt, G. (2006) Integrating blue and green water flows for water resources management and planning. *Phys. Chem. Earth, Parts A/B/C*. 31, 753–762.

Jia, Z., Liu, S., Xu, Z., Chen, Y., Zhu, M. (2012) Validation of remote sensed data evapotranspiration over Hai river basin, China *J. Geophys. Res.: Atmos*, 117.

Kim, H. W., Hwang, K., Mu, Q., Lee, S. O., Choi, M. (2012) Validation of MODIS 16 Global terrestrial Evapotranspiration product in various climate and land cover in Asia. *KSCE J. Civ. engineering*. 16, 229-238

Jung, M., Henkel, K., Herold, M., Churkina, G. (2006) Exploiting synergies of global land cover products for carbon cycle modeling. *Remote Sens. Environ.*, vol. 101, no. 4, pp. 534–553.

Kotsuki, S., Tanaka, K., 2015. SACRA – a method for the estimation of global high-resolution crop calendars from a satellite-sensed NDVI. *Hydrol. Earth Syst. Sci.*, 19, pp: 4441–4461.

Leff, B., Ramankutty, N., and Foley, J. A. (2004) Geographic distribution of major crops across the world. vol. 18, B1009,

Loveland, T. R., Reed, B. C., Brown, J. F., Ohlen, D. O., Zhu, Z., and Yang, L. (2000) Development of a global land cover characteristics database and IGBP DISCover from 1 km AVHRR data. *Int. J. Remote Sens.*, vol. 21:6-7, pp. 1303–1330.

McCallum, I., Obersteiner, M., Nilsson, S., and Shvidenko, A. (2006) A spatial comparison of

- four satellite derived 1 km global land cover datasets. *Int. J. Appl. Earth Obs. Geoinf.*, vol. 8, no. 4, pp. 246–255.
- Mu, Q., Zhao, M (2011) Improvement to a MODIS global terrestrial evapotranspiration algorithm. *Remote sensing of environment*, 115, 1781-1800.
- Nakaegawa, T. (2011) Uncertainty in land cover datasets for global land-surface models derived from 1-km global land cover datasets. *Hydrol. Process.*, vol. 25, no. 17, pp. 2703–2714.
- Neidzweidz, T.; Ustrnul, Z.; Szalai, S.; López-Urrea, R.; Montoroa, A.; Mañasa, F.; López-Fustera, P.; Fereres, E. (2012): Evapotranspiration and crop coefficients from lysimeter measurements of mature ‘Tempranillo’ wine grapes. *Agric. Water Manage.* 2012. 112, 13–20.
- NEPAD (New Partnership for Africa’s Development). (2003) Comprehensive Africa Agriculture Development Programme, available at: <http://www.nepad.org/system/files/caadp.pdf> (last access: 20 January 2018), 102 pp
- Oyoshi, K., Sobue, S., Takeuchi, W., 2013. Development of complicated rice crop calendar in Southeast Asia with time-series MODIS data. *2<sup>nd</sup> International Conference on Agro-Geoinformatics*. pp. 444 – 447.
- Pflugmacher, D., Krankina, O. N., Cohen, W. B., Friedl, M. A., Sulla-Menashe, D., Kennedy, R. E., Nelson, P., Loboda, T. V., Kuemmerle, T., Dyukarev, E., Elsakov, V., and Kharuk, V. I. (2011) Comparison and assessment of coarse resolution land cover maps for Northern Eurasia. *Remote Sens. Environ.*, vol. 115, no. 12, pp. 3539–3553.
- Piracha, A., Majeed, Z., (2011). Water use in Pakistan’s agricultural sector: water conservation under the changed climatic conditions. *International Journal of Water Resources and Arid Environments* 1 (3), 170e179.
- Portmann, F. T., Siebert, S., Döll P., 2010. MIRCA2000—Global monthly irrigated and rainfed crop areas around the year 2000: A new high-resolution data set for agricultural and hydrological modelling. *Global Biogeochem. Cycles*, 24, GB1011.
- Postel, S. L. (1999), *Pillars of Sand: Can the Irrigation Miracle Last?*, W.W. Norton, New York.
- Ramoelo, A., Majozi, N., Mathieu, R., Jovanovic, N, Nickless, A., Dziki, S. (2014) Validation of Global Evapotranspiration Product (MOD16) Using Flux Tower Data in the African Savanna, South Africa. *Remote sensing*. 6, 7406-7423.

- Ramankutty N, Mehrabi Z, Waha K., 2018. Trends in Global Agricultural Land Use: Implications for Environmental Health and Food Security. *Annu. Rev. Plant Biol* 69 (4), pp: 1–14.
- Ran, Y., Li, X., and Lu, L. (2010) Evaluation of four remote sensing based land cover products over China. *Int. J. Remote Sens.*, vol. 31, no. 2, pp. 391–401.
- Rockström, J., Falkenmark, M., Karlberg, L., Hoff, H., Rost, S., Gerten, D., (2009) Future water availability for global food production: The potential of green water for increasing resilience to global change. *Water Resour. Res.*, 45, doi:10.1029/2007WR006767.
- Rost, S., Gerten, D., Bondeau, A., Lucht, W., Rohwer, J., and Schaphoff, S. (2008) Agricultural green and blue water consumption and its influence on the global water system, *Water Resour. Res.*, 44, W09405, doi:10.1029/2007WR006331.
- Sakti, A. D., Takeuchi, W., Wikantika, K., 2017. Development of Global Cropland Agreement Level Analysis by Integrating Pixel Similarity of Recent Global Land Cover Datasets. *Journal of Environmental Protection*, 8 (12), pp. 1509-1529.
- Sakamoto T., Yokozawa M., Toritani H, (2005) A crop phenology detection method using time-series MODIS data, *Remote Sens. Environ.*, vol. 96, pp. 366-374.
- Sakti, A. D., Takeuchi, W., Wikantika, K. (2017). Development of Global Cropland Agreement Level Analysis by Integrating Pixel Similarity of Recent Global Land Cover Datasets. *Journal of Environmental Protection*, 8 (12), pp. 1509-1529.
- Sakti, A. D., Takeuchi, W. (2018) Estimation of Global Crop Calendar and Intensity Using the MODIS NDVI Time Series from 2001 to 2015. *International Symposium on Remote Sensing 2018*
- Savenije, H.H.G. (2004) The importance of interception and why we should delete the term evapotranspiration from our vocabulary. *Hydrological Processes* , 18, 1507–1511
- See, L., Fritz, S., You, L., Ramankutty, N., Herrero, M., Justice, C., Becker-Reshef, I., Thornton, P., Erb, K., Gong, P., Tang, H., van der Velde, M., Ericksen, P., McCallum, I., Kraxner, F., and Obersteiner, M. (2015) Improved global cropland data as an essential ingredient for food security. *Glob. Food Sec.*, vol. 4, pp. 37–45.
- See, L. M. and Fritz, S. (2006) A method to compare and improve land cover Datasets: Application to the GLC-2000 and MODIS land cover products. *IEEE Trans. Geosci. Remote*

- Sens., vol. 44, no. 7, pp. 1740–1746.
- See, L., Schepaschenko, D., Lesiv, M., McCallum, I., Fritz, S., Comber, A., Perger, C., Schill, C., Zhao, Y., Maus, V., Siraj, M. A., Albrecht, F., Cipriani, A., Vakolyuk, M., Garcia, A., Rabia, A. H., Singha, K., Marcarini, A. A., Kattenborn, T., Hazarika, R., Schepaschenko, M., van der Velde, M., Kraxner, F., Obersteiner, M. (2015) Building a hybrid land cover map with crowdsourcing and geographically weighted regression. *ISPRS J. Photogramm. Remote Sens.*, vol. 103, pp. 48–56.
- Siebert, S., Döll, P. (2009) Quantifying blue and green virtual water contents in global crop production as well as potential production losses without irrigation. *J. Hydrol.*, doi:10.1016/j.jhydrol.2009.1007.1031.
- Siebert, S., Henrich, V., Frenken, K., and Burke, J. (2013) Update Of The Digital Global Map Of Irrigation Areas to Version 5, Rheinische Friedrich-Wilhelms-University, Bonn, Germany/Food and Agriculture Organization of the United Nations, Rome, Italy.
- Smith, M., CROPWAT – A computer program for irrigation planning and management, Irrigation and Drainage Pap. 46, Food and Agric. Org. of the U. N., Rome, 1992.
- Sulser, T., Ringler, C., Zhu, T., Msangi, S., Bryan, E., and Rosegrant, M. W. (2010) Green and blue water accounting in the Ganges and Nile basins: implications for food and agricultural policy, *J. Hydrol.*, 384, 276–291, doi:10.1016/j.jhydrol.2009.10.003.
- Suputra, D. P. A., Ambarwati, I. G. A., and Tenaya, I. M. N. (2012) Faktor-faktor yang mempengaruhi alih fungsi lahan studi kasus di Subak Daksina, Desa Tibubeneng, Kecamatan Kuta Utara, Kabupaten Badung. *E-Journal Agribisnis dan Agrowisata*, vol. 1, no. 1, pp. 61–68.
- Tateishi, R., Uriyangqai, B., Al-Bilbisi, H., Ghar, M. A., Tsend-ayush, J., Kobayashi, T., Kasimu, A., Hoan, N. T., Shalaby, A., Alsaaidh, B., Enkhzaya, T., Gegentana, Sato, H. P. (2011) Production of global land cover data – GLCNMO. *Int. J. Digit. Earth*, vol. 4:1, pp. 24–49.
- Tateishi, R., Hoan, N. T., Kobayashi, T., Alsaaidh, B., Tana, G., and Phong, D. X. (2014) Production of global land cover data – GLCNMO2008. *J. Geogr. Geol.*, vol. 6, no. 3, pp. 99–122.
- Tchuenté, A. T. K., Roujean, J. L., and de Jong, S. M. (2011) Comparison and relative quality assessment of the GLC2000, GLOBCOVER, MODIS and ECOCLIMAP land cover data sets at the african continental scale. *Int. J. Appl. Earth Obs. Geoinf.*, vol. 13, no. 2, pp. 207–219.

- Tsendbazar, N., De Bruin, S., Fritz, S., and Herold, M. (2015) Spatial Accuracy Assessment and Integration of Global Land Cover Datasets. September, pp. 15804–15821.
- Pokhrel, Y., Hanasaki, N., Koirala, S., Cho, J., Yeh, P. J. F., Kim, H., Kanae, S., and Oki, T. (2012) Incorporating anthropogenic water regulation modules into a land surface model, *J. Hydrometeorol.*, 13, 255–269, doi:10.1175/JHM-D-11-013.1.
- UNFCCC. Decision 1/CP.21: Adoption of the Paris Agreement. Paris Climate Change Conference; 2015 Nov 30–Dec 11; Paris, France
- Vancutsem, C., Marinho, E., Kayitakire, F., See L., and Fritz, S. (2013) Harmonizing and combining existing land cover/land use datasets for cropland area monitoring at the African continental scale. *Remote Sens.*, vol. 5, no. 1, pp. 19–41.
- Villholth, K. G. (2003) Groundwater irrigation for smallholders in Sub-Saharan Africa – a synthesis of current knowledge to guide sustainable outcomes, *Water Int.*, 38, 369–391, doi:10.1080/02508060.2013.821644.
- Waha, K., Van Bussel, L. G. J., Müller, C., 2012. Climate-driven simulation of global crop sowing dates. *Global Ecol. Biogeogr* (21).
- Waldner, F., Fritz, S., Di Gregorio, A., Plotnikov, D., Bartalev, S., Kussul, N., Gong, P., Thenkabail, P., Hazeu, G., Klein, I., Löw, F., Miettinen, J., Dadhwal, V.K., Lamarche, C., Bontemps, S., Defourny, P. (2016) A Unified Cropland Layer at 250 m for Global Agriculture Monitoring. *Data*, 1, 3.
- Wua, W., Yua, Q., Youb, L., Chenb, K., 2018. Global cropping intensity gaps: Increasing food production without cropland expansion. *Land Use Policy*, 02, 032.
- Zhang, N. and Tateishi, R. (2013) Integrated use of existing global land cover datasets for producing a new global land cover dataset with a higher accuracy: A case study in eurasia. *Adv. Remote Sens.*, vol. 2, pp. 365–372.
- Zabel, F., Putzenlechner, B., Mauser, W., 2014. Global Agricultural Land Resources. A High Resolution Suitability Evaluation and Its Perspectives until 2100 under Climate Change Conditions. *PLOS ONE*, 9 (9).

